Characterization of the mechanisms regulating dyskerin SUMOylation

Hélène Bensoussan

A thesis submitted to McGill in partial fulfillment of the requirements of the degree of **Master of Science**

Department of Anatomy and Cell Biology

McGill University, Montréal, Québec

August 2017

INDEX

ABBREVIATIONS

AAA+ ATPases	ATPases associated with diverse cellular activities
ALT	Alternative lengthening of telomere
APB	ALT-associated promyelocytic leukemia protein body
AsO3	Arsenic trioxide
ATM	Ataxia telangiectasia mutated protein
ATR	Ataxia telangiectasia and Rad3-related protein
BioID	Proximity dependent biotin identification
BLM	Bloom syndrome protein
BirA	Bifunctional ligase/Repressor A
BRCA1	Breast cancer type I susceptibility protein
BRET	Bioluminescence resonance energy transfer
CAB box	Cajal body box
CIP	Calf intestinal alkaline phosphatase
CR4/5	Conserved region 4/5
CR7	Conserved region 7
Cryo-EM	Cryo-electron microscopy
CST	CTC1/STN1/TEN1 complex
CTC1	Conserved telomere maintenance component 1
DAXX	Death domain-associated protein 6
DC	Dyskeratosis Congenita
D-loop	Displacement loop
DDR	DNA damage response

DOC	Sodium deoxycholate
DSB	Double stranded break
FISH	Fluorescent *in situ* hybridization
FRET	Fluorescent resonance energy transfer
HH	Hoyeraal-Hreidarsson
HR	Homologous recombination
hTR	Human telomerase RNA
hTERT	Human telomerase reverse transcriptase
hTRmin	Minimal hTR
IF	Immunofluorescence
IκBα	Nuclear factor kappa B inhibitor alpha
IFD	"Insertion in fingers" domain
KR-TRF1	KillerRed TRF1
KAP1	KRAB domain-associated protein 1
LB	Luria broth
MEF	Mouse embryo fibroblast
MDM2	Mouse double minute 2
MS	Mass spectrometry
kDa	Kilodalton

NAF1	Nuclear assembly factor 1
NOP 10	H/ACA ribonucleoprotein complex subunit 3
NF- κB	Nuclear factor κB
NHEJ	Non-homologous end joining
NHP2	H/ACA ribonucleoprotein complex subunit 2
NiNTA	Nickel-charged nitrilotriacetic acid
NoLS	Nucleolar localization sequence
OB	Oligonucleotide/oligosaccharide binding
PBS	Phosphate-buffered saline
PI	Propidium iodide
PIAS	Protein inhibitor of activated stat
PML	Promyelocytic leukemia protein
POT1	Protection of telomeres 1
PTM	Post-translational modification
PUA	Pseudouridine synthase and archaeosine transglycosylase
RAD51	DNA repair protein RAD51 homolog 1
RAP1	Repressor activator protein 1
RING	Really interesting new gene
H/ACA RNP	H/ACA ribonucleoprotein

ROS	Reactive oxygen species
RPA	Replication protein A
rRNA	Ribosomal RNA
RTEL1	Regulator of telomere elongation helicase 1
SAE1/2	SUMO activating enzyme 1 and 2
SAINT	Significance analysis of intercactome
ScaRNA	Small Cajal body associated RNA
SENP	SUMO/sentrin specific proteases
SHQ1	Protein SHQ1 homolog
SIM	SUMO interacting motif
Smt	Suppressor of Mif2
SMUG1	Selective Monofunctional Uracil-DNA Glycosylase 1
SnoRNA	Small nucleolar RNA
SSC	Saline sodium citrate
STN1	Suppressor of Cdc thirteen
STUbL	SUMO-targeted ubiquitin ligase
SUMO	Small-ubiquitin like modifiers
T-loop	Telomere loop
TCAB1	Telomerase Cajal body protein 1
TEL-patch	TPP1 glutamate and leucine-rich patch
TEN	TERT essential N-terminal
TEN1	Telomeric pathways with Stn1

TERRA	Telomeric repeat-containing RNA
TIF	Telomere dysfunction induced foci
TIN2	TRF1-interacting protein
TPP1	Previously known as TINT1 (TIN2 interacting protein), PTOP (POT1 and TIN2 organizing protein) and PIP1 (POT1 interacting protein)
TRBD	Telomerase RNA-binding domain
TRF1	Telomere repeat binding factor 1
TRF2	Telomere repeat binding factor 2
$TRF2^{\Delta B \Delta C}$	TRF2 dominant negative
Ubc9	Ubiquitin conjugating enzyme 9

LIST OF FIGURES

LIST OF TABLES

ABSTRACT

Telomeres protect the ends of chromosomes from chromosome degradation, DNA damage recognition and chromosome fusion. The enzyme telomerase maintains their length by adding *de novo* telomeric-repeats during genomic replication. While not expressed in somatic cells, 85% of cancer cells express telomerase, giving them unlimited proliferative capacities. Therefore, it is a potential target for cancer therapy. Dyskeratosis Congenita (DC) is a rare premature aging disease that can be caused by mutations in *DKC1*, the gene encoding the evolutionary conserved protein dyskerin. This protein is essential for telomerase RNA stability and hence telomerase activity. DC phenotypes include premature telomere shortening and depletion of highly proliferative tissues. Dyskerin has previously been found to be modified by Small-Ubiquitin Like Modifiers (SUMO), a post translational modification involved in the regulation of multiple cellular pathways. The SUMOylation cycle involves multiple factors: the E1 activating enzyme, the Ubc9 E2 conjugating enzyme and an E3 SUMO ligase to facilitate the transfer of SUMO to its target. Some mutations in dyskerin SUMOylation sites are DC-associated. However, very little is known about dyskerin post translational modification. This study focuses on characterizing the mechanisms regulating dyskerin SUMOylation. We first find SUMOylation of dyskerin to be cell cycle regulated, peaking in S phase and G2/M. We further find that some different types of DNA damage, whether global or telomere-specific, have differential effects on dyskerin protein levels and SUMOylated states. Through the silencing of SUMO specific proteases (SENPs), we determine SUMOylated dyskerin to be mainly nucleolar. We aim to identify SUMO-dependent dyskerin partners with a BioID and more specifically the E3 ligase involved in its SUMOylation. This study is key to have more insight on the interactions and functions impacted in SUMO deficient dyskerin and its role in telomerase.

RESUME

Les télomeres protègent les extremités des chromosomes contre la degradation, la reconnaissance de dommage a l'ADN et la fusion des chromosomes. L'enzyme télomerase entretien leur longueur par l'ajout *de* novo de séquences télomeriques au cours de la réplication du génome. Alors que l'enzyme n'est pas exprimée dans les cellules somatiques, 85% des cellules cancéreuses expriment la télomerase leurs procurant une capacité de prolifération infinie. Ainsi, c'est une cible potentielle pour le traitement du cancer. La Dyskératose Congénitale (DC) est une maladie rare de vieillissement prématurée qui peut être causée par des mutations dans *DKC1*, le gène codant la protéine dyskérine conservée au cours de l'évolution. Cette protéine est essentielle pour la stabilité de l'ARN de la télomerase et donc pour son activité. Les phénotypes de DC inclus le raccourcissement prématuré des télomeres et l'épuisement des tissues hautement proliférants. Il a été prouvé que dyskérine se fait SUMOyler, une modification post-traductionnelle impliquée dans la régulation de multiples mécanismes cellulaires. Le cycle de SUMOylation inclus plusieurs facteurs : un enzyme d'activation E1, un enzyme de conjugation Ubc9 et un E3 ligase de SUMOylation pour faciliter le transfert du SUMO à sa cible. Certaines mutations dans les sites de SUMOylation de dyskérine sont associées à DC. Cependant, ses modifications post-traductionnelles sont très peu étudiées. Cette étude se focalise sur la caractérisation des mécanismes régulant la SUMOylation de dyskérine. Tout d'abord, nous avons découvert que la SUMOylation de dyskérine est dépendante du cycle cellulaire, plus élevée en phase S et G2/M. De plus, nous avons trouvé que certains types de dommages à l'ADN, qu'ils soient globaux ou télomériques, ont différents effets sur le taux de protéines dyskérine et sur sa SUMOylation. Avec le silençage par l'ARN des protéases spécifiques aux SUMOs (SENPs), nous avons déterminé que la dyskérine SUMOylée est principalement nucléolaires. On voudrait identifier les partenaires de la dyskérine dépendant de sa SUMOylation en utilisant une BioID et plus précisement identifer sa

E3 ligase de SUMOylation. Cette étude est essentielle pour avoir plus de ressources sur les intéractions et les fonctions qui sont affectées par la dyskérine déficiente pour la SUMOylation et son rôle dans la télomerase.

ACKNOWLEDGEMENTS

I would like to strongly thank my supervisor **Dr. Chantal Autexier** for taking me into her lab and giving me the opportunity to get introduced to scientific research as well as her amazing team. It has been a pleasure to work for such a strong and passionate supervisor full of life!

I would like to acknowledge **Patrick Lambert-Lanteigne** for being my mentor and putting up with my questions for two years. He has been a great teacher: patient, attentive, never judging and always ready for a good laughter!

I want to thank the lab members in general, **Deanna MacNeil, Patrick Lambert-Lanteigne, Josephine Chu, Phillipe Rousseau and Jeffery Wang** for making these two years such an enjoyable roller coaster ride, for always being supportive in the low moments and positive-attitude viruses at others.

I would like to thank **Christian Young** for being so helpful and patient for the flow cytometry analysis and **Halil Bagci** for helping with the BioID analysis using ProHits out of his own time.

I would like to thank the members of my committee **Dr. Pierre Thibault**, **Dr. Heidi McBride** and my mentor **Dr. Craig Mandato** for their time and their good advice.

This research was made possible thanks to the support of the **Lady Davis Institute/ TD Bank Studentship Award**.

I want to thank my entire family for being so supportive during my studies and especially my parents for giving me the opportunity to travel across the world to do what I love.

Finally, I would like to dedicate my thesis to my grandfather **Claude Bensoussan** who passed away last year. He has always been here to encourage me in my studies and was proud even in the smallest achievement. This work is for you Papy.

PREFACE

This research thesis is the original work of the student presenting it today, Hélène Bensoussan Some parts of the literature review include sections written by the student in a review published in 2016 as a co-author[1].

Dr. Li Lan kindly provided the KillerRed-TRF1 plasmid and suggestions on the protocol to use for light exposure.

Dr. Pierre Thibault kindly provided us with HEK293 cells stably overexpressing His-SUMO3.

Shusen Zhu cloned the pLenti-Flag-dyskerin plasmid from the pcDNA3.1 Flag-dyskerin plasmid kindly provided to us by Dr. François Dragon.

The His-SUMO3 Flag-dyskerin HEK293 cell line used in this study was engineered by Patrick Lambert-Lanteigne through the infection of His-SUMO3 expressing HEK293 cells with the pLenti-Flag-dyskerin plasmid.

Dr. Titia de Lange kindly provided us with the pLPC-NMycTRF2$^{\Delta B\Delta M}$ plasmid.

Dr. Marc Fabian kindly provided the pcDNA3.1 neo Myc-BirA* plasmid and gave suggestions on how to proceed with the BioID experiment.

Dr. Koren Kathleen Mann kindly provided us with arsenic trioxide for the DNA damage experiments.

Dr. Stéphane Richard kindly provided some siGFP for the SENP silencing experiments.

Dr. Denis Faubert and Josée Champagne performed the tryptic digestion and the Mass Spectrometry Analysis of the BioID samples at the IRCM.

Halil Bagci, a PhD student from Jean-François Cote's lab kindly performed the analysis with ProHits of the mass spectrometry data obtained from the BioID experiment.

LITERATURE REVIEW

I. Telomeres and telomerase

1) Telomeres

In 1985, Elizabeth Blackburn and Carol Greider discovered a ribonucleoprotein containing reverse transcriptase activity which they termed telomerase[2,3]. The discovery of this enzyme was a breakthrough to better understanding the "end replication problem".

a. End replication problem

DNA polymerases can only replicate DNA in a 5' to 3' direction[4,5]. This is not a problem for the replication of the leading strand but the issue arises to replicate the lagging strand in a 3' to 5' direction. RNA primers bind the lagging strand acting as anchors for the DNA polymerase to synthesize DNA in a 5' to 3' direction creating 100-300 nucleotide Okazaki fragments which are then fused together by the DNA ligase I [6,7]. However, removal of the terminal RNA primer leaves the 3' end of the lagging strand unreplicated[8]. Olovnikov and Watson predicted that with this process, the ends of linear chromosomes would shorten during each replication cycle and create a single stranded 3' end[9,10]. To prevent genetic information loss after each cell cycle and genomic instability, linear chromosome ends are protected by stretches of nucleotide repeats known as telomeres. In accordance with the 3' end chromosome replication problem, each chromosomal replication leads to telomere shortening, between 50 and 200 nucleotides per cycle (Figure 1b)[11]. The cells have a limited proliferation capacity of about 40 to 60 divisions known as the Hayflick limit when the telomeres reach a critical length and the cells enter replicative senescence (Figure 1c)[12]. This process is now also known as cellular aging

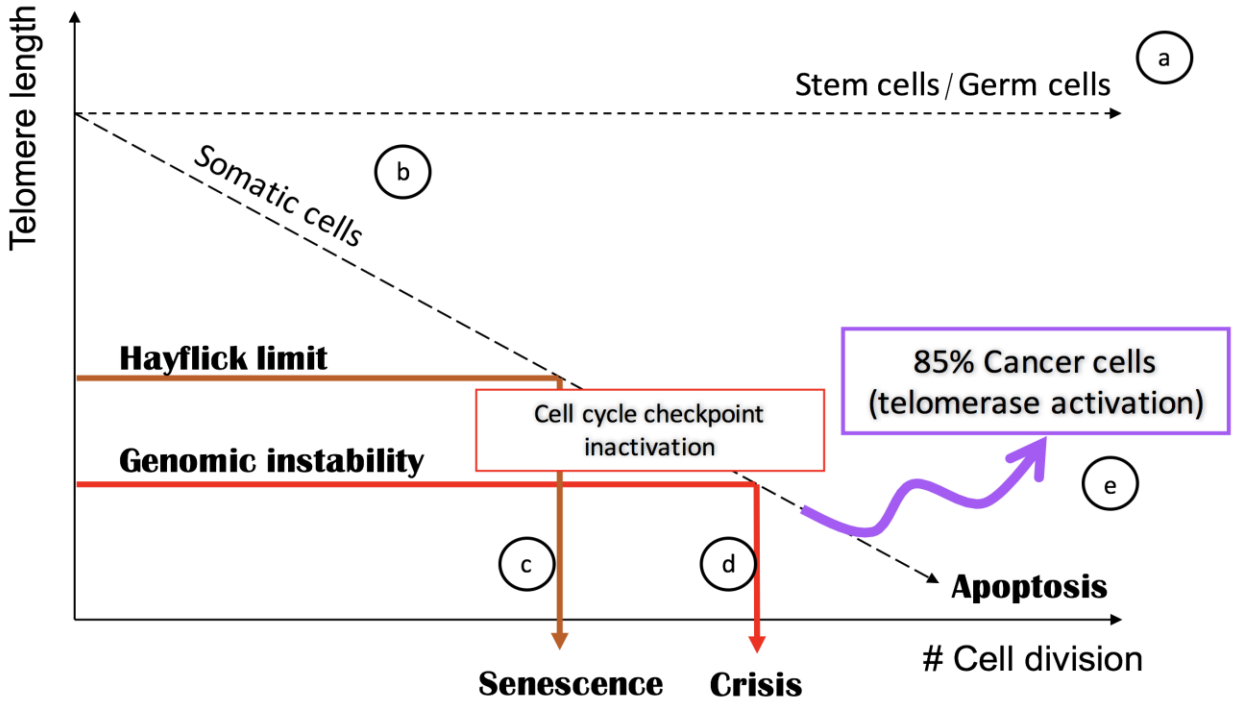

Figure 1. Telomeres, the molecular clocks. a) Telomere length is maintained in stem cells and germ cells where telomerase is expressed. (b) Telomeres shorten at each cell cycle in somatic cells. (c) The Hayflick limit represents the approximate number of cell divisions that can occur before its telomeres are too short and cell cycle checkpoints drive the cell to replicative senescence. (d) Inactivation of these checkpoints leads to further shortening of telomeres and to telomere crisis and apoptosis. (e) The re-expression of telomerase in cancer cells allows them to bypass cell death checkpoints and gives them unlimited proliferation capacities.

b. Structure and function of telomeres

In eukaryotes, telomeres are G-rich nucleotide tandem repeats. Their sequence varies among species with the most common repeat being TTAGGG in vertebrates[13]. Average telomere length also differs from one species to another: for example, humans have 10 to 20 kilobase pair-long telomeres whereas telomeres in mice are 10 to 30 times longer[14,15]. This heterogeneity however does not influence their conserved function. Telomeres are essential to protect linear chromosomes from degradation, fusion and being detected as DNA damage, therefore maintaining genomic integrity. This function is assisted by a group of telomere-associated proteins known as the shelterin complex: the Telomeric Repeat binding Factors 1 (TRF1) and 2 (TRF2), the TRF1

INteracting protein (TIN2), the Repressor Activator Protein 1 (RAP1), the Protection Of Telomeres 1 (POT1) and the protein previously known as TINT1 (TIN2 interacting protein)[16], PTOP (POT1 and TIN2 organizing protein)[17] and PIP1 (POT1 interacting protein)[18] (aka TPP1) (Figure 2)[19]. TRF1 and TRF2 bind the double-stranded telomeric DNA stabilizing and protecting telomeres. TIN2 binds both TRF1 and TRF2, linking the two shelterin proteins together while also anchoring TPP1. POT1 binds the G-rich single stranded telomeric DNA through its Oligonucleotide/Oligosaccharide Binding (OB) domain while also binding to TPP1. Finally, RAP1 binds both TRF2 and TIN2 and was shown to be essential for TRF2 stabilization at telomeres[20,21]. The proper recruitment and binding of these proteins mediates the protection of telomeres from the DNA damage response (DDR) through the formation of a higher structure known as the Telomere loop (T-loop)[22]. The single stranded 3' overhang forms a lariat-shaped structure and displaces upstream double stranded telomeric DNA forming a Displacement loop (D-loop). The telomeres can also form higher order structures such as G-quadruplex DNA, stacking of planar arrays formed by four guanines that are hydrogen-bonded. The spontaneous formation of these structure is possible due to the G-rich nature of telomeric DNA[22,23]. These higher order structures are disrupted during S phase for telomere replication[24].

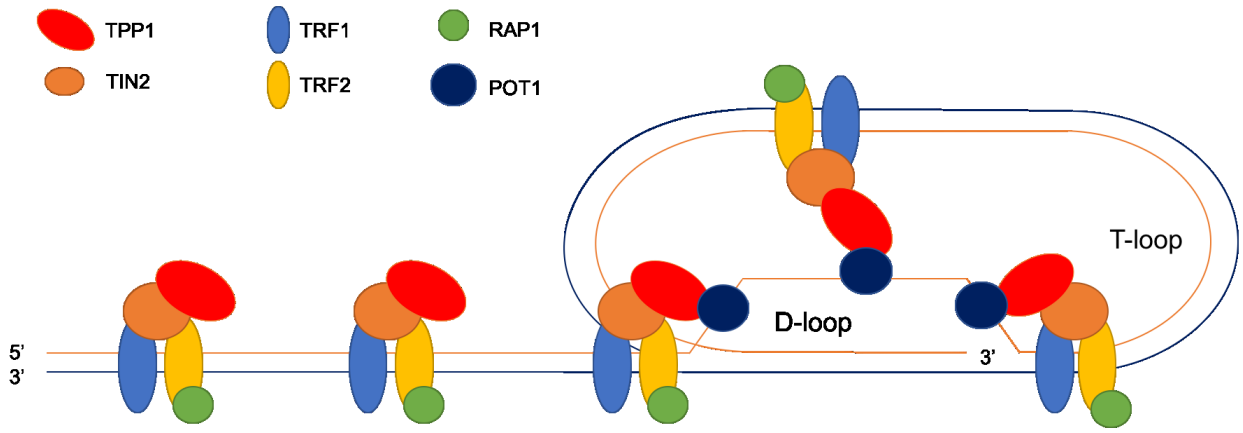

Figure 2. Schematic representation of the shelterin complex at the telomeres and the formation of a T-loop and D-loop from the G-rich 3' overhang. Blue strand represents the leading strand while the orange strand represents the lagging strand.

2) Telomerase

The discovery of telomeres opened a new research area dedicated to understanding the mechanisms involved in the regulation of telomere maintenance, how some cells (such as stem, progenitor and cancer cells) can proliferate past the Hayflick limit (Figure 1a and e) and how telomere length is maintained or elongated with increasing cellular divisions. Telomerase became the answer to understanding telomere maintenance and elongation in eukaryotes.

a. Nobel prize discovery

The telomerase enzyme was initially discovered in *Tetrahymena* at the University of California, Berkeley by Elizabeth Blackburn and Carol Greider. These Nobel prize winners' work provided the first evidence for a reverse transcriptase elongating telomeres[2,3]. Oligonucleotides mimicking *Tetrahymena* telomeric repeats can be extended in cell-free *Tetrahymena* extracts and this activity is specific to the 3' G-rich telomere strand[3]. They also showed that this synthesis is species template-independent as yeast telomere oligonucleotides can be extended as well in *Tetrahymena* extracts with the addition of *Tetrahymena* telomeric repeats. These results prove that telomere

elongation occurs through *de novo* synthesis with the kinetics of an enzymatic activity. Two years later they purified this enzyme and characterized a ribonucleoprotein complex responsible for this reverse transcriptase activity from an RNA template which they termed telomere terminal transferase and later became known as telomerase[2].

b. The human telomerase, a ribonucleoprotein complex

This ribonucleoprotein is made of two main catalytic subunits: the human Telomerase Reverse Transcriptase (hTERT) and the human Telomerase RNA (hTR) acting as an RNA template with a telomeric-template guiding the complex to telomeres in S phase. Although both units are sufficient *in vitro* for telomerase activity[2,25], additional components are necessary *in vivo* for its assembly and function including four scaffold proteins known as the H/ACA proteins.

c. H/ACA ribonucleoprotein subunits

The term H/ACA is attributed to small non-coding RNAs which possess a conserved 3' secondary structure motif known as the H/ACA motif containing two hairpins separated by a single stranded H-box (5'-ANANNA-3' sequence where N is any nucleotide), ending in a single stranded 3' tail-encoded ACANNN[26]. These H/ACA RNAs assemble into ribonucleoprotein complexes with four H/ACA scaffold proteins upon maturation: the pseudouridine synthase dyskerin; the RNA interacting components H/ACA Ribonucleoprotein complex subunit 2 (NHP2) and H/ACA Ribonucleoprotein complex subunit 3 (NOP10); and a pseudouridylation-catalysis enhancer H/ACA Ribonucleoprotein complex subunit 1 (GAR1)[27]. The assembled H/ACA RNPs can then target RNA molecules for pseudouridylation, an essential post-transcriptional process leading to the isomerization of uridine nucleosides into pseudouridines, guided by the small non-coding H/ACA RNAs[28]. Among this family of RNAs, we can distinguish two groups based on their subcellular localization. The first group are small nucleolar RNAs (snoRNAs) which assemble

into H/ACA RNPs to specifically target ribosomal RNAs (rRNAs) in the nucleolus[29], a subnuclear structure acting as the site of rRNA transcription and processing as well as ribosome assembly[30]. Later, a second group was identified termed small Cajal body-associated RNAs (scaRNAs) which guide the corresponding H/ACA RNPs for pseudouridylation of spliceosomal small nuclear RNAs (snRNAs) in the Cajal Bodies (CB) [28]. CBs are subnuclear dynamic sites also referred to as coiled bodies, as coilin is there main component, where snRNAs are synthesized and processed[31]. ScaRNAs are differentiated from snoRNAs due to their Cajal body box (CAB box). This special structure is a conserved binding domain for the telomerase Cajal body protein 1 (TCAB1) which recruits the complex it binds to the CB. [32]

d. hTR, the telomerase H/ACA RNA

The 451-nt hTR is part of the H/ACA RNA family characterized by the presence of the H/ACA motif previously described. It is known that this motif is necessary for its stability and localization *in vivo* as well as the proper assembly of the telomerase complex and for its trafficking and activity[33,34]. The telomeric template is localized at its 5' end between nucleotides 46 and 53 within the pseudoknot domain also known as core domain (Figure 3). The pseudoknot which extends to approximately nucleotide 200 is essential for telomerase activity as deletions in hTR between nucleotides 170 and 200 lead to reduced telomerase activity *in vitro*[35]. Mutations in this domain have also been associated to shorter telomeres and telomerase deficiency *in vivo*. The localization of these mutations in this highly-conserved region underlines the pseudoknot as a core domain of hTR[35]. The pseudoknot domain is necessary and sufficient for hTERT and hTR assembly *in vitro*[36,37]. Other domains in the hTR are critical for its stability and localization[38,39]. These include conserved region 4/5 (CR4/5) and conserved region 7 (CR7). CR4/5 is situated in the first loop of the 3' secondary structure of the hTR. Its role is not essential for telomerase activity *in vitro* but

its evolutionary conservation highlights its role in telomerase assembly and activity *in vivo*[36,40,41]. CR7 is in the second stem loop of the 3' end and is critical for RNA stability[33]. It also contains a CAB box, grouping hTR to the scaRNA family[42]. This region is critical for the hTR transport to the CB in S phase mediated by the binding of TCAB1[43], a process further described below. Interestingly, it has recently been reported that the H/ACA RNP assembly is not directly necessary for telomerase activity but probably upstream of telomerase activity at the telomeres[44]. After the engineering of a minimal hTR (hTRmin) which lacks the H/ACA motif and is stabilized by additional 3' processing and protection motifs, the hTR/hTERT assembly was shown to be sufficient for telomerase activity and telomere maintenance[44].

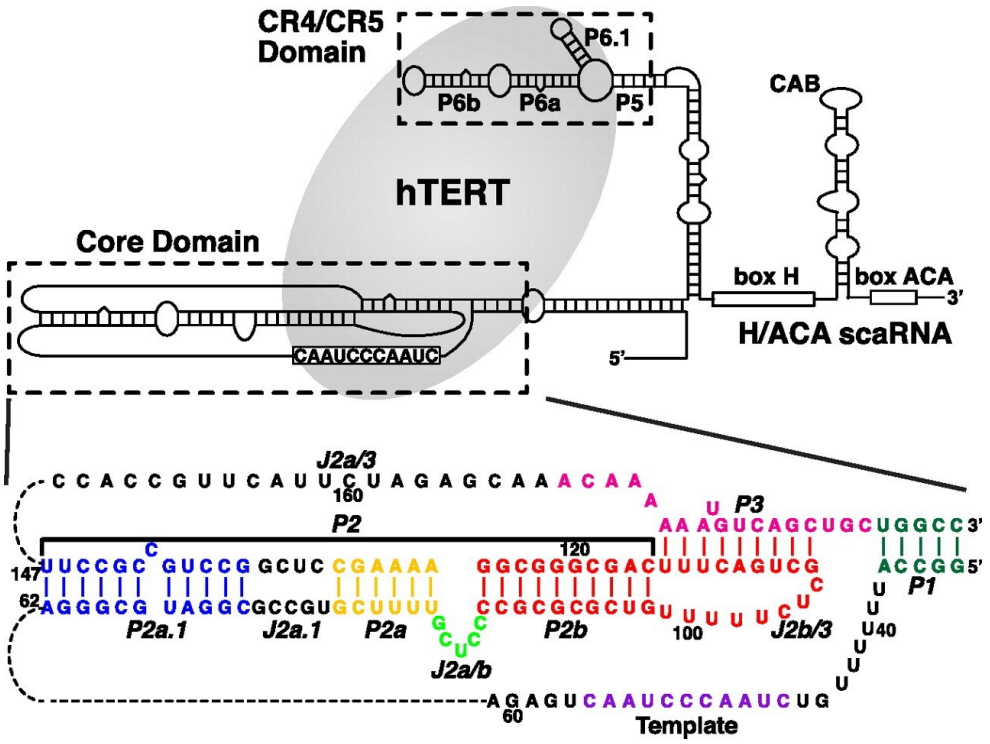

Figure 3. Secondary structure of the human telomerase RNA hTR. The figure includes four key elements of the hTR: the pseudoknot/template (core domain), the CR4-CR5 region, the CR7 containing the CAB box and the H/ACA box. (Zhang, Q et al. 2010. PNAS) Copyright 2010 reprinted with permission from PNAS.

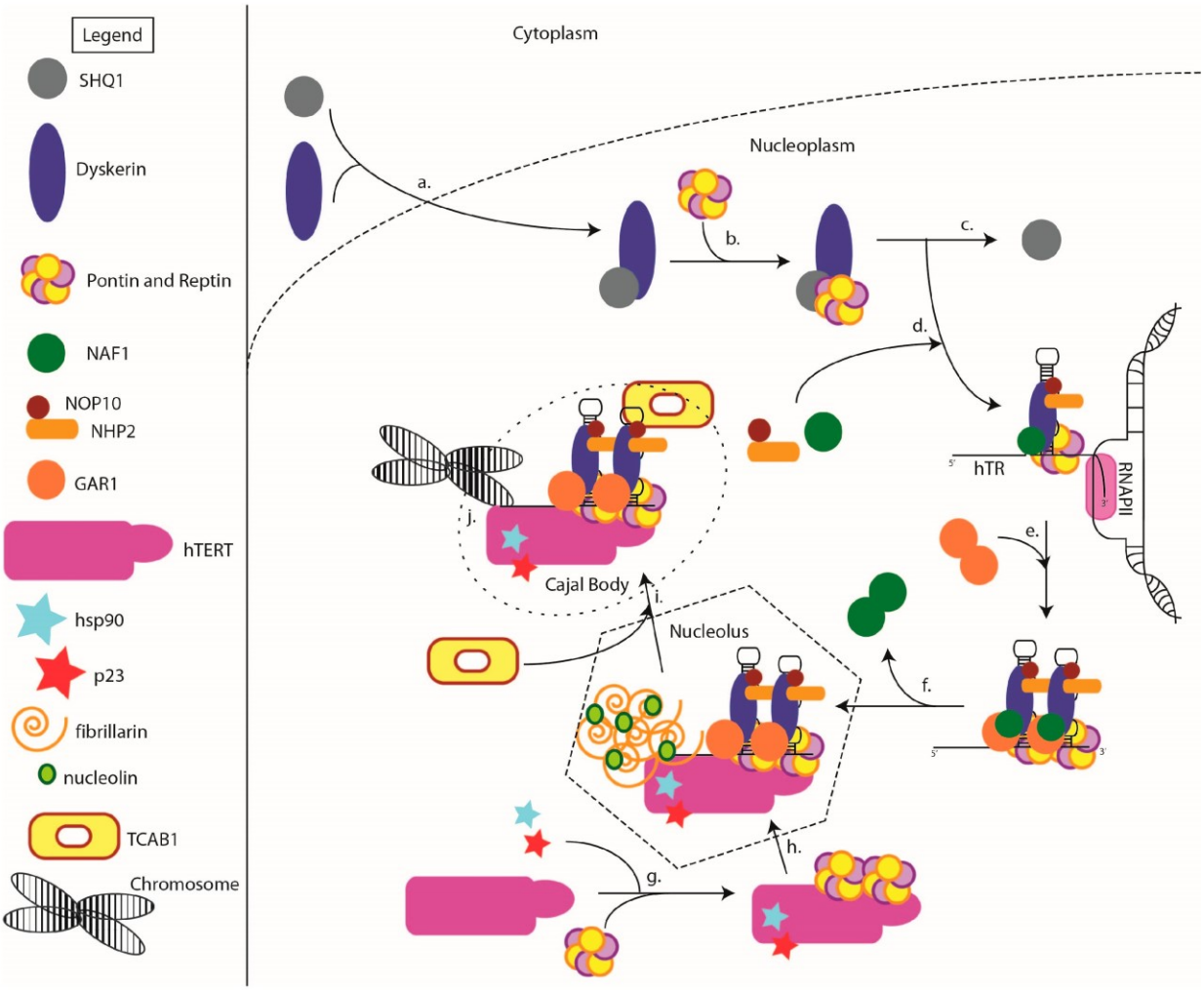

Figure 4. Assembly and Localization of H/ACA Ribonucleoprotein Complex. (**a**) SHQ1 shuttles dyskerin to the nucleoplasm. (**b**) Pontin and reptin bind the SHQ1/dyskerin heterodimer (**c**) facilitating SHQ1 dislocation (**d**) The H/ACA proteins, including NAF1, Nop10 and NHP2 are recruited to the nascent hTR. (**e**) GAR1 displaces NAF1 from the pre-H/ACA RNP complex. (**f**) The mature hTR translocate to the nucleolus where it assembles with hTERT which **(g)** was previously processed by chaperones including reptin/pontin and (**h**) recruited to the nucleolus to form a mature telomerase complex while bound to fibrillarin and nucleolin with the hTR. (**i**) The mature telomerase is transported to the Cajal body mediated by TCAB1 binding to the CAB box of the hTR; (**j**) Telomerase recruitment to telomeres is facilitated by the Cajal body movement to telomeres in S-phase. (MacNeil, D. Bensoussan, H. and Autexier, C. 2016. Genes. MDPI) reprinted with permission from MDPI.

e. hTR assembly to the H/ACA proteins

A closer look at the assembly of hTR with these core proteins at the H/ACA motif reveals a similar interaction to the one observed in the other H/ACA RNPs (Figure 4). Two **full complexes** bind to the hTR, one at each hairpin[45]. Dyskerin and NOP10 interact with hTR while GAR1 and NHP2 are recruited through protein–protein interactions to dyskerin and NOP10, respectively[46,47] (Figure 4d). Although hTR contains a canonical H/ACA motif, it differs from typical human H/ACA sno/scaRNAs as it has not been reported to be involved in pseudouridylation or any RNA post-transcriptional modification activities[47,48]. The role of its 3' H/ACA motif seems to be focused on the regulation of its biological stability and function with respect to telomerase. While the structure of the mature RNP has been accurately described, there are unanswered questions regarding the process of its assembly. One important question is whether all the ribonucleoprotein components assemble as a tetrameric complex prior to being recruited to the RNA or if they assemble with one another while associating with a nascent RNA. The core complex formation is necessary for hTR stability and accumulation *in vivo*[31,49]. The point at which GAR1 interacts with the other core components also remains somewhat of a mystery in the assembly process of the mature H/ACA RNP. While Dyskerin-NOP10-NHP2 colocalize at the site of hTR transcription, GAR1 does not[50]. Therefore, GAR1 must join the complex later to form the mature H/ACA RNP (Figure 4e). The complex preceding GAR1 association is known as the pre-H/ACA RNP and includes the association factor nuclear assembly factor 1 (NAF1). NAF1 cannot bind hTR without the presence of the dyskerin-NOP10-NHP2 trimer[51]. Concordantly, this small protein is essential to the assembly of the pre-H/ACA RNP complex and is not present in the mature H/ACA RNP complex[50,52,53]. From their findings in 2006, Darzacq *et al.* proposed a stepwise RNP assembly model where NAF1 binds to dyskerin in the cytoplasm to stabilize the protein, allowing for the recruitment of the other components (NOP10 and NHP2). Furthermore, NHP2 can only associate

with the pre-H/ACA RNP tetramer in the presence of NOP10. Therefore, NOP10-NHP2 likely bind to dyskerin as a heterodimer. Then, NAF1 can act as a nuclear shuttle, bringing an inactive precursor complex to the nascent hTR to form the pre-H/ACA RNP complex (Figure 4d). Most recently, mutations in the gene encoding NAF1 were identified in pulmonary fibrosis-emphysema patients, causing decreased telomerase RNA accumulation and telomere shortening[54]. While these mutations also affect levels of other H/ACA RNAs, no rRNA pseudouridylation defects or ribosomal pathology is observed in first generation mice with these mutations. These data implicate NAF1 haploinsufficiency specifically in telomere maintenance syndromes and is consistent with an important role for NAF1 in telomerase H/ACA RNP assembly and hTR stability[54]. The above model has however been revisited with the identification of a novel nuclear assembly factor, the protein SHQ1 homolog (SHQ1)[55,56]. SHQ1 co-immunoprecipitates with free dyskerin in the nucleus (Figure 4b) but does not associate with dyskerin when dyskerin is assembled in an H/ACA RNP complex. Moreover, SHQ1 has never been found to simultaneously interact with dyskerin bound to NAF1 (Figure 4c & d)[56]. Grozdanov *et al*. show that SHQ1-binding domain mutants of dyskerin are associated with lower levels of dyskerin and hTR instability[57]. Moreover, SHQ1 mimics RNA-interaction patterns and compete with binding of RNAs to dyskerin[58,59]. Its RNA mimicking function may indicate that it would be dislodged from dyskerin by the RNA component as they compete for the dyskerin RNA binding site. Additionally, endogenous SHQ1 localizes in the cytoplasm and nucleoplasm but is excluded from the nucleoli and the GAR1-rich CB (Figure 4a-c)[56]. This heat shock-like chaperone seems to play a major role in the regulation of free dyskerin levels, protecting the protein from degradation through transient interactions prior to the H/ACA pre-RNP assembly (Figure 4a-d). Finally, two ATPases associated with diverse cellular activities (AAA+ ATPases) pontin and reptin are key elements in the formation and function of a mature H/ACA RNP complex. These two AAA+ ATPases are part of

many transcriptional regulation and chromatin remodeling complexes, and contribute to cellular growth regulation and DNA damage repair[60]. Venteicher *et al.* conducted the first research linking pontin and reptin to the assembly and function of the mature telomerase holoenzyme, showing that the complex not only binds directly to hTERT (Figure 4g) but also to hTR and dyskerin *in vitro* (Figure 4b & d). Additionally, they demonstrated that the assembly and stabilization of the mature RNP is ATP-dependent and cell cycle regulated with a peak of the AAA+ ATPases recruitment in S phase[61]. Further experiments uncovered that SHQ1 removal favors the formation of the pre-RNP complex in a reptin/pontin dependent manner (Figure 4b & c)[60]. All these findings support a stepwise-regulated assembly of the H/ACA RNPs in the nucleolus starting with SHQ1-bound dyskerin shuttling to the nucleoplasm where SHQ1 is displaced by an RNA–dyskerin interaction prior to dyskerin's assembly with NAF1, NOP10, and NHP2 (Figure 4).

f. hTERT, the reverse transcriptase unit

hTERT contains three main domains: the 3' overhang DNA binding domain TERT essential N-terminal (TEN), the telomerase RNA-binding domain (TRBD) localized in the N-terminal extension and the conserved reverse transcriptase domain[62,63]. TERT was first shown to have reverse transcriptase activity *in vivo* by Lingner *et al.* (1997) in Euplotes before it was most specificially shown for hTERT by Nakamura *et al.* (1997)[64,65]. After purifying telomerase from the ciliated protozoan *Euplotes aediculatus*, the cloning and sequencing of the gene encoding p123 (*E. aediculatus* TERT*)* revealed sequences encoding conserved reverse transcriptase motifs situated in the center of the protein also present in the yeast TERT, Est2[64]. While these seven motifs are conserved in all reverse transcriptases, the TERT reverse transcriptase region is also characterized by a unique insertion between two of these motifs named A and B'. The N-terminal side motifs were grouped as the "fingers" while the C-terminal side motifs were termed "palm"

and the insertion was named the "Insertion in Fingers" Domain (IFD). This domain is important for telomerase processivity and recruitment to telomeres[62,66-68]. The structure of the TRBD was discovered in *Tetrahymena* using crystallography and revealed an asymmetric binding of lobes creating an RNA-binding pocket[63,69]. Finally, the TEN domain structure of the *Tetrahymena* was characterized with crystallography and was shown to bind single stranded DNA as well as weakly interacting with RNA[70,71].

g. Localization to Cajal Bodies

After its assembly into a pre-H/ACA RNP complex and following processing in the nucleolus (Figure 4f & h), hTR localizes to the CB where it is found as a mature H/ACA RNP complex bound to GAR1 (Figure 4i)[42,72]. An experiment following dyskerin expression in a time-dependent manner confirms its initial accumulation in the nucleolus and subsequent localization to the coiled bodies[73]. With respect to human telomerase, a better understanding of this trafficking mechanism accompanied the discovery of the CAB box contained in the 3' hairpin of the hTR H/ACA motif, which is a CB-specific localization sequence[74]. As previously mentioned, TCAB1 was identified to bind to the CAB box in scaRNAs and bring them to the CBs[75]. It was later shown that this protein also recruits telomerase to the CBs (Figure 4i)[32,43]. In human cells, mutations in the CAB box sequence prevent TCAB1 from binding to the hTR and impair its recruitment to the CBs[76]. Inversely, depletion of TCAB1 leads to a G1 cell cycle arrest and prevents the recruitment of telomerase to telomeres[77]. Therefore, this protein acts as a scaffold for the mature hTR-H/ACA RNP to localize to the CBs. As additional proof, CBs have been reported to colocalize with telomeres during S phase when telomerase is functional[43]. However, the biological role of this recruitment remains unclear as recent studies have shown that these subnuclear bodies are not essential for telomerase activity *in vivo* in human and mouse cells[34,78,79]. In coilin-depleted human

cells, hTR assembly with hTERT is not affected and the telomerase holoenzyme remains functional[76,78] (Figure 4j). Although hTR is expressed and can assemble into an active telomerase complex with the other components, the ability of the telomerase holoenzyme to repeatedly translocate and synthesize telomeric DNA, a process known as repeat addition processivity is reduced in the absence of CBs[76]. It was recently shown that the CB-core protein coilin associates with a NAF1-free dyskerin in an hTR-dependent manner and that coilin expression decreases dyskerin/hTR assembly, acting as an inhibitor of telomerase assembly or activator of its disassembly[80]. On the other hand, in human cell lines, the overexpression of telomerase components was shown to promote efficient recruitment of the enzyme to telomeres in the absence of CBs[81]. These results suggest that recruitment of the mature complex to CBs facilitates telomere encounters by the telomerase holoenzyme under normal biological conditions, but when telomerase is no longer limiting, these organelles can be bypassed by functional telomerase complexes. Interestingly, the hTRmin previously described and engineered by Vogan *et al.* allowing H/ACA independent accumulation of hTR in human cells shows no defects in telomerase activity and telomere length homeostasis with hTERT overexpression upon knockout of either TCAB1 or coilin[44]. As telomerase is found in low levels in normal human cells, localization to the telomeres likely requires chaperoning mechanisms such as CB accumulation[78,81].

h. Cell cycle dependent assembly and localization

CBs are mobile structures, and therefore have the capacity to move the associated telomerase holoenzyme to its target when needed[82]. This movement is proven to be cell-cycle dependent with a two-fold increase of hTR localization at the telomeres and CBs during S phase[83,84]. However, Vogan *et al.* recently showed that general hTR levels and telomerase assembly remain constant

throughout cell cycle progression. In fact, TCAB1 association to the CAB box of hTR seems to be the telomerase maturation step that is regulated by the cell-cycle. Association of TCAB1 to hTR peaks in S phase and is diminished in G2/M. Therefore, the role of TCAB1 may not only be to regulate the trafficking of telomerase to the CBs, but also to modulate access of active telomerase to the telomeres[85]. Observing the cell-cycle regulation of the mature complex provides insights on the stepwise assembly of the pre-RNP complex to the telomerase catalytic subunit hTERT. Tomlinson *et al.* showed that hTR accumulates first at the CBs in G1 and beginning of S phase, unassociated to hTERT. hTR and hTERT are only found to colocalize in S phase, suggesting that hTERT assembles with hTR once at the CBs, at which point the telomerase holoenzyme becomes mature and active[84]. Interactions of TCAB1 with dyskerin, hTR, and hTERT have also been previously reported, providing additional evidence that the mature telomerase holoenzyme is assembled once located at the CBs[43]. In further studies, the same group demonstrated that hTERT is essential for hTR localization to the CBs during S phase in cancer cell lines. These two findings seem contradictory as the second implies that hTR association to hTERT is essential for its recruitment to CBs. The maturation pathway is partially clarified by Lee *et al.* who reported that hTERT associates with the pre-H/ACA RNP in the fibrillar component of the nucleolus while bound to nucleolin, a nuclear protein involved in RNA biogenesis[86,87]. This step occurs prior to the recruitment of the mature telomerase to the CBs by TCAB1 where the telomerase holoenzyme becomes catalytically active[87] (Figure 4g–i).

i. Recruitment activity

Telomerase recruitment and activity are tightly regulated by multiple processes and interactions. One of them is the shelterin protein TPP1, which contains a glutamine and leucine rich patch (TEL-patch) in its OB domain. The function of the TEL-patch involves hTERT recruitment and

translocation on the telomere that is being elongated[88,89]. Further study of this recruitment shows the TEL-patch to interact with the hTERT TEN domain[89]. Furthermore, the IFD was recently characterized to foster recruitment of hTERT to the telomere in a TPP1 dependent manner[66,67,90]. Several hTERT variants in the IFD were examined for effects on telomerase activity and telomere recruitment[66,67,90]. Defects in telomere binding are observed for several of these IFD variants and could be rescued by TPP1 overexpression for some of them[66,67]. It was speculated that these recruitment defects may be mediated through conformational changes of the TEN domain, supported by the proximity of the IFD to the TEN domain in recent Cryo-Electron Microscopy (Cryo-EM) mapping of the *Tetrahymena thermophile* TERT[91].

Many other factors other than the shelterin components are involved in telomerase recruitment and activity regulation. For instance, the TRF1 interacting telomerase inhibitor 1 (PinX1) which mediates telomerase recruitment and localization through interaction with hTERT leads to a decrease in hTERT at the telomeres when silenced in HeLa cells[92]. It was also recently reported that for hTERT to be effectively recruited to the telomeres in S phase, TRF1 must vacate the telomere in an ataxia telangiectasia and Rad3-related protein (ATR) / ataxia telangiectasia mutated protein (ATM) dependent manner[93]. TRF1 dissociation from the telomere may be caused by its phosphorylation by ATM, which causes proteasomal TRF1 degradation[94]. Dissociation of TRF1 would also release the 3' telomeric overhang from a protective structure and allow telomere elongation by telomerase. This model is supported by another report of ATM-dependent telomerase recruitment in both mice and humans cells where ATM inhibition is shown to stall telomere elongation while its activation enhances it[95]. Finally, the trimeric complex made of the conserved telomere maintenance component 1 (CTC1), the suppressor of Cdc thirteen (STN1) and the telomeric pathways with Stn1 (TEN1) known as the CST complex is also involved in telomerase regulation with a dual role. Extensive studies conducted in its yeast ortholog show that

the CST complex can recruit the telomerase enzyme to the G-rich overhang in the first step allowing extension of the G-rich overhang[96]. Through another domain, it is then capable of recruiting the necessary machinery to fill-in the C-rich strand leading to the inhibition of telomerase and detachment from the telomeres. Later, CST has been reported to inhibit telomerase activity in in a POT1 dependent manner in human cell lines[97]. Mutated versions of POT1 are unable to negatively regulate telomerase, causing defects in telomere processing and leading to unstable extended 3' overhangs due to CST depletion at the telomere and uncontrolled telomere elongation. Overall, the numerous proteins involved in telomerase regulation highlight the importance of a tight regulation of this enzyme which can also be observed through the consequences arising following their defects.

3) Telomere and telomerase in disease

a. Cancer

While telomerase expression is restricted to highly proliferative stem cells and germline cells, it is found to be expressed in 85% of cancer cells. More specifically, the expression of hTERT in these cells confers them with unlimited dividing capacity as hTERT expression is the limiting factor for telomerase activity in somatic cells[98]. The *hTERT* promoter possesses many transcription factor binding domains revealing a tight control of the promoter [98]. This regulation is necessary as hTERT needs to be silenced in somatic cells and expressed in others for cellular immortalization such as in stem and progenitor cells. In cancer, mutations are often found in the *TERT* promoter leading to increased transcription of the gene and translation of the protein[99-101]. Interestingly, most of these malignant cells still display short telomeres[102-104]. Therefore, telomerase activity must arise after the critical shortening of telomere. These cells can usually bypass the Hayflick limit and therefore replicative senescence. This step is known as crisis and is usually due to the impaired activation

of DNA damage checkpoints such as p53 and the retinoblastoma protein[105] (Figure 1d). p53 mutations are one of the most common forms of deficiencies leading to cancer[106]. Once the cell enters crisis, the telomeres are so short that genomic integrity is lost and chromosomal ends start to fuse between sister chromatids as well as between different chromosomes, a process known as telomere fusions. This recombination leads to genomic instability and drives the expression of hTERT hence the assembly and activity of telomerase. This process allows the escape of cell death and the immortalization of the cell which can now sustain its telomeres indefinitely.

b. Premature aging diseases, Dyskeratosis Congenita

Dyskeratosis Congenita (DC) is a rare premature aging disease that touches 1 in a million people. Patients are diagnosed at approximately age 10 and display physical symptoms such as nail dystrophy, leukoplakia and abnormal skin pigmentation. In most cases, the patients die prematurely due to deficiencies in highly replicative tissues leading to stem cell depletion and bone marrow failure at around 40-50 years old[107]. DC was originally discovered in the 1900s in the X-linked recessive form, arising from a mutation in the *DKC1* gene in distal Xq28 which encodes dyskerin[108]. It was initially hypothesized that the disease was caused by defects in ribosome maturation as dyskerin was mainly known as a pseudouridine synthase required for rRNA maturation and ribosome assembly until Mitchell *et al.* linked DC to telomerase defects. They found that DC patients have low levels of hTR and reduced telomerase activity as well as telomere length below average[109]. Nowadays, other forms of the disease have been identified such as autosomal recessive and autosomal dominant forms caused by mutations in NOP10 and NHP2 or in the telomerase components hTERT and hTR respectively[51,110,111]. The mutations in hTR are localized either in the pseudoknot, impairing telomerase activity, or at the 3' end impairing its association with the H/ACA scaffold proteins and therefore its stability and localization. Some of

these mutations are localized in the H/ACA box[112]. Mutating the CAB box impairs hTR localization to the CB, exemplified by the C408G mutant hTR identified in autosomal DC patients[34,113]. Other hTR mutations located in the CAB box are associated to bone marrow failure syndromes[114]. The direct consequence of these mutations in DC patients is underlined in earlier research where the homozygous knock out of mouse TR displays DC-like phenotypes after a few generations[115]. The clustering of DC-linked mutations in telomerase and telomere associated components underlines the importance of telomere misregulation in DC. Mutations in telomere-associated components as well as dyskerin have also been linked to other premature aging diseases such as Hoyeraal-Hreidarsson, a severe form of DC[116]. Furthermore, several studies show DC patients are more prone to developing cancer than healthy individuals[117,118]. The role and regulation of telomerase and its components, such as dyskerin are therefore essential for a better understanding of how it is implicated in aging and cancer and to translationally apply this knowledge to the development of therapeutic strategies.

II. Dyskerin

Dyskerin is an evolutionary conserved nucleolar protein of 58 kilodaltons (kDa). It was found in humans following the identification of mutations in the *DKC1* gene in DC patients. However, other members of this family in other species had already been identified.

1) Dyskerin orthologs

The first dyskerin ortholog was found in yeast (Cbf5) where it was shown to have affinity for centromere DNA as well as a microtubule binding site such that deletion of this site would cause cell cycle arrest[119]. A few years later, Cbf5 was found to be involved in rRNA biogenesis which explains the cell cycle arrest caused by dyskerin mutations leading to reduced ribosomal synthesis. Additional orthologs were identified over the years such as in the rat (NAP57)[120], as well as in *Drosophila* (Nop60B)[121] and *Arabidopsis* (AtNAP57)[122] showing an important evolutionary

conservation of the protein across species and highlighting its multiple key functions in regulating cellular processes. More strikingly, deletion of these homologs is lethal for the organism[123,124].

2) Human dyskerin discovery

It was in 1998 that the human *DKC1* gene was fully cloned and identified as a member of this family following the discovery of multiple missense mutations in this gene[108]. The peptide analysis showed dyskerin to be a lysine-rich hydrophilic protein containing putative nuclear localization sequences and Nucleolar Localization Sequences (NoLS), phosphorylation sites as well as a specific pseudouridine synthase and archaeosine transglycosylase (PUA) domain which is a conserved RNA-binding sequence[125]. Finally, a TruB homologous sequence was identified, a conserved sequence important for RNA pseudouridylation, an essential post-transcriptional process leading to the isomerization of uridine nucleosides into pseudouridines which is guided by small non-coding RNAs[28]. Additional research proved dyskerin localizes to the nucleoplasm first then accumulates in the nucleolus. It also associates with CB but not if its NoLS is interrupted[73]. These experiments proved in parallel that some DC mutations were not causing dyskerin mislocalization and that the phenotype may therefore arise from a loss of function. It is now clear that this protein family plays many roles in cellular maintenance and mainly as a core component of H/ACA ribonucleoprotein including three other scaffold proteins previously described.

3) Dyskerin roles

The importance of dyskerin in regulating cellular pathways is highlighted through the dramatic phenotype observed in DC patients. As discussed previously, dyskerin is a key H/ACA protein. Both snoRNAs and scaRNAs bind the PUA domain of dyskerin to target/direct dyskerin-mediated pseudouridylation[126-128]. Loss of dyskerin results in a significant reduction of H/ACA snoRNAs[129] and reduction in hTR[130] as dyskerin binding is important for their stability. The impact on scaRNAs remains to be studied but we could predict the same effect. While its role associated

to H/ACA RNAs, RNA maturation and hTR stability have been covered, the pseudouridine synthase has also been associated to other cellular mechanisms such as mitosis and DNA damage.

a. Dyskerin and cellular proliferation

A study conducted by Alawi *et al.* showed a mitotic specific role for dyskerin where dyskerin levels are increased in G2/M and loss of dyskerin activates a mitotic spindle-assembly checkpoint and cell cycle arrest[131]. These findings agree with a previous publication from this group implicating a role for dyskerin in cell growth that is independent of p53 and telomerase by depleting telomerase negative cells of dyskerin[129]. These dyskerin depleted cells displayed abnormal morphology, cell cycle arrest and multi-polar mitotic spindles.

b. Dyskerin and DNA damage

Dyskerin depletion is correlated to increased DNA damage. In mutant dyskerin mouse embryo fibroblasts (MEFs), an increase in γH2Ax foci, marker of double stranded breaks (DSBs) is observed compared to wild type MEFs with 10-15% localized to telomeres. Moreover, these dyskerin deficient MEFs are more susceptible to treatment with the DNA damaging chemotherapeutic drug etoposide and display a significant increase in γH2Ax foci, as well as γH2Ax protein levels. The downstream activators of the DDR were also highly increased in mutant cells compared to wild type cells suggesting that dyskerin mutant MEFs are hypersensitive to DNA damage. Interestingly, they presented that the DDR activation is independent of telomere length[132]. As mentioned, DC is also linked to mutations in the genes *hTR* and *hTERT* as well as in genes encoding the other H/ACA scaffold proteins, *NHP2, NOP10*, and even in genes encoding shelterin proteins such as *TINF2* encoding the shelterin protein TIN2. The phenotypes observed with each mutation can vary. For example, mutations in *hTR* and *hTERT* require many generations for an

intense phenotype to manifest while patients with either *DKC1* or *TINF2* mutations display severe phenotypes from the first generation. The similar phenotypes observed with mutations in dyskerin and TIN2 might hint at a common role that is not fully understood between the two proteins. Similar to cells from dyskerin-deficient patients, *TINF2*-related DC cells present an increased DDR[133]. The same way that hTERT was shown to have a function on cell growth independent of its role in telomerase[134], dyskerin could be involved in another cellular process such as the DDR. An extensive study on the effect of different chemical stresses on the subunits of H/ACA RNPs showed that their expression is not regulated the same way following each type of treatment. This suggest that they might play different roles upon DNA damage[135]. Overall, dyskerin is most often downregulated following DNA damage inducing treatments. Finally, dyskerin was shown to associate with the single-strand-selective monofunctional uracil-DNA glycosylase 1 (SMUG1) which is involved in DNA repair[136]. The study was mainly focused on presenting the role of SMUG1 in rRNA processing but it would be interesting to study the impact of this interaction on DNA damage.

c. Dyskerin in cancer

The first general link between dyskerin and cancer was observed in DC patients who have increased susceptibility to developing malignancies[117]. The susceptibility is linked to the extreme shortening of telomeres in DC cells. As telomeres shorten, the cell eventually reaches the Hayflick limit and must go through replicative senescence. However, multiple studies have shown that p53 expression in dyskerin deficient mouse cells is impaired due to poor mRNA translation due to failed ribosome biogenesis[137]. To date less evidence linking defects in dyskerin and altered ribosome biogenesis has been reported[138]. While p53 mRNA levels are not affected, one study showed that recruitment of p53 mRNA to the polysomal fractions is decreased resulting in

decreased p53 protein levels. The same was reported for p53's downstream target, p27. The translation of this downstream tumor suppressor in *DKC1* mutant mice as well as in pituitary tumor samples with the dyskerin mutation S485G was shown to be significantly reduced [137,139]. These misregulations lead to a deficient DNA damage checkpoint when these cells pass the Hayflick limit which increases the chances of cancer[118]. A different study has however shown that downregulation of dyskerin has no effects on p53 expression[129]. After these studies, a growing interest in understanding the levels and role of dyskerin in tumors arose. Montanero *et al.* conducted the first study looking at expression and function of dyskerin in human lung, breast and colon carcinomas[140]. The analysis of dyskerin mRNA levels shows that dyskerin levels vary greatly between different cancer types with some having low levels of dyskerin mRNA. Additionally, they looked at rRNA pseudouridylation and found that it is positively correlated to dyskerin mRNA levels. Lower levels seem to increase neoplastic transformation suggesting dyskerin could act as a tumor suppressor[118,140]. Low dyskerin levels are however associated to reduced telomerase activity and they showed that breast tumors with lower dyskerin levels were associated with better prognosis. On the other hand, wild type dyskerin is often found to be upregulated in cancer cell lines. While some studies show that this upregulation mainly drives increased cell proliferation and protein biosynthesis in breast cancer and prostate cancer [140,141], others associate the increased dyskerin protein level to increased telomerase activity resulting from increased levels of hTR. One study in neuroblastoma patient samples looked at enriched cluster of genes and identified snoRNA RNP-associated genes with *DKC1* being at the top of the list. They saw a correlation between the expression of the telomerase complex and tumor survival and concluded that this increase in snoRNA RNPs in neuroblastoma causes elevated telomerase activity[142].

4) Post-translational modification

Although extensive research has been conducted on the various functions of dyskerin in the regulation of cellular mechanisms, very little is known about the mechanisms regulating dyskerin in all those functions. One would expect such a dynamic protein to be highly post-translationally modified. Post-translational modifications (PTMs) are one of the most common modifications involved in protein regulation. These include phosphorylation, ubiquitination as well as SUMOylation. Evidence for PTMs in dyskerin was proposed when higher molecular weight species of the protein were observed after SDS-PAGE and Western blotting[143]. Dyskerin has been predicted to be phosphorylated at multiple sites (Ser21, Ser387, Ser451, Ser453, Ser 455, Thr 458, Ser 485, Ser494, Ser 513) (Uniprot ID O60832) [110]. Furthermore, dyskerin was identified as a target for ubiquitination on K39 in a large scale study of the ubiquitin-modified proteome[144]. More direct proof of dyskerin PTMs was provided in a large-scale proteomics study using multidimensional liquid chromatography-tandem mass spectrometry to identify SUMO targets induced by oxidative stress where dyskerin was identified as a hit protein[145-147]. Confirmation of dyskerin SUMOylation was published in 2013 where Brault *et al.* showed that the lysine- rich dyskerin possesses multiple sites that are post-translationally modified, both *in vitro* and *in vivo* in consensus motifs known as SUMOylation sites which are modified by small ubiquitin-like modifers (SUMOs)[130]. Several of the reported dyskerin SUMOylation sites were subsequently confirmed by mass spectrometry (MS)[148]. Overexpression of SUMO1 or SUMO2 led to higher molecular weight dyskerin species which was inhibited when SUMOylation essential proteins, such as the E2 conjugating enzyme Ubc9 were not added *in vitro*[130]. Using cycloheximide to inhibit protein synthesis, Brault *et al.* showed that dyskerin SUMOylation stabilizes the protein. Furthermore, they found that X-linked DC causing mutations located in these SUMOylation sites were linked to decreased hTR levels and impairment in telomere maintenance.

III. SUMOylation

SUMOylation is one of the most recent lysine-specific post-translational modifications discovered and it covalently binds SUMOs to a lysine residue located in consensus sequences. SUMO was first identified in yeast as a Suppressor of Mif2 (Smt) activity and suppressor of cell death in another study where it was named Smt3 and sentrin respectively[149,150]. This modification is highly conserved from yeast to humans including invertebrates such as *C. elegans* and *Drosophila* as well as plants. Studies in each of these systems show SUMOylation to resemble closely the ubiquitination pathway while acting in more various ways such as the modification of protein-protein interactions, protein localization, protein activity and protein stability.

1) Dynamic post-translational modifiers

SUMOs are small 15kDa proteins containing a Gly-Gly motif allowing them to form an isopeptide bond with a lysine residue. This residue needs to be present in a specific sequence known as a SUMOylation consensus motif ΨKXD/E where Ψ is a hydrophobic residue, K is the modified lysine residue, X is any amino acid and D/E is an acidic residue. Although this motif was the first discovered and most conserved, variants have been identified since such as the inverted D/EXKΨ, the negatively charged amino-acid-dependent SUMOylation motifs or even non-conserved motifs[151-155]. The SUMO family in humans includes four isoforms, SUMO 1 to 4 (Table 1). SUMO 2 and 3 share 97% homology and are therefore grouped in the same category when studied as no structural nor functional difference between the two has yet been observed. Each possess a consensus lysine residue allowing a SUMO partner to bind covalently to it and hence the formation of SUMO2/3 chains/branches on the protein[156]. SUMO1 shares 50% homology with SUMO2/3 and lacks the additional branching site making it impossible for this isoform to form branches[157]. It is therefore found at mono-SUMOylated target sites or capping SUMO2/3 branches[158]. SUMO4 shares 87% homology with SUMO2. It is expressed in the kidney, lymph nodes and spleen whereas

the other homologs are ubiquitously expressed. The SUMO4 gene does not contain any introns and is therefore believed to be a pseudogene[159]. Its role has not been well characterized but it has been associated with the modification of the nuclear factor kappa B inhibitor alpha (IκBα)[160-162]. However this modification may not be similar to SUMOylation as its active site cannot be matured *in vivo*[163]. Recently, a new poly-SUMO isoform was discovered by Liang *et al.* which is mainly involved in the modification of promyelocytic leukemia proteins (PML), the unit of PML nuclear bodies involved in the regulation of multiple cellular processes such as transcription, DNA repair and senescence[164,165]. A large pool of free SUMOs is readily available in a cell as these small proteins are involved in the regulation of many cellular processes. This pool mainly consists of SUMO2/3 suggesting that the formation of branches is the most transient form of SUMOylation and can be further stabilized by SUMO1[158]. This process is highly dynamic as these small proteins are removed efficiently by SUMO/sentrin specific proteases (SENPs) making SUMOylation a very transient process with steady-state levels of SUMOylated proteins being typically <5%[166,167].

2) SUMOylation cycle

Although divergent in their functions, SUMOs and ubiquitin go through a very similar activation and binding cycle (Figure 5). The SUMOylation cycle involves multiple players to allow for a dynamic and transient modification, some being conserved for all targets while others display high specificity for targets.

Type	Location	Covalent binding	Branching	Free SUMO
SUMO 1	Nucleus	++	No	+
SUMO 2/3	Nucleus	+++	Yes	+++
SUMO 4	Cytoplasm	-	Unknown	Unknown

Table 1. Four SUMO isoforms in humans display different properties

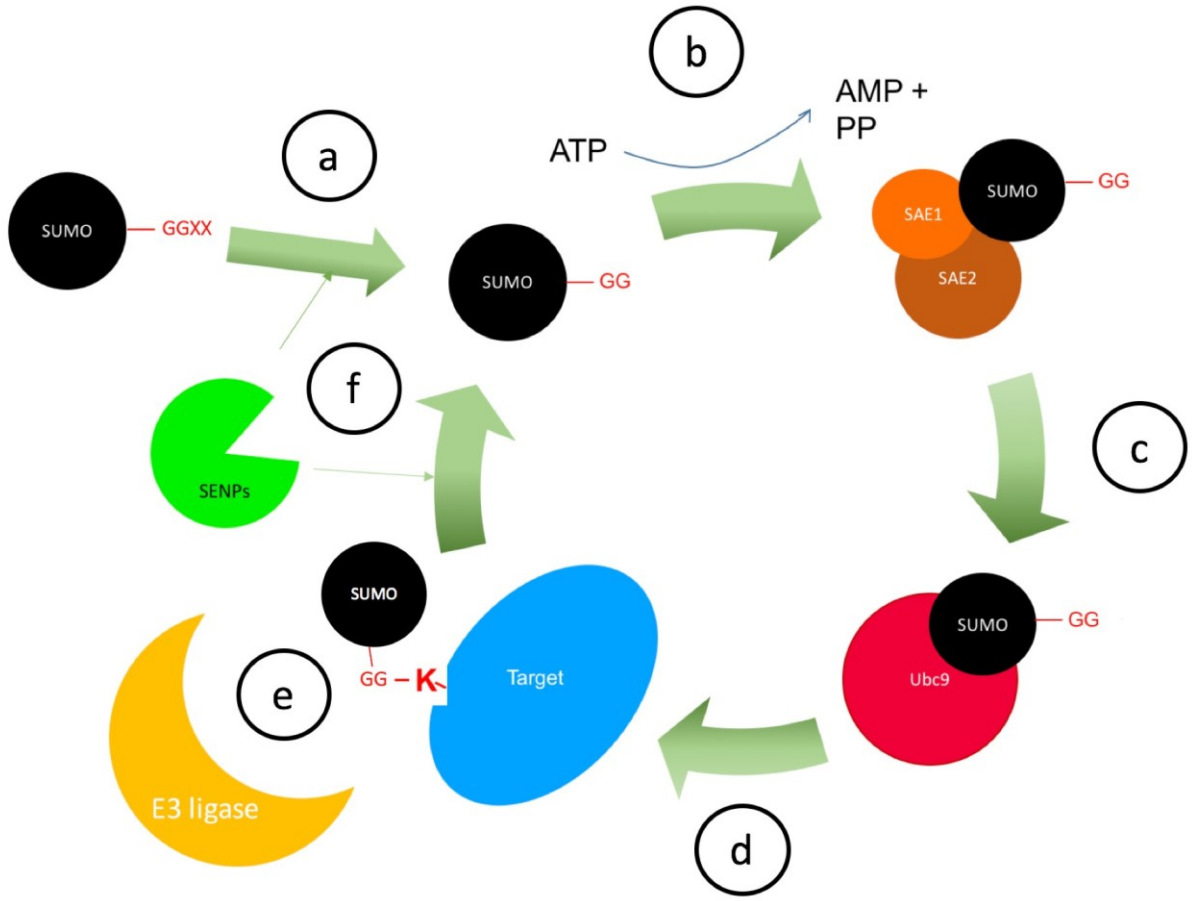

Figure 5. Schematic of the SUMOylation cycle. (a) The SUMO active motif (SUMO-GG) is generated by the cleavage of its C-terminal sequence. (b) SUMO is activated by the SAE1/2 activating enzyme which (c) transfers it to the Ubc9 conjugating enzyme. (d) Ubc9 transfers the

SUMO to its target protein, (e) facilitated in vivo by a SUMO E3 ligase. (f) The cycle is completed with the removal of SUMO by SENPs.

a. SAE1/2, the SUMO E1 activating enzyme

Once its Gly-Gly motif is exposed following SENP-dependent cleavage of its immature C-terminal sequence (Figure 5a), SUMO is ready to be conjugated to a target protein. The first step of this process starts with its binding to the E1 activating enzyme (Figure 5b), a heterodimer known as SUMO activating enzyme 1 and 2 (SAE1/2) conserved for all SUMOylation events and across species [156,168,169]. The SAE1 is 38kDa and homologous to the yeast Uba2p while SAE2 is a 72kDa protein homologous to the yeast Aos1p, where Uba2p and Aos1 are two subunits of the heterodimer Stm3p activating enzyme in yeast[169]. Analysis of the complex showed that the binding of the two subunits leads to the formation of an optimal binding site for SUMO. This complex is homologous to the ubiquitin E1 activating enzyme and acts in an ATP-dependent manner to create a thioester bond with the C-terminus of free SUMO proteins to recruit SUMO to the E2 conjugating enzyme[168].

b. Ubc9, the SUMO E2 conjugating enzyme

After its activation by SAE1/2, the SUMO protein is transferred to an E2 conjugating enzyme known as the Ubiquitin Conjugating enzyme 9 (Ubc9) (Figure 5c). Ubc9 binds to the SAE1/2-SUMO complex for a transesterification reaction where the thioester bond between the activating enzyme and SUMO is transferred to a cysteine residue on Ubc9, Cys93. This enzyme shares an evolutionary conserved sequence of about 140 amino acids with other E2 conjugating enzymes forming a conserved tertiary structure. However, Ubc9 contains an insertion of two critical residues in this region, Asp100 and Lys101 which are essential for its role in transferring SUMO to its target[170,171] (Figure 5d). Multiple experiments have looked at the effect of knocking down Ubc9: while its depletion in DT40 lymphocyte cells leads to abnormal chromosome segregation and eventually apoptosis, it was found that conditional Ubc9 knock out mice present important

intestinal deficiencies and complete Ubc9 knock out mice is embryonically lethal [172-174]. These results reflect that Ubc9 is essential for SUMOylation which in turn is essential for life. Further studies found that, in most cases, Ubc9 is sufficient *in vitro* for transferring SUMO to its target contrary to the conjugation enzyme for ubiquitination[156]. The two-amino-acid insertion was shown to be capable of binding non-covalently the target protein at its SUMOylation consensus site ΨKXD/E[171]. However, *in vivo* the E2 conjugating enzyme requires help from a third player, the E3 ligase, involved in the SUMOylation cycle.

c. The SUMO E3 ligase

While not always necessary *in vitro*, the E3 ligase plays a critical role *in vivo* and is required to facilitate the binding of SUMO to its target[175] (Figure 5e). Contrary to Ubc9 and like ubiquitin E3 ligases, E3 ligases are specific to their substrates and a few have already been identified such as the members of the protein inhibitor of activated Stat (PIAS) family[176], Topors[177], the Ran binding protein 2[178,179] and others[175]. However, while hundreds of these enzyme family members are characterized for ubiquitination, only a dozen are known for SUMOylation. One common characteristic in SUMO E3 ligases is the SUMO interacting motif (SIM). This motif consists of a hydrophobic sequence juxtaposed to acidic residues allowing a non-covalent interaction with SUMO[180]. Further studies uncovered a specific sequence in the hydrophobic patch, V/I-X-V/I-V/I, conserved in each SIM and necessary for SUMO binding[181]. Crystallography studies showed that the organization and variations in these hydrophobic and acidic clusters allows for preferences in binding orientation and SUMO isoform specificity[182-184]. Another characteristic found in E3 ligases in general is known as the really interesting new gene (RING) finger domain[185]. This domain takes the shape of a platform allowing for docking of the E2 conjugating enzyme and

therefore facilitates the transfer of SUMO or ubiquitin to its target. This motif is found in most of the E3 ligases including SUMO E3 ligases (PIAS, Topors).

d. SUMO/Sentrin Specific Proteases

The SENP family initiates and terminates the SUMOylation cycle starting with the maturation of the SUMO by exposing its Gly-Gly motif and ending with its removal from the target protein (Figure 5a and f). SUMO is expressed as a pro-protein and requires further modification to reveal its active Gly-Gly motif and bind to its target, then needs to be cleaved from its targets efficiently. SENPs are therefore responsible for the dynamic and transient nature of the SUMOylation cycle. Six isoforms in this cysteine protease family are found in humans, SENP1-3 and 5-7 and their function is conserved across species: two isoforms are found in yeast while eight have been identified in *Arabidopsis*. Each of them differ in their preferences for SUMO isoforms, sub- localizations and functions (Figure 6). Their non-conserved N-terminal domain has been shown to control their distinct subcellular location while their conserved C-terminal catalytic domain is essential for their specificity in SUMO maturation and displays a triad consensus of three amino acids, His-Cys-Asp[186-189]. Studying the SENP1 crystal structure associated to SUMO1, showed that the structure of SENPs includes a "tunnel" formed by a tryptophan residue allowing for the proper positioning of the SUMO scissile peptide bond in a *cis* conformation. This rearrangement allows for a more efficient cleavage and exposure of the processed C-terminal Gly-Gly motif[190]. While SUMO binding abilities seem to be constant across isoforms, the specificity is regulated by the SENPs catalysis efficiency. This is due to the C-terminal SUMO sequence at the scissile bond which determines which SENP can process them the most efficiently[187,188,190].

SENP1 is mainly nuclear and accumulates at the nuclear envelope and at nuclear foci which sometimes colocalize with PML nuclear bodies (Figure 6). It has been shown to play a role both in SUMO maturation and deconjugation. While active for all SUMO isoforms, it is more efficient in processing SUMO1 than SUMO2 and SUMO3[190,191]. SENP2 is also involved in both functions although it is more active in deconjugation and more specific to SUMO2 than SUMO1 and SUMO 3[189]. Its cellular localization is similar to that of SENP1 although it cycles between the nucleus and the cytoplasm[192]. SENP3 and 5 are very similar; they localize mainly to the nucleolus and favor SUMO2/3 maturation and processing over SUMO1 (Figure 6)[189,193]. Their localization is highly correlated to the processes they have been implicated in, most specifically rRNA biogenesis but also the mitotic apparatus through the SUMOylation regulation of Borealin, a cell cycle associated protein and spindle assembly[194-198]. Finally, SENP6 and SENP7 are both mainly involved in SUMO chain editing, which is consistent with their specificity for SUMO2 and SUMO3 (Figure 6)[189,199-201]. The editing activity can be attributed to additional loop structures found in both SENP6 and 7 but not in the other isoforms as deletion of these loops shows reduced catalytic activity[199,200]. These SENPs are mainly localized in the nucleoplasm[192]. Therefore, SENPs are essential for regulating SUMO bioavailability.

Subcellular localization specificity

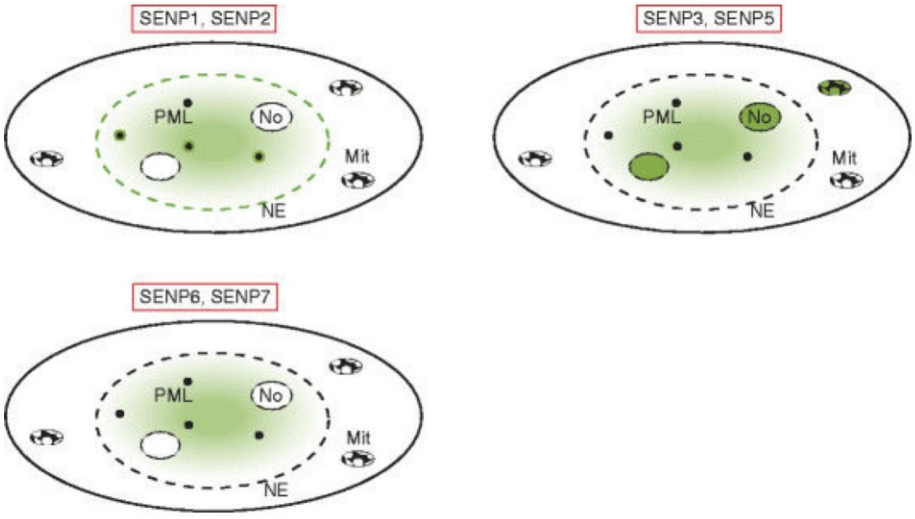

SUMO isoform specificity

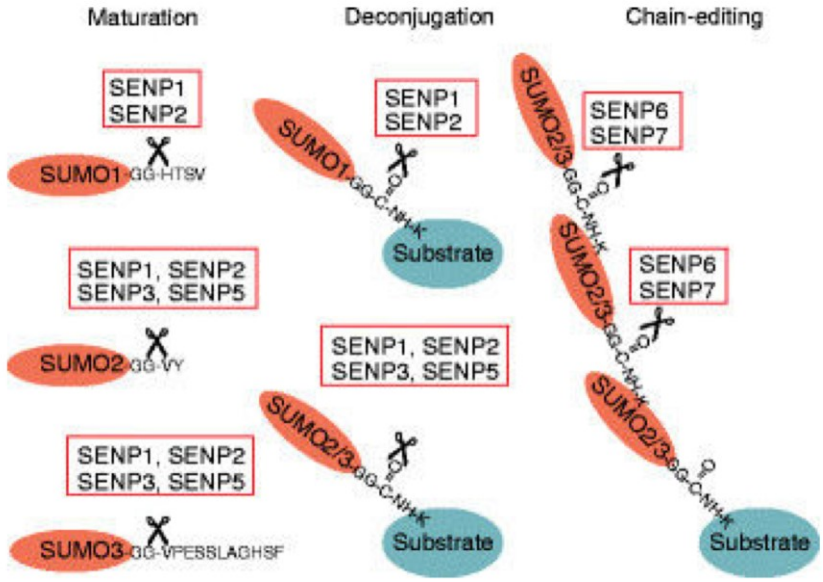

Figure 6. SUMO/Sentrin specific proteases (SENPs) display subcellular localization and SUMO family specificities. SENP1 and 2 are mostly active and concentrated in the nucleoplasm, nuclear envelope and at the PML bodies while SENP 3 and 5 are concentrated in the nucleolus and mitochondria. SENP 6 and 7 are found in the nucleoplasm (top panel). SENP 1-5 have maturation capacity for both SUMO2 and SUMO3. SENP 1 and 2 are more specific to SUMO1, for both maturation and deconjugation. SENP6 and 7 are involved in SUMO2/3 chain editing (bottom panel). (Nayak, A. & Muller, S. 2014. Genome Biology) reprinted with permission from BioMed Central.

3) SUMOylation cellular regulation

As previously described, the SUMOylation cycle resembles the ubiquitination cycle in its cycle. However, the two post-translational modifications diverge in the cellular processes that they regulate. While ubiquitination is mainly restricted to the mediation of protein targeting to the proteasome for degradation, SUMOylation regulates a wide range of functions via the alteration of protein-protein interaction, protein stability, protein activity as well as protein localization[202,203]. Through these mechanism, SUMOylation has been shown to regulate transcription, cell cycle, DNA damage, ubiquitin-mediated degradation, stress response and multiple other cellular pathways[159,175,202,204]. The cell death and embryonic lethality phenotypes resulting from Ubc9 knockdown *in vitro* in DT40 lymphocytes and *in vivo* in knockout mice is consistent with the role of SUMOylation in a wide range of cellular pathways [172,174]

a. Transcription

SUMOylation has been shown in many cases to be associated with transcription regulation. It can be found to work either as a repressor or an activator of transcription. One study showed that the transcription factor c-Myb was modified at its negative regulator domain by SUMO1 at three lysine residues[205]. These residues work in a stepwise manner where the SUMOylation of the first site is necessary for the modification of the other two[205,206]. These modifications increase its proteolytic stability while decreasing its transcriptional activity. Another transcription factor regulated indirectly by SUMOylation is the nuclear factor kappa B (NF-κB). When bound to its inhibitor Iκβα, NF- κβ is kept inactive in the cytoplasm. Degradation of this inhibitor is necessary for NF-κβ to localize to the nucleus and activate transcription. This activation is regulated by SUMOylation of Iκβα in the cytoplasm by both SUMO1 and SUMO4, reducing levels of NF-κβ mediated transcription[160,161,207]. On the other hand, SUMO can also act as a positive regulator of

transcription such as with p53. The transcription factor p53 regulates many cellular processes through promoter binding and transcription upregulation of genes implicated in cell cycle and apoptosis and acts as a tumor suppressor. The protein expression is tightly regulated, kept at low levels in normal conditions and upregulated in response to stress with a rapid turnover as well as actively transported between the cytoplasm and nucleus. This control is regulated both directly and indirectly by SUMOylation. It was shown that p53 is SUMOylated *in vitro* and *in vivo* at K386 in its C-terminus by SUMO1, increasing its binding affinity and transactivation[208,209]. This SUMOylation is mediated by the E3 ligase Mouse double minute 2 (MDM2) as deleting the MDM2 binding domain in p53 abolishes its SUMOylation[210]. This PTM enhances p53 nuclear import. However, recent studies challenge these results showing that p53 SUMOylation reduces its transcriptional activity by enhancing its nuclear export[211]. Further studies showed this site to be modified by SUMO2/3 mediating both activation and repression of p53-targeted genes[212]. Interestingly, this process is also tightly regulated indirectly by SUMO through MDM2 SUMOylation on its K446 residue[209,213]. Moreover, MDM2 has ubiquitination E3 ligase activity. SUMOylation of the E3 ligase prevents its self-ubiquitination at this site and increases MDM2-dependent ubiquitination[214]. Studies showed that MDM2-dependent mono-ubiquitination of p53 controls its export while poly-ubiquitination controls its degradation[215].

b. Relationship with ubiquitin

While involved in many other cellular processes, SUMOylation is still intertwined with ubiquitination[202,203]. It was first found that SUMOylation competes with ubiquitination on lysine residues to protect proteins from degradation and increase their stability. One example is phosducin, a G-protein coupled signal transducer, which is less stable and targeted by ubiquitination when SUMOylation is deficient. It has increased binding affinity to one of its

downstream effector in its SUMOylated state[216]. Some studies report this competition to occur at different lysine residues as the mutation of the SUMOylated lysine residue increases its ubiquitination and protein degradation showing that SUMOylation blocks ubiquitin from binding adjacent lysine residues, increasing the stability of the protein[205,209,216]. In other proteins, SUMO was shown to compete directly at lysine residues that were known to be modified by ubiquitin such as K21 in the transcription factor inhibitor IκBα and K466 in the ubiquitin E3 ligase MDM2 protecting them from degradation and respectively inhibiting NF-κB-mediated transcription and enhancing p53 ubiquitination and degradation[207,214]. After these findings, it was surprising to find that SUMO promotes ubiquitination of some proteins. A proteomic study showed that SUMO2-bound protein enriched lysates are associated to increased amounts of ubiquitin and that treatment with the proteasome inhibitor MG132 leads to increased amounts of SUMO2 conjugated targets[217]. SUMO has also been shown to recruit ubiquitin E3 ligases to induce targeting to the proteasome and degradation of the protein. These ligases are known as SUMO-targeted ubiquitin ligases (STUbLs) and are characterized by the presence of SIMs, like SUMOylation E3 ligases which allows them to be recruited by SUMO branches or chains on a target protein[218]. This hydrophobic domain encounters a hydrophobic cluster in SUMO and the intercalating of the β-strands in each of these domains sets the proper orientation for this transient interaction[219]. While SUMOylation E3 ligases are recruited to promote SUMOylation, STUbLs are recruited to ubiquitinate these targets. They can cap the SUMO chain or bind ubiquitin to a different lysine residue to poly-ubiquitinate the target and direct it to the proteasome[219,220]. The first STUbL discovered was Ulps1 following a special yeast interaction assay known as two-hybrid interaction assay that identified multiple SIM domains in the protein[218,221]. The most studied mammalian STUbLs is RNF4 which regulates degradation of PML proteins. PML associate and aggregate into membrane-less nuclear bodies known as PML bodies. They have been shown to be involved in the DDR, stress

regulation, cell apoptosis and senescence and have a tumor suppressor function[222,223]. PML bodies have been shown to be modified by SUMO1 for proper assembly of the nuclear bodies[224]. However, they are also modified by SUMO2 to recruit the E3 ligase RNF4. This protein is part of the RING domain family of proteins which have been found to often have multiple SIM domains suggesting a possible recruitment by SUMOylation chains for ubiquitination[225]. PML associates with the retinoic-associated receptor alpha which diffuses PML bodies through delocalization of PML[226]. Upon stress induction by treatment of cells with arsenic trioxide (AsO3), this complex is degraded through the SUMOylation-mediated degradation of PML by RNF4-mediated ubiquitination. This process is dependent on the K160 PML residue as its mutation abolishes the recruitment of the 11S proteasome[226]. Immunofluorescence studies show increased PML bodies are formed when using an siRNA against RNF4 as PML is not being degraded[227]. Later, RNF4 was shown to have STUbLs activity on multiple other proteins[228,229]. The ortholog of this STUbL is conserved in *Sacchromyces cerevisiae* as Usl2, the Slx5/Slx8 heterodimer. Multiple SIM domains are located in Slx5 and only one in Slx8, which are essential for its function such as the ubiquitination of the SUMOylated form of the E3 ligase Siz2, a yeast PIAS ortholog. A study reported that Uls2 prefers poly-SUMO chains and that it mono-ubiquitinates their terminal SUMO[220]. The RNF4-dependent formation of these hybrid SUMO-ubiquitin chains was shown to recruit another family of receptor proteins containing a tandem SUMO and ubiquitin interacting motif (tSIM-UIM)[230]. As expected, this family included proteasomal proteins such as proteasome subunit S5a of the 19S regulator complex as well as lysosomal proteins[230,231] However it also recruits DNA damage factors such as the Breast cancer type I susceptibility protein (BRCA1) revealing a role for SUMOylation and STUbLs in DNA damage regulation[232].

c. DNA damage

One of SUMOylation's many functions include the regulation of the DDR pathway[167]. Cells have evolved a complex machinery to maintain their genomic integrity which detects DNA damage such as single stranded breaks and DSBs with various checkpoints capable of regulating cell cycle, DNA repair as well as transcription modification and chromatin remodeling for an instant response to stress[233]. Many of the DDR proteins are SUMOylated to initiate their recruitment to the DNA damage site or to recruit downstream effectors and activate their activity in the repair pathway. Upon the generation of a DNA lesion, single strand DNA-binding replication protein A (RPA) is recruited and binds to the overhangs of the DSBs. RPA is crucial for the activation of the ATR signaling cascade and the DDR. RPA70, one of the three RPA subunits is SUMOylated *in vivo* on residues K449 and K577 in SENP6 knockdown cells. This model displays increased replication defects and DNA breaks. The study further showed that RPA70 SUMOylation is essential for its replacement by the DNA repair protein RAD51 homolog 1 (RAD51) at the DSB and for homologous recombination (HR) as RPA70 SUMO deficient mutants show decreased localization of RAD51 at damage foci[167,234].

Furthermore, the role of the Bloom syndrome protein (BLM) helicase at damaged replication forks and the formation of the D-loop for HR are also SUMOylation-mediated mechanisms. BLM is SUMOylated at residues K317 and 331 and the modification is necessary for RAD51 binding at the DSB[235]. Ouyang *et al.* also show that SUMO-mutant BML cells present increased γH2Ax foci, increased cell death and inhibition of HR. BML SUMOylation is hypothesized to indicate a breakage at the replication fork[235].

The proliferating cell nuclear antigen is also a key organizer of DDR factors at the stalled replication fork and this process is regulated by its various PTMs. Its K164 residue can be both SUMOylated and ubiquitinated. Its SUMOylation recruits the Regulator of telomere elongation

helicase 1 (RTEL1) at the replication fork and inhibits spontaneous recombination[236].

Another downstream effector of HR recruited at DSBs is BRCA1. The protein assembles into multiple complexes including proteins containing a tSIM-UIMs such as Rap80[232]. Therefore, the complex requires SUMOylation of proteins at the DSB site such as the cell cycle checkpoint protein known as Mediator of DNA damage Checkpoint 1. The SUMOylation of this checkpoint protein is shown to be essential for proper recruitment of BRCA1 as the mutation of its SUMOylated lysine residue abolishes its recruitment to DSBs[237]. Moreover, this recruitment is also regulated by the formation of SUMO-ubiquitin hybrid chains as RNF4 depletion prevents BRCA1 localization with γH2Ax *in vivo* [232].

A more general study looked at the involvement of different SUMO isoforms in the DDR and showed that SUMO2/3 mainly act in the non-homologous end joining (NHEJ) pathway while SUMO1 is involved in all repair pathways. Most interestingly, they showed that unconjugated SUMO1 also plays a role interacting with SIMs such as those found in Rad51, increasing its accumulation at DSBs[238]. A recent study reports the importance of STUbLs at DNA damage sites. Their model proposes these E3 ligases act as a "cleaning crew" of SUMO2/3 chain accumulation at DNA damage sites allowing for the proper activation of the downstream DDR effectors[239-241].

d. Telomeres

Many of the telomere associated proteins have been shown to be SUMOylated, especially in yeast models[242]. The importance of the mechanisms for telomere maintenance is highlighted through a significant increase in telomere elongation when SUMOylation is inhibited[243]. Therefore, many of these SUMOylation targets inhibit telomerase activity. One example is Cdc13, a telomere length regulator protein which has been associated to both telomerase recruitment or inhibition. SUMOylation of this protein at K909 increased its affinity with the STN (Stn1/Ten1) complex,

the yeast ortholog of a CST subunit involved in telomerase inhibition and C-strand fill-in[244]. This study also identified additional telomere proteins that are SUMOylated such as RAP1. This protein binds to TRF2 and is essential to protect telomeres from being recognized as DNA damage and inhibiting NHEJ. RAP1 is known to be a negative regulator of telomere length[245]. Interestingly, a study showed that SUMOylation of this protein inhibits its role in preventing NHEJ as depletion of the STUbL Uls1 leads to telomere fusions by NHEJ while the inhibition of SUMO chain formation bypasses the Uls1 mutation and leads to reduced telomere fusion[246]. What remains unclear is why the regulation of RAP1 by SUMOylation would only have negative effects. Further studies need to be conducted to understand better this mechanism[242].

Furthermore, two studies were published simultaneously reporting that Tpz1, the TPP1 yeast ortholog is SUMOylated at K242 and SUMO deficient Tpz1 mutant cells display clear elongation of telomere and significantly decreased STN complex binding to telomeres. A weak interaction was detected with a two-hybrid interaction assay between Stn1 and SUMO-Tpz1 but not between Ten1 and SUMO-Tpz1. Therefore, Tpz1 SUMOylation inhibits telomerase activity through the recruitment of the STN complex at telomeres, similarly to the function of Cdc13 SUMOylation[247,248]. Research conducted in mammalian cells identified TRF1 and TRF2 to also be targeted by SUMOylation. One study shows that TRF2 poly-SUMOylation mediated by the E3 ligase PIAS1 recruits the STUbL RNF4 for its ubiquitination and degradation. This process would most likely target a fraction of TRF2 as the shelterin protein is essential for telomere maintenance and protection. The second study focused on SUMOylation of shelterin proteins in cancer cell lines which maintain their telomeres by the Alternative Lengthening of telomeres (ALT) mechanism. This mechanism emerged in cell lines that do not express telomerase and rely on HR of telomere repeats to maintain the length of their telomeres and preserve their unlimited proliferation capacity[249]. One characteristic of these cancers is ALT-associated PML bodies (APBs) where

telomeres localize at PML bodies, a site enriched in DNA repair factors therefore an ideal site for telomere recombination[250]. In this study, they show that SUMOylation of the two shelterin components TRF1 and TRF2 by the E3 ligase MMS21 is necessary for telomere recruitment at the PML bodies and therefore for APB formation in these ALT cell lines[251]. However, the mechanism by which their SUMOylation recruit telomeres to PML bodies is not yet characterized. The involvement of SUMOylation for targeting telomeres for DNA repair was also described in yeast by Churikov *et al.* where they showed using a chromatin immunoprecipitation assay that eroded telomeres are enriched in SUMOylated telomere-bound proteins in the absence of telomerase, and promotes their relocalization to the nuclear pore complex for DNA damage repair. Knowing the Uls2 to physically interact with nuclear pore complexes, they found that the STUbLs mediate the recognition of the SUMOylated eroded telomeres and traffic them to the nuclear pore complex where they undergo recombination[252].

4) SUMOylation in diseases

Seeing the diversity of roles SUMOylation plays in cellular processes, it can only be predicted that the malfunction of this PTM is involved in many diseases[253]. A first range of diseases linked to SUMOylation are neurodegenerative diseases[254]. These cases involve premature degradation of neuronal populations which can be due to an improper SUMOylation dependent regulation of proteasomal degradation of target proteins. Multiple SUMO substrates have been linked to neuronal diseases such as Tau in Alzheimer's disease, Huntingtin in Huntington's disease or α-synuclein in Parkinson's disease[254,255]. SUMOylation is also related to heart disease. It was shown that depletion of SUMO1 in cardiac tissues leads to heart failure. This is due to the impaired SUMOylation of the Lamin A protein in the extracellular matrix, representative of the consequences arising from mutations in the SUMOylation consensus site of the protein where the glutamate is modified to glutamine or lysine: E203G and E203K[253,256]. Additionally, many cancer

cell lines have been linked to SUMOylation deficiencies. One of the first causes is due to mutations leading to the overexpression of SUMOylation activators such as SUMO isoforms[257], Ubc9 or SUMO E3 ligases. For example, the upregulation of the SUMO E3 ligase PIAS3 has become a hallmark of cancer[258] while the upregulation of Ubc9 has already been linked to multiple cancer types such as ovarian cancer and human lung adenocarcinomas[259-261]. SENP overexpression is associated with cancer. For example, SENP1 overexpression in the prostate increases susceptibility for tumor growth[262]. Seeing how SUMOylation regulates the expression and activity of key transcription factors and tumor suppressors, its upregulation can lead to the dysregulation of oncogenes. p53 has been extensively shown to be regulated by SUMOylation and the loss of p53 is one of the main causes of cancer[106]. The same dramatic effect is observed for the NF-κB transcription factor as its upregulation is highly correlated to inflammation and cancer[263,264]. Another cause of cancer can be the use of SUMO by telomerase-defective cells to maintain their telomere length and proliferative capacity which creates survivors that should have gone through replicative senescence[252,265].

IV. Rational and objectives of the research

The goal of my master thesis research was to characterize the molecular mechanisms that regulate dyskerin SUMOylation. This project included determining if dyskerin SUMOylation is cell cycle regulated, assessing if dyskerin SUMOylation could be stimulated by DNA damage, identifying in which subcellular compartment dyskerin is SUMOylated, and finally identifying the E3 ligase regulating dyskerin SUMOylation. I discovered that dyskerin SUMOylation is cell cycle regulated with a peak in S phase and G2/M, time points which corresponds to key functions of dyskerin. Moreover, I show that certain genotoxic stresses such as AsO_3 treatment can increase dyskerin protein levels and induce dyskerin SUMOylation and that dyskerin SUMOylation can also be increased by inducing telomere-specific damage. Following the silencing of specific SUMO

proteases, I found that a pool of SUMOylated dyskerin is concentrated in the nucleolus and that SENP3 is involved in the dyskerin SUMOylation cycle. Finally, I have engineered the necessary constructs and cell lines to use an unbiased biotinylation proximity based identification assay that has the potential to identify proteins in close proximity to dyskerin (10nm) or having weak interactions with the protein which may allow us to identify the E3 ligase involved in dyskerin SUMOylation.

MATERIALS AND METHODS

I. Cell culture and plasmids

HEK293 cells were the only cells used in this study. Stably expressing His-SUMO3 HEK293 cells genetically modified for facilitated Mass Spectrometry analysis were kindly provided by Dr. Pierre Thibault[266]. Stably expressing Flag-dyskerin HEK293 cells and His-SUMO3 Flag-dyskerin HEK293 cells were created by transfecting Mock HEK293 cells and His-SUMO3 HEK293 cells respectively with a pLenti-Flag-dyskerin construct. This construct was made by Shusen Zhu: pcDNA3.1 Flag-dyskerin (kindly provided by Francois Dragon, Université du Québec à Montréal) was digested with EcoRV and ClaI for 3 h at 37 °C. Enzymes were inactivated 20 min at 65 °C. The overhang was filled-in by adding dNTPs and Klenow fragment with a 15 min incubation at 25 °C. The sample was loaded on an agarose gel and the corresponding band was extracted. The pLentiCMV/TO vector plasmid was digested with EcoRV for 3 h at 37 °C then dephosphorylation of the vector was done with Calf intestinal alkaline phosphatase (CIP) (NEB, M0290S) for 50 min at 37 °C. Insert and vector were ligated with the T4 DNA ligase (Invitrogen, 15224-017) for 24 h at 14 °C. Ligation product was transformed into Stbl3 bacteria. Plasmids were digested as well as sequenced to confirm the correct insert. The stable cell lines expressing this vector were infected and selected by Patrick Lambert-Lanteigne. All cells were cultured in Dulbecco's Modified Eagle's medium (Wisent) completed with 10% Fetal Bovine Sera (Wisent) and an antibiotic solution containing 10,000 units/mL of penicillin, 10,000 µg/mL of streptomycin and 25 µg/mL of Gibco Amphotericin B (Invitrogen, #15240-062). Selection was maintained with puromycin (2 µg/ml, Wisent) for the Flag-DKC1 vector and neomycin (500 µg/ml, Multicell) for the His-SUMO3 vector. The pCMV KR-TRF1 plasmid was obtained from Dr. Li Lan's lab[267]. The TRF2 dominant negative pLPC-NMycTRF2$^{\Delta B \Delta M}$ plasmid was provided by Dr. Titia de Lange[268]. 5 µg of the latter plasmid was digested with 20 U of XhoI (NEB,

R0146S) and HindIII (NEB, R0104S) in Buffer 2 (NEB, B7002S) for 1 h at 37 °C. TRF2$^{\Delta B\Delta M}$ encoding sequences were extracted from an agarose gel. 5 µg of pcDNA3.1 hygro (+) vector was digested in parallel in the same conditions and the enzymes were deactivated at 65 °C for 20 min. It was then incubated with 10 U of CIP for 30 min at 37 °C. TRF2$^{\Delta B\Delta M}$ inserts were cloned into a pcDNA3.1 hygro (+) vector (in ratios 1:3, 1:5 and 1:10) with 1 µl of T4 DNA ligase for ligation, 1 h at 37 °C. DH5α bacteria were transformed with the pcDNA3.1 TRF2$^{\Delta B\Delta M}$ plasmid. The cloning was confirmed through sequencing of the plasmid.

MycBirA* insert from pcDNA3.1MycBirA* neomycin plasmid kindly provided by Dr. Marc Fabian was cloned into the pcDNA3.1 (+) hygro vector using NheI (NEB, R0131S) and HindIII (NEB, R0104S). *DKC1* was amplified with a polymerase chain reaction from the pcDNA3.1 Flag-dyskerin plasmid using the following primers: 5'-GGGGGTACCAGCGGATGCGGAAGTAA-3' (forward) and 5'-CCCTCTAGACTACTCAGAAACCAATTCTAC-3' (reverse) and cloned in the MycBirA* pcDNA3.1 (+) hygro plasmid using KpnI (NEB, R3142S) and XbaI (NEB, R0145S) in CutSmart buffer (NEB, B7204S). BirA*HA insert from pcDNA3.1BirA*HA neomycin (Addgene, #36047) was cloned into the pcDNA3.1 (+) hygro vector using NheI (NEB, R0131S) and PmeI (NEB, R0560S) in CutSmart buffer. DKC1 was amplified with PCR using the following primers: 5'-ATGCGCTAGCATGGCGGATGCGGAAGTAATTA-3' (forward) and 5'-GGGACCGGTACTCAGAAACCAATTCTACCTCT-3' (reverse) and cloned in the BirA*HA pcDNA3.1 (+) hygro plasmid using NheI and AgeI (NEB, R0552S). The digestion and cloning conditions followed were the same as for the TRF2$^{\Delta B\Delta M}$ plasmid. His-SUMO3 HEK293 cells were transfected with each of the four constructs using lipofectamine 2000 (Invitrogen) and selected with hygromycin (200 µg/ml, Wisent).

II. RNA interference

The sequences of siRNA oligonucleotides used were 5'-CAA UAA GGA GCU ACU GCU AdTdT-3' and 5'-GUU AUU CCU CGA UGA CGA UdTdT-3'[269] for SENP3 (Cell signaling, D20A10) and 5′-GGA CCA GCU UUC GCU UUC UdTdT-3′ and 5'-CCU GGU CGA AAG CGA AAG AdTdT-3' for SENP1 (Cell signaling, D16D7)[270]. An siGFP (5'-AAC ACU UGU CAC UAC UUU CUCdTdT-3' and 5'-UUG UGA ACA GUG AUG AAA GAGdTdT-3') was used as a control[271]kindly provided by Dr. Stéphane Richard. 12 pmol of each siRNA were preincubated with lipofectamine RNAiMax (Invitrogen) in OptiMEM (Gibco) then added to the antibiotic free medium containing His-SUMO3 Flag-DKC1 HEK293 cells in a 6 cm plate. The medium was changed 5 h later with complete DMEM. The transfected cells were incubated for 72 h then collected in ice-cold Phosphate-Buffered Saline (PBS).

III. Immunoblots and antibodies

Cells were lysed in mRIPA buffer (50 mM Tris HCl pH 8.0, 150 mM NaCl, 10 mM $MgCl_2$, 1% NP-40, 0.5 % sodium deoxycholate (DOC), 1 mM phenylmethylsulfonyl fluordie, complete Protease Inhibitor Cocktail (Roche), 20 mM N-Ethylmaleimide), incubated 20 min on ice then centrifuged at 4 °C at 15,000 rpm. Protein concentration was assessed using a Bradford Assay. 10-40 µg of samples were loaded on SDS-PAGE, electrophoresed 90 min at 90 V then transferred to a polyvinylidene difluoride membrane (Millipore) for 2 h at 70 V. Membranes were blocked in 5 % non-fat dry milk PBS-Tween (PBS-T) 0.05 % for 1 h at room temperature then incubated in corresponding primary antibodies overnight at 4 °C: anti-dyskerin (1:2000) (Santa cruz, sc-48794), anti-SUMO2 (1:1000) (Invitrogen, #51-9100), anti-TRF1 (1:4000) (abcam, #ab1423), anti-TRF2 (1:1000) (Millipore, #05-521), anti-Flag (1:4000) (Proteintech, 20543-1-AP), anti-TCAB1 (1:8000) (NovusBiologicals, NB100-68252), anti-HA (1:1200) (Cell Signaling, #2367), anti-Myc (1:2000) (Santa Cruz, #sc-40), anti-6xHis (1:500)

(Clontech, #631212), anti-PML (1:500) (Santa Cruz, sc- 9862), anti-SENP1 (1:1000) (Cell Signaling, #11929) or anti-SENP3 (1:1000) (Cell Signaling, #5591) antibodies. Membranes were washed 5 min 3 times with PBS-T 0.05% then incubated in secondary antibodies anti-rabbit or anti-mouse (1:10000), corresponding to the primary antibody, for 1 h at room temperature. Membranes were washed 5 min 3 times with PBS-T 0.05% then developed with ECL2 Western Blotting Substrate (ThermoScientific) and exposed on 8x10" Scientific autoradiography films (Progene, 39-20810) as well as revealed using direct blue-excited fluorescence with the STORM imager 840 (General Electric, 63-0035-59). The program ImagQuantTL was used for their analysis and quantification.

IV. Fluorescent *in situ* hybridization (FISH) and Immunofluoresence (IF)

80 % confluent cells on a sterile coverslip in a 6-well plate were washed twice with PBS and the coverslips were transferred to a new 6-well plate while remaining cells were pelleted for input samples. The coverslips were incubated 10 min at room temperature in 10% acetic acid 4% formaldehyde solution for cell fixation then washed twice for 5 min in PBS. Cells were left in 70 % ethanol at 4 °C overnight. Cells were rehydrated for 5 min in 50 % deionized formamide, 2X saline-sodium citrate (SSC) buffer then the denaturing step was conducted 10 min in 70 % deionized formamide, 2X SSC at 85 °C. The coverslips were put cell-side down on 40 µl of pre-hybridization mixture (hybridization buffer, 50% deionized formamide, 1 µg/µl of *E.coli* tRNA, 25 ng/µl of 50 nt random primer)(hybridization buffer: 10 % dextran sulfate, 2 mM vanadyl ribonucleotide complex, 0.002mg/ml nuclease-free BSA) in a humid chamber and incubated for at least 1 h at 37 °C. Coverslips were transferred to 40 µl of hybridizing solution containing Cy3-labeled telomeric peptide nucleic acid probe (Panagene) in pre-hybridization mixture and left overnight at 37 °C. Coverslips were transferred to a 6-well plate and washed twice in a bacterial incubator shaker at 110 rpm for 30 min in 50 % deionized formamide, 2X SSC then washed 10

min three times in PBS. Cells were blocked 1 h in 5% BSA. Three washes of 10 min were conducted in PBG (1% cold fish gelatin, 0.5% BSA in PBS). Coverslips were incubated cell-side down in anti-γH2AX (Millipore, #05-636) for DNA damage detection or anti-TCAB1 (1:50) (NovusBiologicals, NB100-68252), anti-HA (1:50) (Cell Signaling, #2367) and anti-Myc (1:50) (Santa Cruz, #sc-40) diluted in PBG. The incubation in the primary antibody was performed overnight at 4 °C. Coverslips were washed 3 times 10 min in PBG and coverslips were incubated cell-side down in the corresponding fluorescent secondary antibody: donkey Fluorescin FITC anti mouse (1:250) (Jackson IR, 715-095-150) and donkey Cy3 anti-rabbit (1:250) (Jackson IR, 711-165-152) for 1 h in the dark at room temperature. If a simple IF for two different primary antibodies was conducted, the experiment started at the 30 min washes in 50% deionized formamide, 2X SSC. At the secondary antibody step, coverslips were incubated cell-side down in both donkey Fluorescin FITC anti mouse (Jackson IR, 715-095-150) and donkey Cy3 anti-rabbit (Jackson IR, 711-165-152) for 1 h in the dark at room temperature. Coverslips were washed 3 times 10 min in PBG then fixed with nail polish to glass slides and kept at 4 °C.

V. Nickel-charged Nitrilotriacetic Acid (NiNTA) affinity purification

Two 15 cm plates were collected in 5mL of ice-cold PBS. 500 µl was kept for input analysis. Cells were pelleted and lysed in 800 µl of Guanidine Hydrochloride Lysis buffer (GuHCl, 6 M Guanidine HCl, 20 mM sodium phosphate, 500 mM NaCl, 10 mM imidazole, pH 8.0), and lysates were sonicated 3 times 5 sec pulses at 40 % amplitude on ice with a Fischer Scientific 550 Sonic dismembrator. Cells were centrifuged 20 min at 15000 rpm. 50 µl of slurry Nickel resin (Qiagen, #30310) was washed twice with PBS and once with GuHCl (Spin for 2 min at 3000 rpm). Lysates were transferred to the pre-washed resin and rotated at 4 °C overnight. The supernatant was removed and beads were washed once with GuHCl, once with Urea washing buffer 1 (8 M urea, 20 mM sodium phosphate, 500 mM NaCl, 10 mM imidazole, pH 8.0) and

twice with Urea washing buffer 2 (8 M urea, 20 mM sodium phosphate, 10 mM imidazole, 500 mM NaCl, pH 6.3). Beads were eluted in 50 µl of elution buffer (2.5X laemlli buffer- define, 200 mM imidazole), rotated for 15 min then boiled 5 min at 95 °C. Analysis of the samples was done with SDS-PAGE and immunostaining against dyskerin and SUMO2.

VI. Cell cycle

2 mM of thymidine was added to a 30 % confluent 10 cm plate of HisSUMO3-Flag-dyskerin HEK293 cells for 18 h. Media was washed twice with PBS then changed for thymidine free DMEM for 9 h. 2 mM thymidine were supplemented again for a second block and kept for 17 h. Cells synchronized in G1/S phase were released and collected every hour for 12 h. Cells were trypsinized and washed once with PBS then resuspended in 1 ml of ice-cold PBS. 4 mL of ice-cold absolute ethanol was added drop by drop while vortexing gently for storage at -20 °C. Fixed cells were pelleted and resuspended in 100 µL of 200 µg/mL of RNaseA in PBS. Cells were incubated 30 min at 37 °C. 50 µl of Propidium Iodide (PI, 1 mg/ml in PBS) was added and samples were left at room temperature for 10 min before the flow cytometry analysis on a BD LSR Fortessa (BD Biosciences, SanJose) using laser 561 mm and filter 610/20 nm. Three key time points were identified: 0 h, 4 h 30 and 9 h corresponding to G1, S and G2/M phase, respectively. An asynchronous sample was collected as a control. Following this analysis, cells collected at 0h, 4 h 30 and 9 h were washed twice with PBS, 10 % was kept in absolute ethanol for flow cytometry analysis and the other 90% was used for NiNTA affinity purification.

VII. DNA damage treatments

Cells were treated with 0.25-1.25 ng/ml of doxorubicin for 24 h or 2 µM AsO_3 for increasing amount of time (1 – 6 h). Cells were scraped in ice-cold PBS. The pellets were lysed in mRIPA buffer, incubate on ice for 20 min and centrifuged for 20 min at 15,000 rpm at 4 °C. Lysates were used for immunoblotting against dyskerin and SUMO2. Immunoblotting against PML was used

as control for the AsO_3 treatment[227]. For telomere-specific DNA damage, two constructs were used: the dominant negative TRF2 (TRF2ΔBΔM)[268] and a chimeric TRF1[267] fused to the phototoxic fluorescent Killer Red protein (KR-TRF1). Two 15cm plates of His-SUMO3 Flag-dyskerin expressing HEK293 cells were transfected with 25 µg of the plasmid (for both) using lipofectamine 2000 and incubated for 24 h, the antibiotic free medium was changed for complete DMEM after 6 h. KR-TRF1 transfected cells were kept in the dark and exposed to light for a determinate amount of time (1-3 h) using a Sylvania 15W fluorescent tube. FISH/IF with a telomeric probe and antibodies against γH2AX (Milllipore, (#05-636) was used to assess Telomere dysfunction Induced Foci (TIF) caused by the proteins encoded by these constructs.

VIII. Bio-ID constructs and streptavidin purification

Immunoblotting was used to confirm expression of the BioID fusion proteins and immunofluorescence to confirm localization of the recombinant protein. Four 80 %-confluent 15 cm plates for each cell type were supplemented with 50 µM D-biotin (Bioshop, 50 µM stock in H_2O) and collected 20 h later. Cells were washed three times with PBS to remove any residual biotin then centrifuged for 5 min at 3000 rpm. The pellet was lysed in RIPA buffer (50 mM Tris HCl pH 7.4, 150 mM NaCl, 1% NP-40, 0.1% SDS, 1% DOC, 1 mM EDTA, 1 mM PMSF, complete Protease Inhibitor Cocktail (Roche)) and supplemented with 250 units of benzonase. Lysates were sonicated 30 secs at 30% amplitude (10-sec bursts with 2 secs of rest in between) then centrifuged for 30 min at maximum speed at 4 °C. 20 µl aliquots were kept for input analysis at -80 °C. In the meantime, 70 µl of slurry Streptavidin-Agarose beads (Millipore) were washed 3 times with RIPA buffer then lysates were added to pre-washed streptavidin beads and incubated on rotor at 4 °C for 3 h. Reactions were centrifuged for 1 min at 2000 rpm at 4 °C. Supernatant was stored at -20 °C and beads were washed 3 times with RIPA buffer and 3 times with 50 mM ammonium bicarbonate pH 8.5 at 4 °C. Beads were resuspended in 100 µl of 50 mM

of Ammonium bicarbonate and samples processed immediately for Mass Spectrometry (MS) analysis at the IRCM proteomic core facility. Input samples were used for immunoblotting against Myc and HA tags.

IX. BioID digestion and LC-MS/MS

The on-bead proteins are digested with 0.5 µg Sequencing Grade Modified Trypsin (Promega) overnight at 37^{o}C with agitation. The supernatants were collected and the beads were washed two times with 100 µl water. The supernatants of each wash were pooled and then reduced and alkylated. The reduction step is done with 9 mM dithiothreitol at 37 ^{o}C for 30 min and, after cooling for 10 min, the alkylation step is done with 17 mM iodoacetamide at room temperature for 20 min in the dark. The supernatants were acidified with trifluoroacetic acid for desalting and removal of residual detergents by MCX (Waters Oasis MCX 96-well Elution Plate) following the manufacturer's instructions. After elution in 10% ammonium hydroxide /90 % methanol (v/v), samples were dried with a Speed-vac, reconstituted under agitation for 15 min in 15 µL of 5 % formic acid and loaded into a 75 µm i.d × 150 mm Self-Pack C18 column installed in the Easy-nLC II system (Proxeon Biosystems). Peptides were eluted with a two-slope gradient at a flowrate of 250 nL/min. Solvent B first increased from 1 to 35% in 105 min and then from 35 to 84% B in 25 min. The HPLC system was coupled to Orbitrap Fusion mass spectrometer (Thermo Scientific) through a Nanospray Flex Ion Source. Nanospray and S-lens voltages were set to 1.3-1.8 kV and 50 V, respectively. Capillary temperature was set to 225 °C. Full scan MS survey spectra (m/z 360-1560) in profile mode were acquired in the Orbitrap with a resolution of 120,000 with a target value at 1e6. The 20 most intense peptide ions were fragmented in the HCD collision cell and analyzed in the linear ion trap with a target value at 2e4 and a normalized collision energy at 28. Target ions selected for fragmentation were dynamically excluded for 25 sec.

X. Protein identification

The peak list files were generated with Proteome Discoverer (version 2.1) using the following parameters: minimum mass set to 500 Da, maximum mass set to 6000 Da, no grouping of MS/MS spectra, precursor charge set to auto, and minimum number of fragment ions set to 5. Protein database searching was performed with Mascot 2.6 (Matrix Science) against the Refseq human protein database (July 29th, 2016). The mass tolerances for precursor and fragment ions were set to 10 ppm and 0.6 Da, respectively. Trypsin was used as the enzyme allowing for up to 1 missed cleavage. Cysteine carbamidomethylation was specified as a fixed modification, and methionine oxidation as variable modifications. Data interpretation was performed using Prohits (version 5.0.2).

RESULTS

I. Dyskerin SUMOylation is cell cycle regulated

It has previously been shown that SUMOylation regulates multiple proteins that are cell cycle regulated such as the cyclin family and p53[272]. Dyskerin plays multiple functions at different phases of the cell cycle. On one hand, it was shown to be part of the active telomerase complex in S phase which corresponds to the optimal activity of the enzyme[273,274]. Dyskerin also acts during mitosis playing an important role for the mitotic apparatus. It was shown to accumulate at perichromosomal regions during mitosis and its depletion induces a G2/M arrest and a spindle assembly checkpoint revealing mitotic defects [129]. We therefore investigated whether dyskerin SUMOylation is regulated in a cell-cycle dependent manner. To do so, we used HEK293 cells stably overexpressing both His-SUMO3 and Flag-dyskerin. First, these cells were synchronized in G1/S phase using a double thymidine block then released from the synchronization and collected every hour for 12 h to characterize their progress in each phase of the cell cycle (Figure 7) Using PI staining and flow cytometry analysis allowed us to distinguish between three time points corresponding to G1, S phase and G2/M at 0 h, 4 h 30 and 9 h respectively.

Untransfected HEK293 control/parental cells (Mock HEK 293) and HEK293 cells expressing His-SUMO3 and Flag-dyskerin were collected at these time points and proteins were extracted. The PI staining analysis of these samples allowed us to confirm that these time points are “in-phase” across the cell cycle between the two HEK293 cell lines used (Figure 8A). Western blot analysis shows that dyskerin protein levels are higher in His-SUMO3 Flag-dyskerin expressing HEK293 cells synchronized in S phase and G2/M compared to dyskerin levels in G1 and the asynchronous samples of both mock and His-SUMO3 Flag-dyskerin expressing HEK293 cells (Figure 8B, compare lanes 7-8 with lanes 1-6). This experiment was repeated a total of 3 times, and levels of dyskerin were quantified by normalizing to actin levels (Figure 8C). We then used a nickel-charged

nitrilotriacetic acid (NiNTA) purification to enrich His-SUMO3 conjugated proteins in the samples from the His-SUMO3 Flag-dyskerin expressing cells. Histidine is known to have a high affinity for nickel ions and the 6X His-tagged SUMO3 conjugated proteins will therefore bind to the resin and allow for the purification of SUMOylated proteins in the lysates. Following the NiNTA purification, Western blot analysis using an antibody against dyskerin revealed protein species of higher molecular weight than the 58 kDa expected for dyskerin and may represent SUMOylated forms of dyskerin (Figure 8B and 8D, upper panel). We have previously reported that dyskerin migrates at about 70 kDa which might be indicative of posttranslational modifications[130]. The first observed band slightly above 70 kDa (labeled non-specific) appeared in all samples including the mock HEK293 samples. We concluded that it is likely a non-specific protein revealed by the dyskerin antibody as no protein should be pulled down in the mock HEK293 samples. The protein species at about 90 kDa (labeled SUMOylated dyskerin) is observed in all His-SUMO3 expressing samples but is absent in the Mock HEK293 cell control samples. We hypothesize that it is a SUMOylated state of dyskerin that may be cell-cycle independent. However, we also observe a higher molecular weight protein species at about 110 kDa (labeled SUMO (n) dyskerin) which is more intense in both S phase and G2/M synchronized His-SUMO3 expressing HEK293 cells compared to G1 and the asynchronous sample, and which correlates with the increased dyskerin protein levels observed in S and G2/M phases in the input samples. (Figure 8D, upper panel, compare lanes 7-8 to lanes 5-6). Western blot analysis using an antibody against SUMO2/3 revealed the SUMO 2/3-conjugated protein pool at different time points of the cell cycle (Figure 8D, bottom panel). As predicted, no signal was detected in the control samples as they are not expressing the His-SUMO3 protein (Figure 6D, bottom panel, lanes 1-4). We found an enrichment in global SUMOylated proteins in S phase and G2/M compared to G1 and asynchronous samples (Figure 8D, bottom panel, compare lanes 7-8 to 5-6).

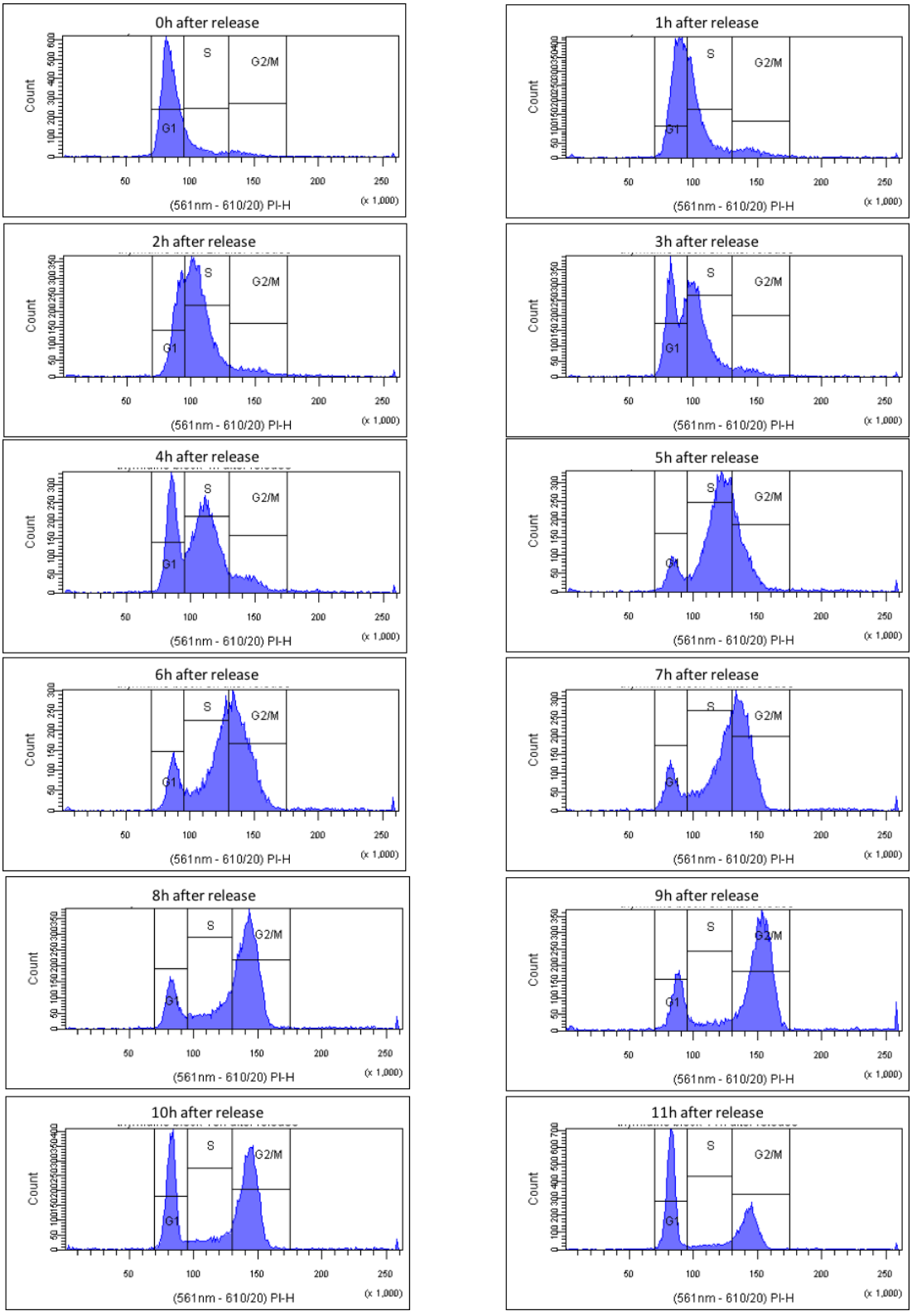

Figure 7. Cell cycle progression of HEK293 cells stably expressing His-SUMO3 Flag-dyskerin. FACS analysis results after PI staining of samples synchronized with and released from a thymidine block and collected every hour for 12 h.

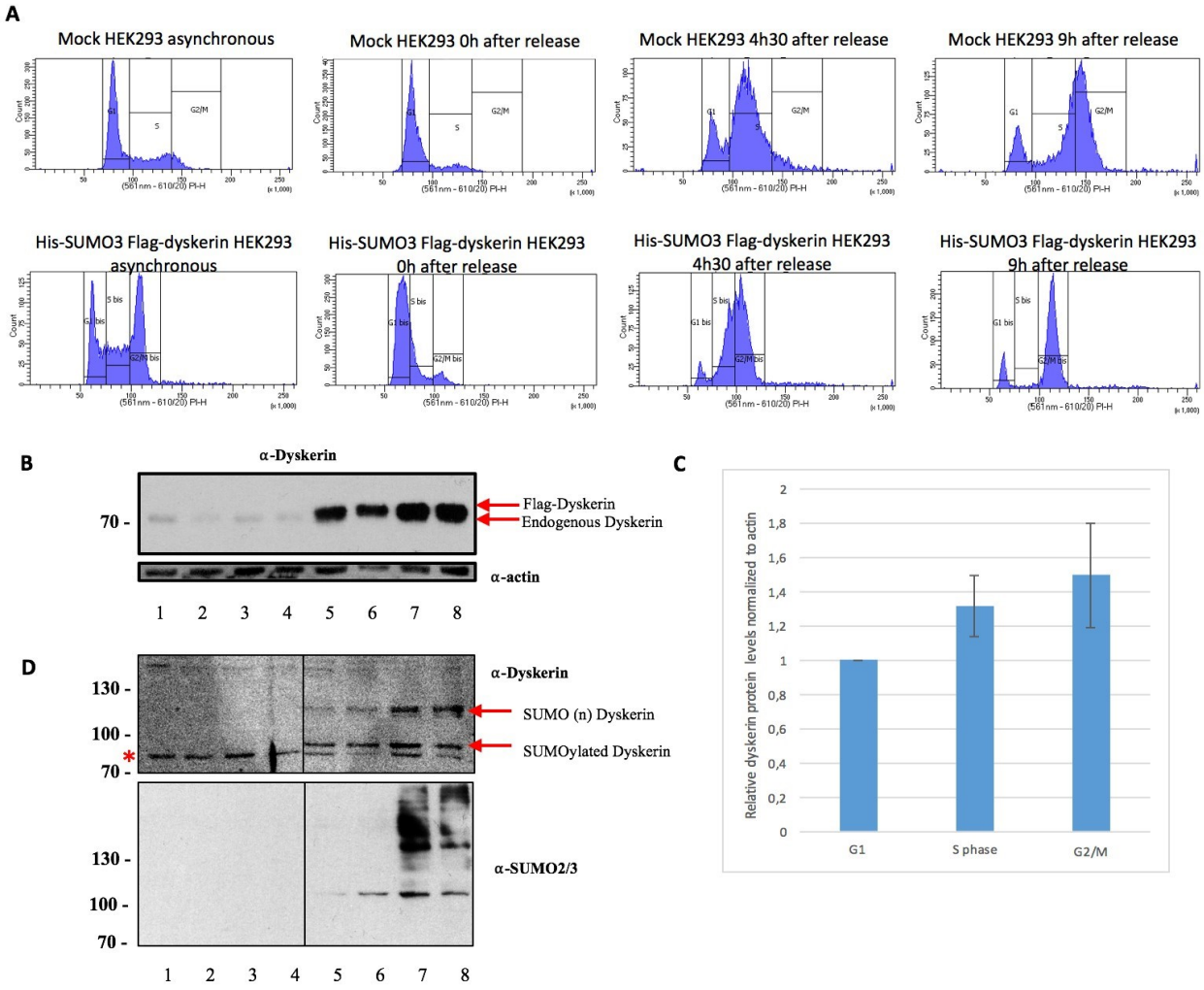

Figure 8. Dyskerin SUMOylation is cell-cycle regulated. A) FACS analysis results of both Mock HEK293 and HEK293 cells stably expressing His-SUMO3 Flag-dyskerin after releasing them from a thymidine block at time point 0 h, 4 h 30 and 9 h corresponding to G1, S phase and G2/M, respectively. B) Dyskerin protein levels are increased in S phase (lane 7) and G2/M (lane 8) and decreased in G1 (lane 6) compared to the asynchronous sample (lane 5) in HEK293 cells stably expressing His-SUMO3 Flag-dyskerin. Mock HEK293 asynchronous and synchronized in G1, S phase and G2/M (lane 1-4) were used as a control. Actin blot was used as loading control. C) Quantification of the input membrane blotted against dyskerin and normalized to actin (n=3). D) NiNTA purification results after blotting against dyskerin (top panel) and SUMO2/3 (bottom panel) shows higher molecular weight dyskerin SUMOylation species ($SUMO_{(n)}$ Dyskerin) and higher levels of global sumoylated proteins both in S phase (lane 7) and G2/M (lane 8). (*) denotes a non-specific band following immunoblotting. Molecular Weight markers were used for each gel and are indicated on left of the gels in kDa

II. Global DNA damage affects dyskerin protein levels and SUMOylation

SUMOylation is known to recruit multiple DDR factors at DNA damage sites and to activate repair factors such as RNF4 and BRCA1 previously discussed [239,275,276]. Furthermore, it has been shown that global SUMOylated protein levels increase upon introduction of stress[277]. Previous studies have tested the effect of multiple genotoxic stressors on the SUMOylation of their proteins of interest[147]. Dyskerin depleted cells have been shown to be more sensitive to genotoxic stress and dyskerin was shown to interact with DNA repair factors such as SMUG1 implicating that dyskerin mays play a role in DNA damage pathways[132,137,278]. Moreover, a study on the effect of DNA damaging agents on the protein levels of H/ACA proteins showed that each protein is differentially regulated by different DNA damages[135]. Therefore, we were curious to see if DNA damage can affect dyskerin SUMOylation levels. The study examining H/ACA RNP protein levels observed reduced dyskerin levels upon doxorubicin treatments[135]. Dyskerin depleted cells are also more sensitive to doxorubicin treatment[137,278]. Hence, we tested the effect varying doses of doxorubicin have on dyskerin protein levels and SUMOylation. HEK293 and His-SUMO3 Flag-dyskerin stably overexpressing HEK293 cells were treated with increasing concentrations of doxorubicin (0.25, 0.5 and 1.0 μM), a DNA intercalating agent for 24 h (Figure 9). We observed a negative correlation between the concentration of doxorubicin used versus the total dyskerin protein levels in His-SUMO3 Flag-dyskerin stably overexpressing cells (Figure 9A, lanes 5-8). Total dyskerin protein levels were slightly increased with the lowest dose of 0.25 nM (Figure 9A, upper panel, lane 6) while higher concentrations led to a gradual decrease of dyskerin protein level (Figure 9A, lanes 7-8). This experiment was repeated twice, and levels of dyskerin were quantified by normalizing to actin levels (Figure 9B). When analyzing the amount of SUMOylated proteins enriched by the NiNTA purification following these treatments, it does not seem that doxorubicin has an impact on total protein SUMOylation levels (Figure

9C). We were unable to detect higher molecular weight protein species possibly representative of dyskerin SUMOylation after the NiNTA purification and immunoblotting using an antibody against dyskerin (data not shown). Either the decrease in dyskerin protein levels may not be linked to a change in its SUMOylation or dyskerin SUMOylation levels are too low to detect. The experiment will need to be repeated and results confirmed. To further understand the effects of genotoxic stress on dyskerin protein levels and SUMOylation states, we investigated the effect of As_2O_3, a genotoxic chemical which creates DSBs through the synthesis of Reactive Oxygen Species (ROS)[279]. This treatment has been shown to increase global protein SUMOylation as well as PML SUMOylation in particular[146,225,227]. To test its effect on dyskerin SUMOylation, we treated HEK293 and His- SUMO3 Flag-expressing HEK293 cells with 1 μM As_2O_3 for different time points ranging from 1 h to 4 h (Figure 10). Likely due to low endogenous levels of dyskerin, we did not observe variations in dyskerin levels and SUMOylation upon treatment of mock HEK293 cells (data not shown). We subsequently used only the sample from untreated mock HEK293 cells as a control. After western blot analysis using antibodies against dyskerin, we observed that dyskerin protein levels increase in His-SUMO3 Flag-expressing HEK293 cells with increasing time of AsO_3 treatment (Figure 10A top panel, lanes 2-6). Immunoblotting against SUMO2/3 revealed one band in the mock HEK293 sample also found in the samples from His-SUMO3 Flag-dyskerin overexpressing samples (labeled SUMOylated protein), and thus likely not specific to dyskerin. (Figure 10A middle panel, lanes 1-6). The upper band is detected only in HEK 293 stably overexpressing His- SUMO3 Flag-dyskerin (labeled SUMO-Flag dyskerin) and increases in intensity with AsO_3 treatment and could therefore be specific to dyskerin (Figure 10A, middle panel, compare lanes 2- 6 to lane 1). To understand if this increase was correlated to an increase in dyskerin SUMOylation, we performed a NiNTA purification of the cells after the same treatments. Higher molecular weight protein species at approximately 90

kDa (labeled SUMO-dyskerin) corresponding to SUMOylated dyskerin were

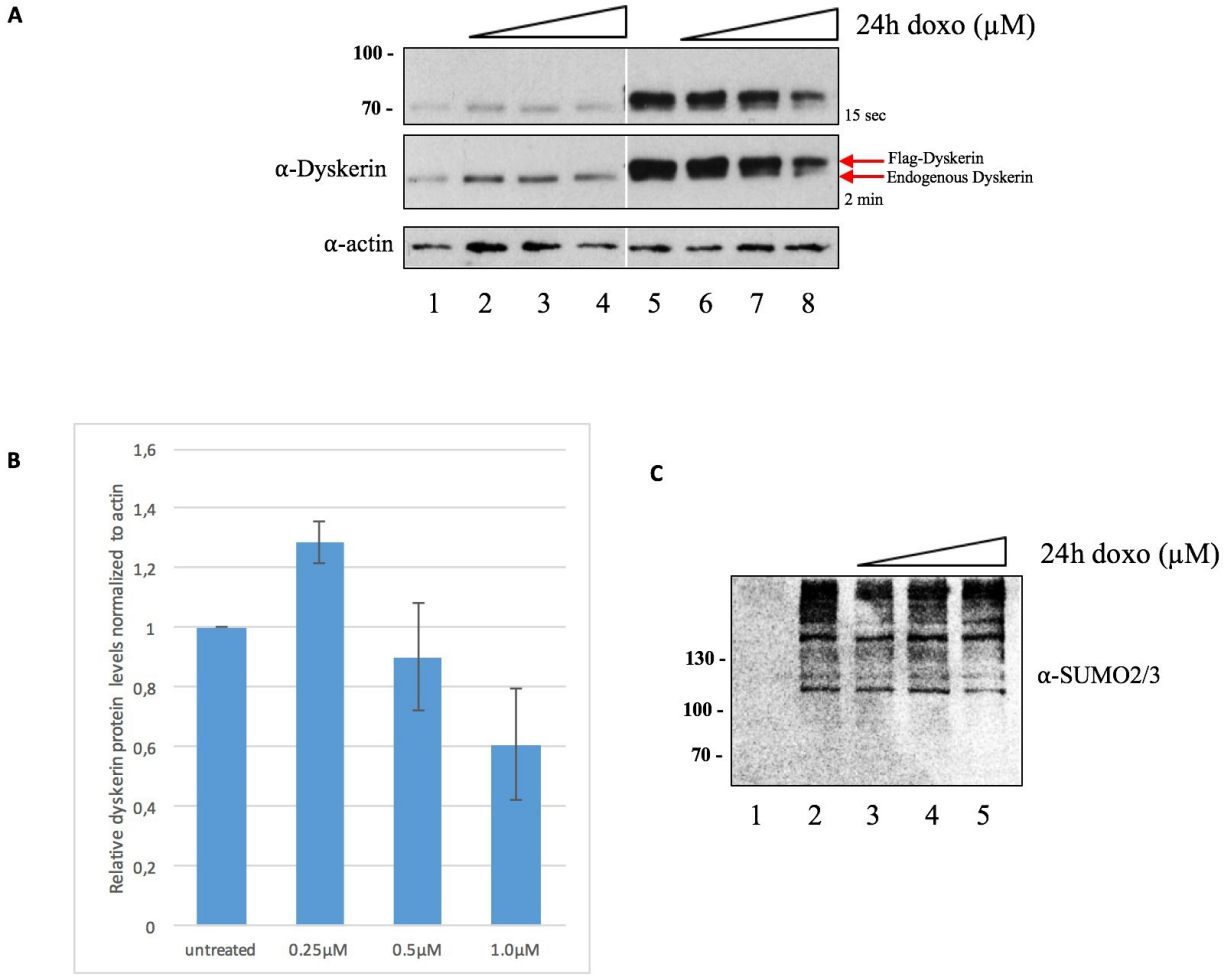

Figure 9. Doxorubicin treatment decreases dyskerin protein levels. A) Mock HEK293 cells (lane 1-4) and HEK293 cells stably expressing His-SUMO3 Flag-dyskerin (lane 5-8) were untreated (lanes 1 and 5) or treated with increased amount of doxorubicin 0.25 μM (lane 2 and 6), 0.5 μM (lane 3 and 7) and 1.0 μM (lane 4 and 8) for 24 h. Immunoblot against dyskerin with different film exposure times, 15 secs (top panel) and 2 min (middle panel) exposure. Actin blot was used as loading control. B) Quantification of total dyskerin protein levels were normalized to actin (n=2). C) SUMO2/3 blot after NiNTA purification of HEK293 cells stably expressing His-SUMO3 Flag-dyskerin (lane 2-5) treated with increasing amount of doxorubicin 0.25 μM (lane 3), 0.5 μM (lane 4) and 1.0 μM (lane 5) for 24 h and untreated Mock HEK293 cells (lane1) and HEK293 cells stably expressing His-SUMO3 Flag-dyskerin (lane 2) as controls. Molecular Weight markers were used for each gel and are indicated on left of the gels in kDa.

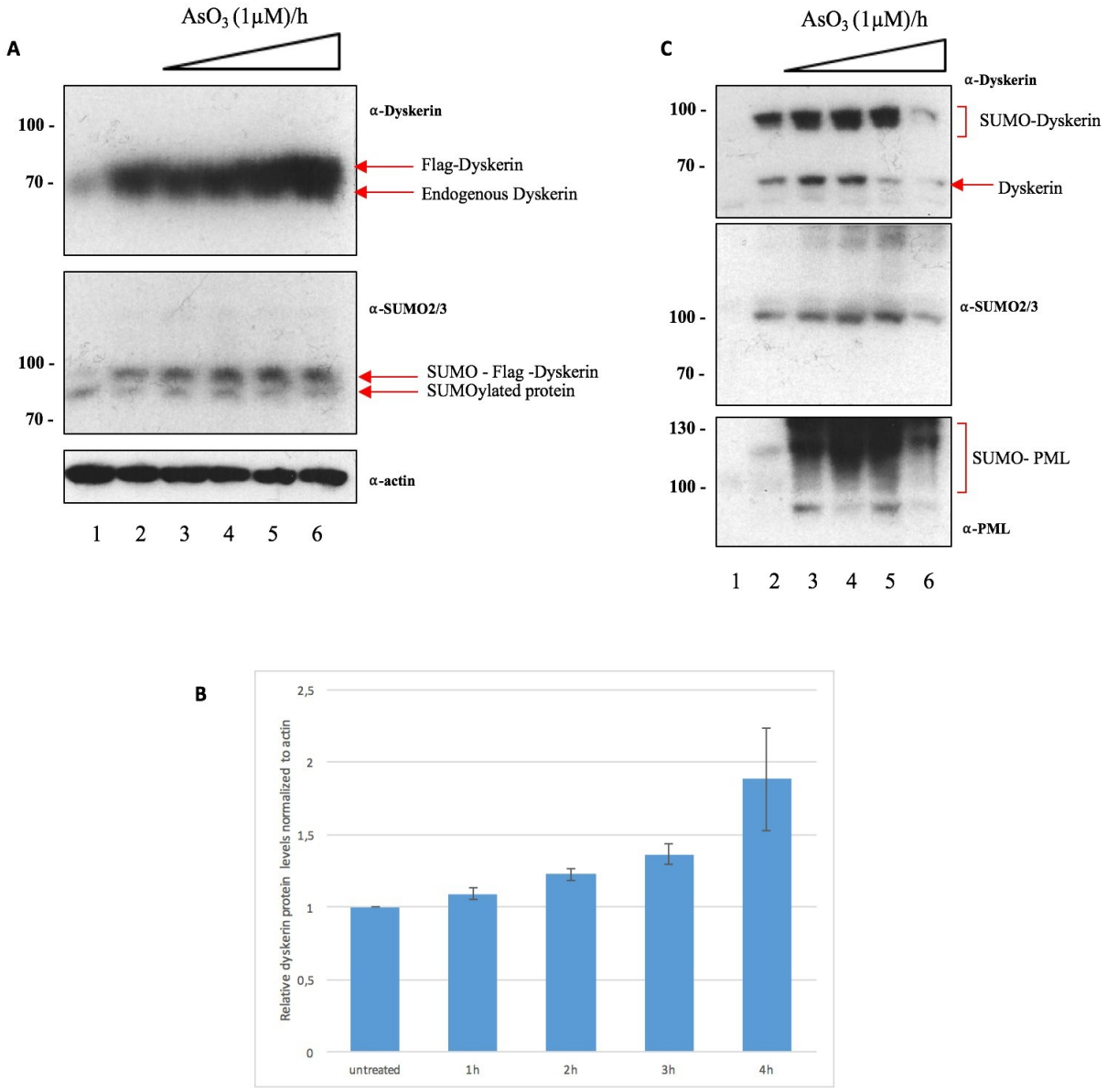

Figure 10. Dyskerin protein levels and SUMOylation are affected by arsenic. HEK293 cells stably expressing His-SUMO3 Flag-dyskerin treated with 1µM of AsO3 for increasing time: 0h (lane 2) 1h (lane 3) 2h (lane 4) 3h (lane 5) 4h (lane 6) and Mock HEK293 cells (untreated control) (lane 1) A) Input of samples blotted against dyskerin and SUMO2/3. Actin blot was used as loading control. B) Quantification of the dyskerin blot signal normalized to actin (n=2). C) NiNTA purification elution blotted against dyskerin, SUMO2/3 and PML as a control of arsenic-triggered SUMOylation. Molecular Weight markers were used for each gel and are indicated on left of the gels in kDa.

observed in the samples from cells expressing His-SUMO3 and Flag- dyskerin, but not in the sample from mock HEK293 cells (Figure 10C, upper panel, compare lanes 2-6 to lane 1). Interestingly, this molecular weight is similar to the one of the protein observed in the SUMO2/3 blot of the input samples and which we propose could correspond to SUMO-Flag dyskerin (Figure 10A, bottom panel, lanes 2-6). A protein slightly below 70 kDa (labeled dyskerin) was also pulled down from the purification (Figure 10C, upper panel, compare lanes 2-6 to lane 1) and may represent non-SUMOylated dyskerin. Since there is evidence that telomerase acts as a dimer, two molecules of dyskerin are expected to be found in each complex[274]. This protein could correspond to endogenous or Flag-dyskerin that were bound to the SUMOylated dyskerin species and enriched during the purification. We observed that levels of the 90 kDa species increased after the AsO_3 treatment between 1 h and 3 h showing that AsO_3 may induce dyskerin SUMOylation. However, levels of the 90 kDa species substantially decreased after 4 h of treatment. The same pattern of global SUMOylated proteins was detected when using an antibody against SUMO2/3 with an increase of SUMOylation between 1 and 3 h of treatment and an important reduction at 4 h of treatment (Figure 10C, middle panel, compare lanes 3-5 to 1 and 6). We also assessed levels of SUMOylated PML after AsO_3 treatment since arsenic has been reported to increase SUMOylation of PML[226]. As previously mentioned, PML is the main component of stress-induced nuclear bodies also known as PML bodies. These dynamic and heterogeneous structures have been associated to inflammation, stress, and diseases such as cancer. They play a role in regulating apoptosis and cellular senescence and are a main site of PTMs[165,280]. The link between PML bodies and SUMOylation arose when it was found that PML, which acts as a “hand holder” for the PML bodies, is SUMOylated[224,281]. We observed a similar increase in PML SUMOylation with increasing time of AsO_3 treatment (Figure 10C bottom panel), as reported in the literature. We also observed a decrease in PML SUMOylation at

4h of AsO_3 treatment like the decrease in dyskerin SUMOylation we observed (Figure 10C, compare lanes 6 in upper and lower panels). As SUMOylated PML has been reported to recruit ubiquitin E3 ligases and target PML to the proteasome for degradation, we hypothesize that arsenic triggers a SUMO-dependent degradation pathway increasing dyskerin SUMOylation and possibly degradation through the recruitment of STUbLs. Since one function of dyskerin is telomerase-specific, we assessed the location of the DNA damage created upon AsO_3 treatment using FISH/IF (Figure 11). We found that the γH2AX foci (green) were dispersed in the nucleus and that they were not localized at the telomere foci (red).

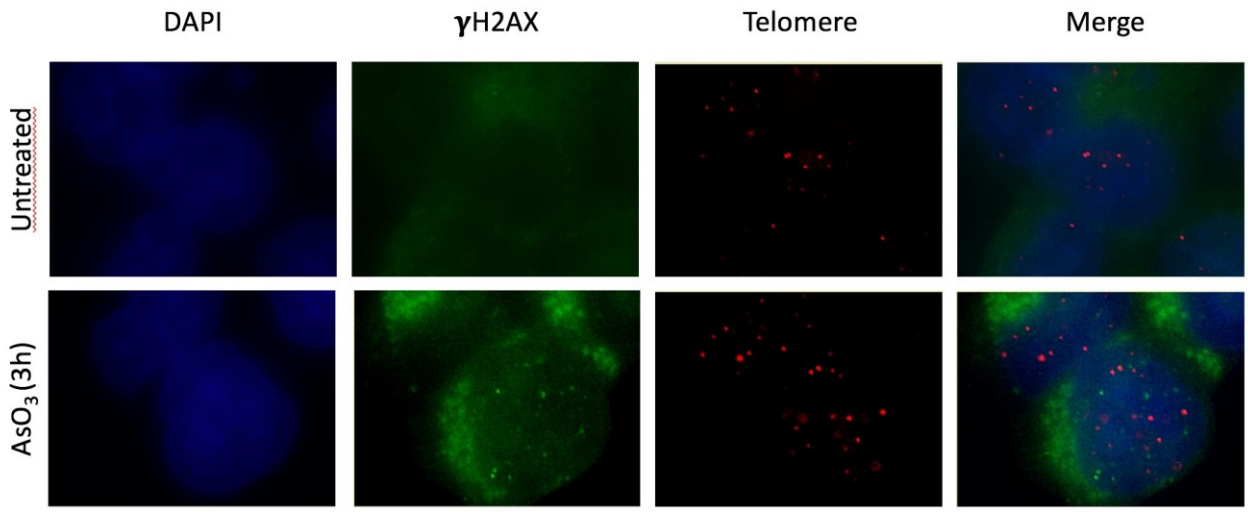

Figure 11. Arsenic treatment creates global DNA damage. FISH/IF of His-SUMO3 Flag dyskerin expressing HEK293 cells for untreated (top lane) and 3 h of AsO_3 treatment (bottom lane) Red foci represent telomeres and green foci represent γH2AX.

III. Telomere-specific damage affects dyskerin protein levels and SUMOylation

When telomeres are unprotected and exposed, such as temporarily, during DNA replication or when they become critically short, they activate a DDR[282,283]. Some mechanisms such as the expression of the telomeric repeat-containing RNA (TERRA) and its binding and accumulation at short telomeres are involved in in the activation of the DDR. This DDR can result in Homology-directed repair if telomerase is not expressed in the cells to rescue the telomere loss[284]. However, when telomerase is expressed, TERRA leads to telomerase nucleation at short telomeres[285]. Other mechanisms have been found to regulate telomerase recruitment at shorter telomeres. Live imaging of the trafficking of the telomerase enzyme reveals multiple short interactions at telomeres while observing a few rare long-lasting interactions[286]. This dynamic of the complex is probably due to probing short telomeres in need of elongation. Many studies have shown that telomerase gets preferentially recruited to short telomeres in yeast[287] as well as in humans[288] and that this preference can be mediated by the low cellular expression of telomerase as well as extracellular pH[289,290]. Moreover, telomerase nucleolar localization was shown to increase upon DNA damage introduction in human lung fibroblast[291] and additional research focused on hTERT further linked telomerase to DNA damage repair[292]. Furthermore, the yeast telomerase RNA nucleoplasmic localization was shown to be mediated by SUMOylation linking telomerase recruitment and SUMOylation[293]. Dyskerin being part of the telomerase complex, we hypothesized that its SUMOylation might be regulated by telomere-specific damage. Our first approach involved the use of the KillerRed-TRF1 (KR-TRF1) construct which expresses a fusion protein of the photosensitizer KillerRed (KR) and the shelterin protein TRF1[267]. KR is a red fluorescent chromophore which synthesizes ROS when activated by light[294,295]. Hence, the expression of KR fused to TRF1 will localize the ROS at telomeres and induce telomere-specific damage[267]. This fusion protein has previously been characterized and shown to induce TIFs[267] After transiently

transfecting His-SUMO3 Flag-dyskerin expressing HEK293 cells with KR-TRF1 and exposing them to light for 3h, we performed a FISH/IF to check that our experimental conditions induce TIFs. As expected, we observed TIFs, measured as the colocalization of γH2AX and telomeres in the KR-TRF1 expressing His-SUMO3 Flag-dyskerin HEK293 cells (Figure 12). The expression of the fusion protein was confirmed using western blot analysis against TRF1 (Figure 13A). We then examined the effect of the presence of TIFs on dyskerin protein levels. We transfected His-SUMO3 Flag-dyskerin HEK293 cells with KR-TRF1 and exposed the cells to light for 1 or 3 h. Dyskerin levels in His-SUMO3 Flag-dyskerin expressing HEK293 cells not transfected with KR-TFR1 and in Mock HEK293 cells were also assessed as controls. First, we found that dyskerin levels were lower in KR-TRF1 transfected His-SUMO3 Flag-dyskerin HEK293 cells upon exposure to light compared to dyskerin levels in similar cells not exposed to light (Figure 13B, compare lanes 3-4 to lane 2). Dyskerin levels were most reduced when cells were exposed to light for 3h (Figure 13B lane 4). This experiment was repeated three times for 1h light exposure, twice for 3h exposure and levels of dyskerin were quantified by normalizing to actin levels (Figure 13C, left graph). Interestingly, when looking at the other H/ACA proteins we found that, while NOP10 levels appeared unaffected in cells harboring telomere damage, NHP2 protein levels increased (Figure 13B) The expression levels of the H/ACA proteins were assessed once and quantified by normalizing to actin levels (Figure 13C, right panel). Interestingly, blotting the same input samples with an antibody against the Flag epitope revealed smears (labeled SUMO(n)-Flag-dyskerin) in the samples from cells exposed to light and expressing KR-TRF1 that could not be observed in the HEK293 cells expressing His-SUMO3 and Flag dyskein not expressing KR-TRF1 (Figure 13D, compare lanes 3 and 4 to lane 2). The decrease of non-SUMOylated Flag-dyskerin (labeled Flag-dyskerin) was observed upon expression of KR-TRF1 in cells subjected to light for 3 h, when immunoblotting was performed against Flag, similarly as when immunoblotting was

performed against dyskerin (compare Figure 13A and D, lanes 4). We hypothesize that the Flag antibody might be more sensitive than the dyskerin antibody allowing the detection of higher molecular weight SUMO-dyskerin species induced by the KR-TRF1 mediated telomeric damage. This data remains preliminary and the experiment will have to be repeated and the results confirmed.

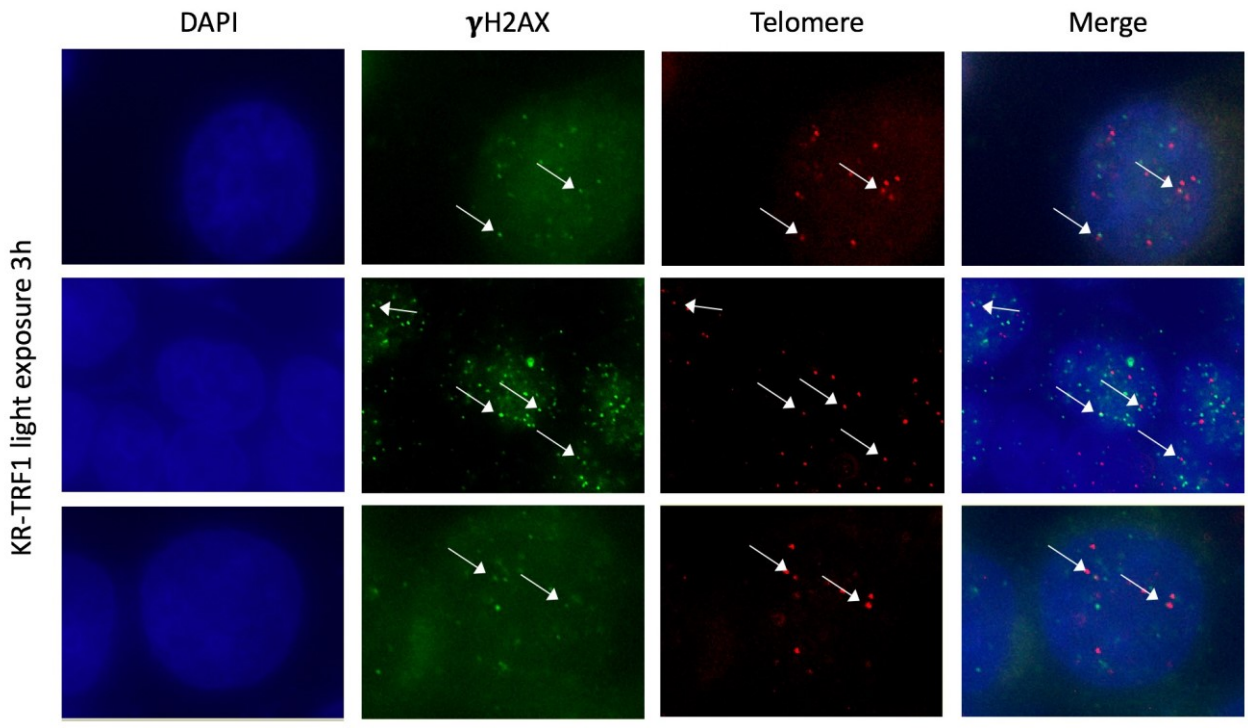

Figure 12. Telomere specific damage induced by light exposure of cells expressing KillerRed-TRF1. FISH/IF of His-SUMO3 Flag dyskerin expressing HEK293 cells transfected with KillerTRF1 and exposed to light for 3h. Red foci represent telomeres and green foci represent γH2AX. White arrows indicate colocalization of signals representing TIFs.

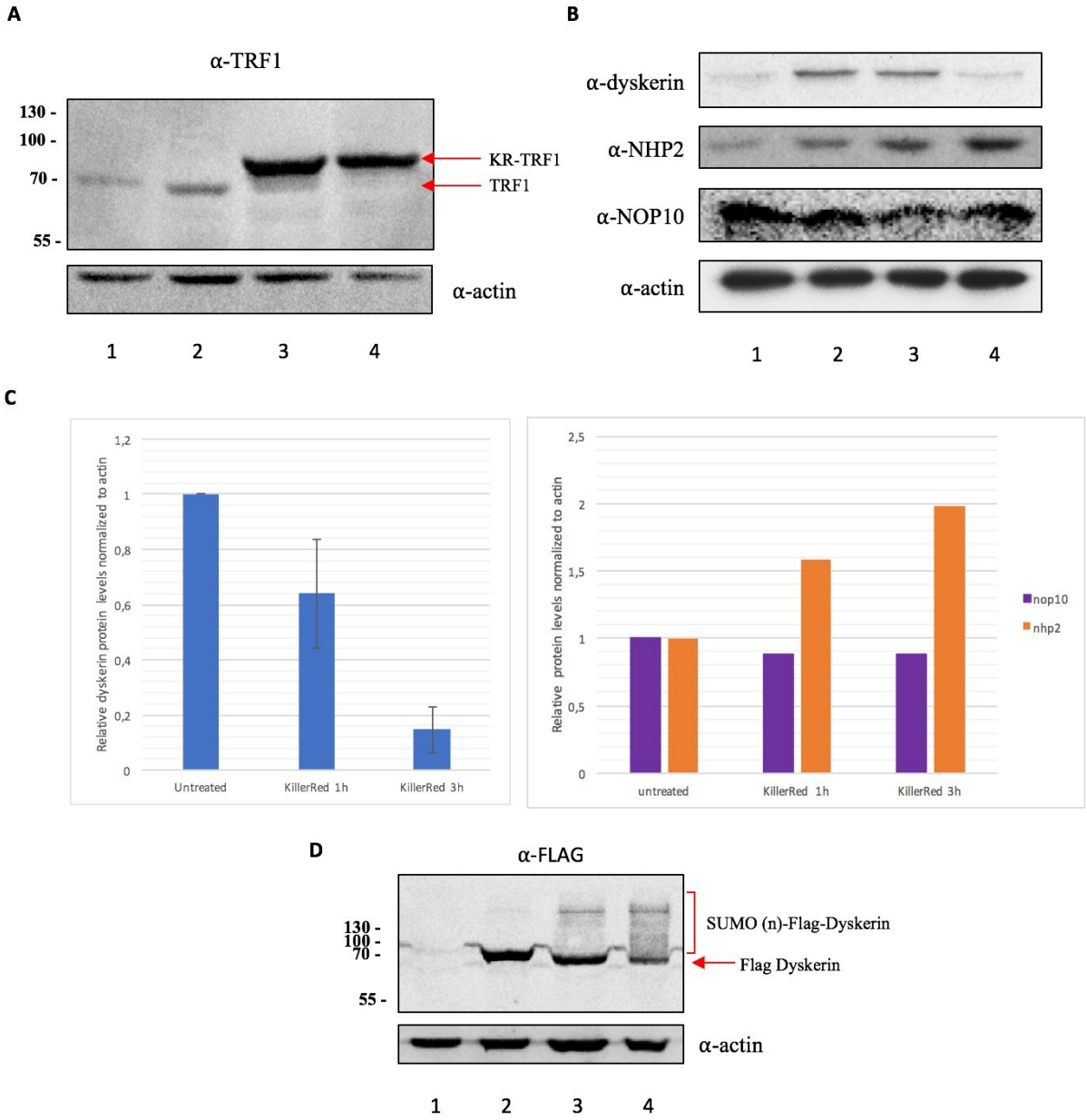

Figure 13. KillerRed-TRF1 expression leads to decreased levels of dyskerin protein levels and differentially affects the H/ACA proteins. HEK293 cells stably expressing His-SUMO3 Flag- dyskerin and transiently expressing the KR-TRF1 fusion protein exposed to light for 1 h (lane 3) and 3 h (lane 4). Mock HEK293 cells (lane 1) and HEK293 cells stably expressing His-SUMO3 Flag-dyskerin (lane 2) but not KR-TRF1 were used as controls. A) Immunoblotting against TRF1 was performed to confirm the expression of the fusion KillerRed-TRF1 protein, expected molecular weight of about 80 kDa. Actin blot was used as a loading control. B) Input samples blotted against dyskerin, NHP2, and NOP10. Actin blot was used as a loading control. C) Quantification of dyskerin protein levels (left panel) after light exposure for 1 h (n=3) and 3 h (n=2) and quantification of NHP2 and NOP10 protein levels (n=1) normalized to actin. D) Input samples blotted against Flag. Actin blot used as loading control. Molecular Weight markers were used for each gel and are indicated on left of the gels in kDa

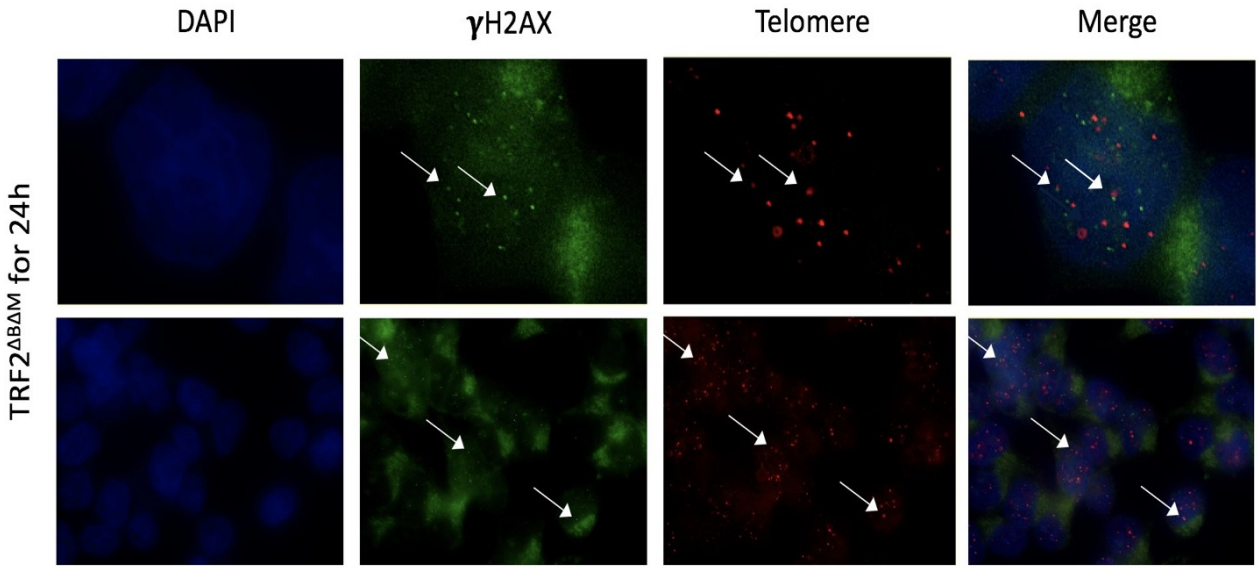

Figure 14. Telomere specific damage induced by the expression of the TRF2 dominant negative. FISH/IF of His-SUMO3 Flag-dyskerin expressing HEK293 transfected with the TRF2 dominant negative construct for 24 h. Red foci represent telomeres and green foci represent γH2AX. White arrows indicate colocalization of signals representing TIFs

We also used a second approach to induce telomere specific damage. We expressed a dominant negative version of the shelterin protein TRF2 truncated on both its N terminal and C-terminal ends ($TRF2^{\Delta B\Delta M}$)[268] which leads to unprotected telomeres and the formation of telomere-specific damage[296]. We confirmed the induction of telomere-localized damage using FISH/IF after transfecting His-SUMO3 Flag-dyskerin HEK293 cells with the TRF2 dominant negative construct (Figure 14) and the expression of the $TRF2^{\Delta B\Delta M}$ by Western analysis (Figure 15A, left panel). Immunoblot analysis against dyskerin showed an increase in dyskerin levels in $TRF2^{\Delta B\Delta M}$-expressing His-SUMO3 Flag-dyskerin expressing HEK293 cells compared to the same cells not expressing $TRF2^{\Delta B\Delta M}$ (Figure 15A, right panel, compare lane 3 to 2). The experiment was repeated 3 times and dyskerin protein levels were quantified and normalized to actin (Figure 15B). We also blotted the same samples with an antibody against the Flag epitope (Figure 15C).

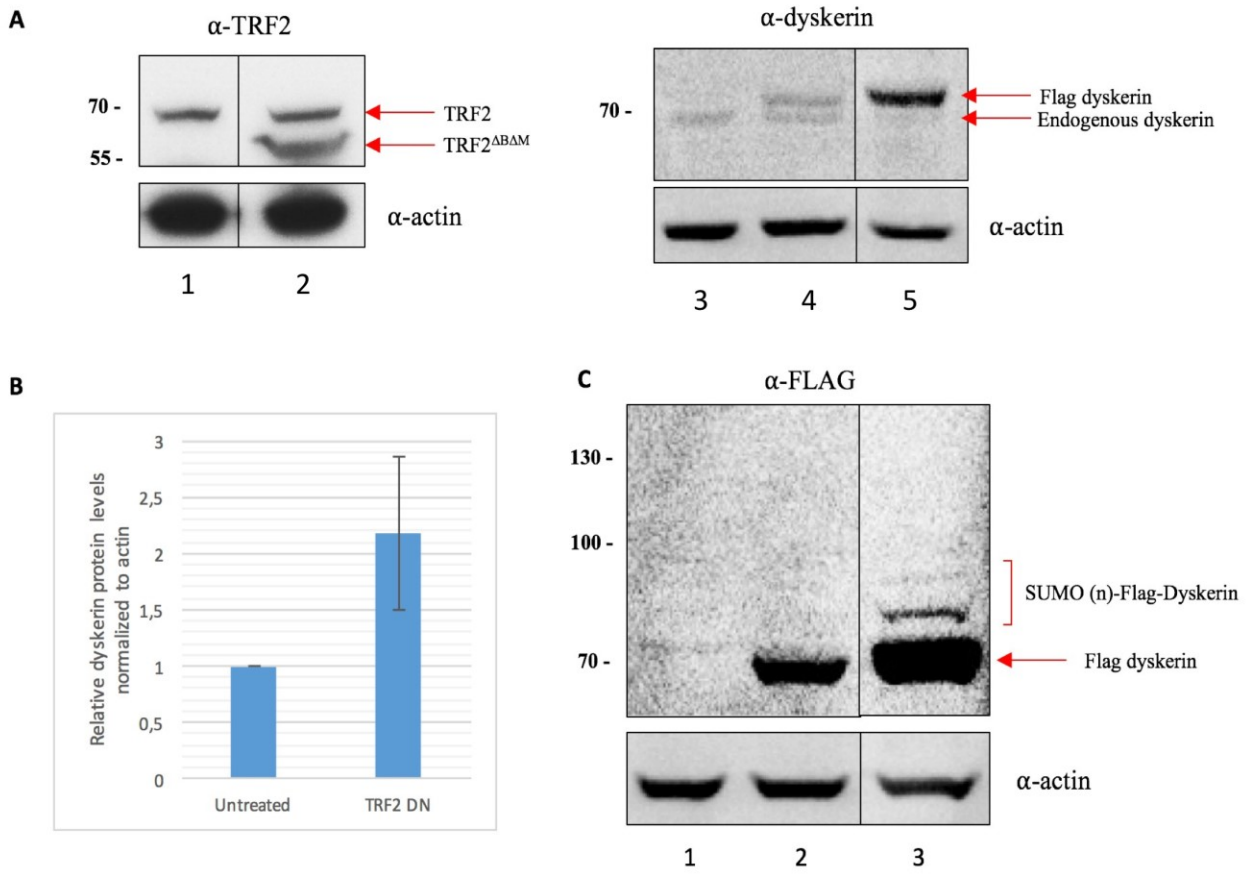

Figure 15. The TRF2 dominant negative induced telomere damage affects dyskerin protein levels and SUMOylation. A) Input samples blotted against TRF2, confirming the expression of the dominant negative TRF2ΔBΔM, expected molecular weight of about 55-60 kDa (left panel) and dyskerin (right panel). HEK293 cells stably expressing His-SUMO3 Flag-dyskerin transiently expressing the truncated dominant negative TRF2 (TRF2ΔBΔM) (lane 2 and 5). Mock HEK293 cells (lane 3) and HEK293 cells stably expressing only His-SUMO3 Flag-dyskerin were used as controls (lane 1 and 4). B) Quantification of dyskerin protein levels 24 h after TRF2ΔBΔM transfection (n=3) C) Input samples blotted against Flag reveals higher molecular weight species of Flag-dyskerin (SUMO (n)-Flag-Dyskerin) in cells expressing TRF2ΔBΔM (lane 3). Mock HEK293 cells (lane 1) and HEK293 cells stably transiently expressing only His-SUMO3 Flag-dyskerin (lane 2). The black boxes indicate the cropping of the lanes from the same membranes. Actin was used as a loading control for A and C. Molecular Weight markers were used for each gel and are indicated on left of the gels in kDa.

Similarly, we observed higher levels of Flag-dykerin in the cells expressing TRF2$^{\Delta B \Delta M}$ compared to the cells not expressing TRF2$^{\Delta B \Delta M}$ (Figure 15C, compare lane 3 to 2). We also observed higher molecular weight species around 80 kDa and 90 kDa (labeled SUMO(n)-Flag-dyskerin). This western blot was also only done once and the experiment should be repeated before further interpretation. For both telomere specific damage inducing approaches, a NiNTA purification should be performed to assess if the observed higher molecular weight species of dyskerin are specific to SUMOylation.

IV. SENP3 is involved in regulating dyskerin SUMOylation

As explained previously, the SENPs display high heterogeneity in their subcellular localization as well as in the SUMO isoforms that they deconjugate (Figure 6). To investigate the potential localization of SUMOylated dyskerin and if there is one predominant SUMO isoform that is conjugated to dyskerin we silenced SENP1 and SENP3, which are mainly active in the nuclear envelope and the nucleolus respectively. Transfection of siRNAs against either SENP1 or SENP3 in His-SUMO3 Flag-dyskerin HEK293 cells decreased SENP1 and SENP3 levels by about 80% of endogenous levels in His-SUMO3 Flag-dyskerin HEK293 cells that were mock transfected or transfected with a siGFP (Figure 16A, top panels, compare lanes 3-4 to lanes 1-2 for SENP3 and lanes 7-8 to lanes 5-6 for SENP1). Lanes 3 and 4 and lanes 7 and 8 are a duplicate of the experiment with the same siRNA, either SENP1 or SENP3. The silencing experiments were repeated 3 times total and SENP 1 and SENP3 protein levels for each siRNA was quantified and normalized to actin levels (Figure 16B). While no significant change in dyskerin protein levels was observed following SENP1 silencing (Figure 16A, bottom panel, lanes 5-8), we observed an increase in dyskerin protein levels following SENP3 silencing (Figure 16A, bottom panel, compare lanes 3-4 to lanes 1-2). The experiment was repeated twice and dyskerin protein levels were quantified and normalized to tubulin (Figure 16C). Additionally, a slight shift in molecular weight of dyskerin

was induced by SENP3 silencing which could correspond to the addition of one SUMO protein (Figure 16A, bottom panel labeled SUMOylated dyskerin). This result is consistent with the function and nucleolar nature of dyskerin as SENP3 is most active in the nucleolus. Also, dyskerin has been shown previously in our lab to be modified by SUMO2/3 which are the isoforms favored by SENP3[130,193]. This is also consistent with the lack of effect from SENP1 silencing as it is mainly active in the nuclear envelope[189].

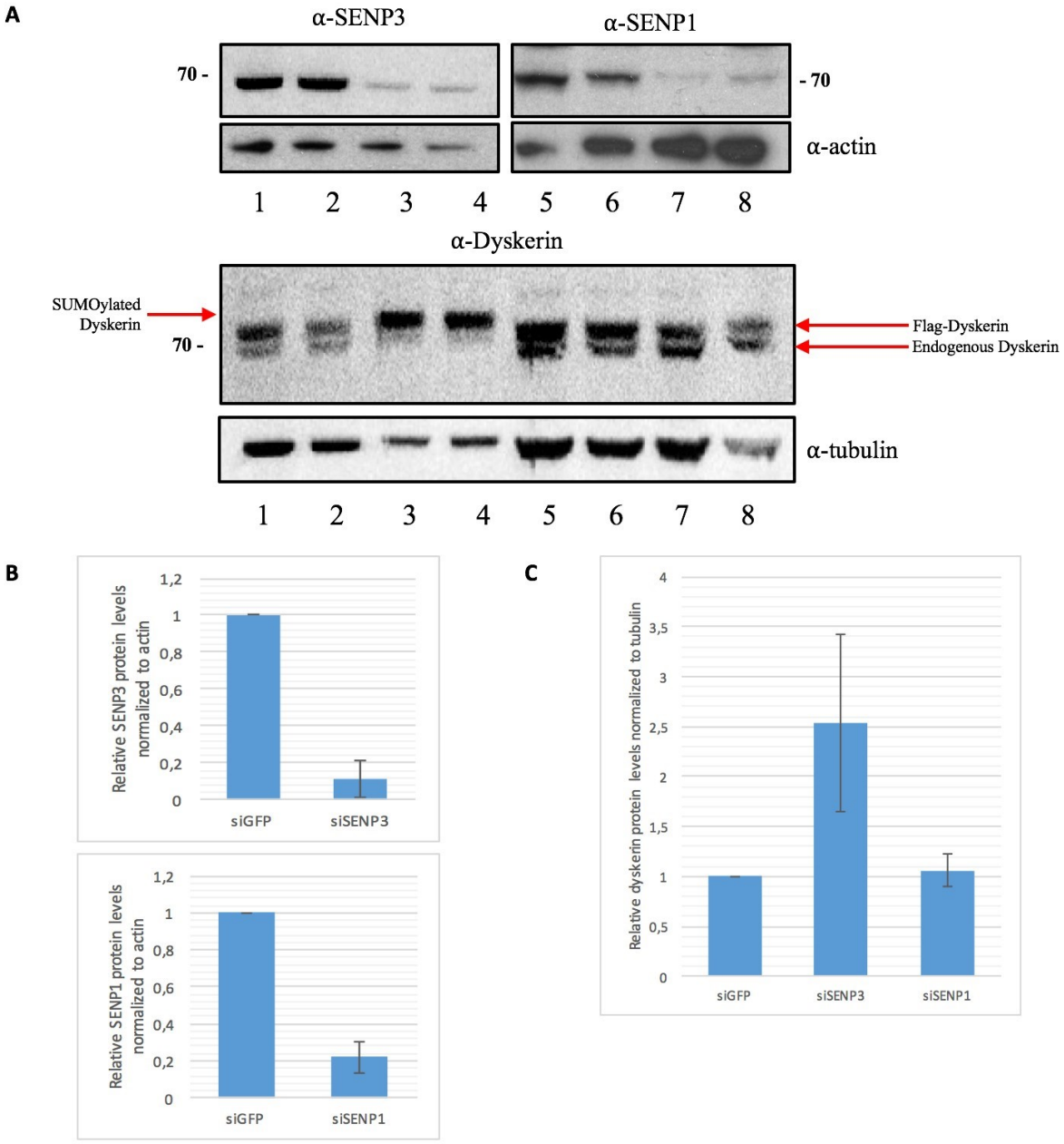

Figure 16. SENP3 silencing leads to increased dyskerin protein levels and stabilized SUMOylation of dyskerin. HEK293 cells stably expressing His-SUMO3 Flag-dyskerin transfected with siSENP3 (lane 3-4) and siSENP1 (lane 7-8). Lanes 3 and 4 for siSENP3, and 7 and 8 for siSENP1, represent samples from two different experiments loaded on the same gel. HEK293 cells stably expressing His-SUMO3 Flag-dyskerin untreated (lane 1) and transfected with siGFP (lane 2) were used as controls. A) Input samples blotted against SENP3 (top left panel, lane 1-4) SENP1 (top right panel, lane 5-8) with actin as a loading control and dyskerin (bottom panel) with tubulin as a loading control. B) Quantification of total SENP3 and SENP1 protein levels normalized to actin (n=3). C) Quantification of dyskerin protein levels for each sample normalized to tubulin (n=3). Molecular Weight markers were used for each gel and are indicated on left of the gels in kDa.

V. Identification of the E3 ligase using a proximity dependent biotin identification

The E3 ligase involved in the SUMO cycle is analogous to the ubiquitin E3 ligase and is necessary *in vivo* to transfer the SUMO protein from the Ubc9 conjugating enzyme to its target (Figure 5). While hundreds of ubiquitin E3 ligases have already been identified, only a few have been characterized for SUMOylation. However, we suspect that an important pool of these enzymes still must be discovered. Therefore, instead of following a biased approach targeting the few E3 ligases discovered, we used an unbiased approach involving a proximity dependent biotin identification (BioID) to attempt to identify the E3 ligase involved in dyskerin SUMOylation. This technique is based on the fusion of a bait protein to the *E.Coli* biotin ligase Bifunctional ligase/Repressor A (BirA). While highly specific as a wild type protein, a mutant BirA (BirA*), R118A makes the enzyme promiscuous. Therefore, any protein located near (10nm) or having a weak interaction with the chosen bait protein that is fused to the mutant BirA will be tagged by biotinylation at lysine residues[297]. Using streptavidin beads, these proteins are purified and analyzed by MS. For our experiment, we used dyskerin as our bait protein and fused it to BirA* either at the N-terminus or C-terminus of dyskerin also tagged with Myc and HA respectively (Figure 17). Using two constructs is important in case the fusion at one terminus affects the structure and function of the fusion protein, but also in case dyskerin SUMOylation sites are biotinylated by BirA*, and affect the interaction or function of SUMOylation dependent interactors that we are trying to identify. His-SUMO3 Myc-BirA*-dyskerin stably expressing HEK293 cells and His-SUMO3 HA-BirA*-dyskerin stably expressing HEK293 cells were generated. Similarly, His-SUMO3 Myc-BirA* and His-SUMO3 HA-BirA* expressing HEK293 cells were also generated. Including these controls is necessary for the MS analysis to identify and exclude the non-dyskerin specific proteins that are biotinylated such as keratin and other naturally biotinylated proteins as well as proteins that BirA* alone would interact with. Prior to performing MS, it is

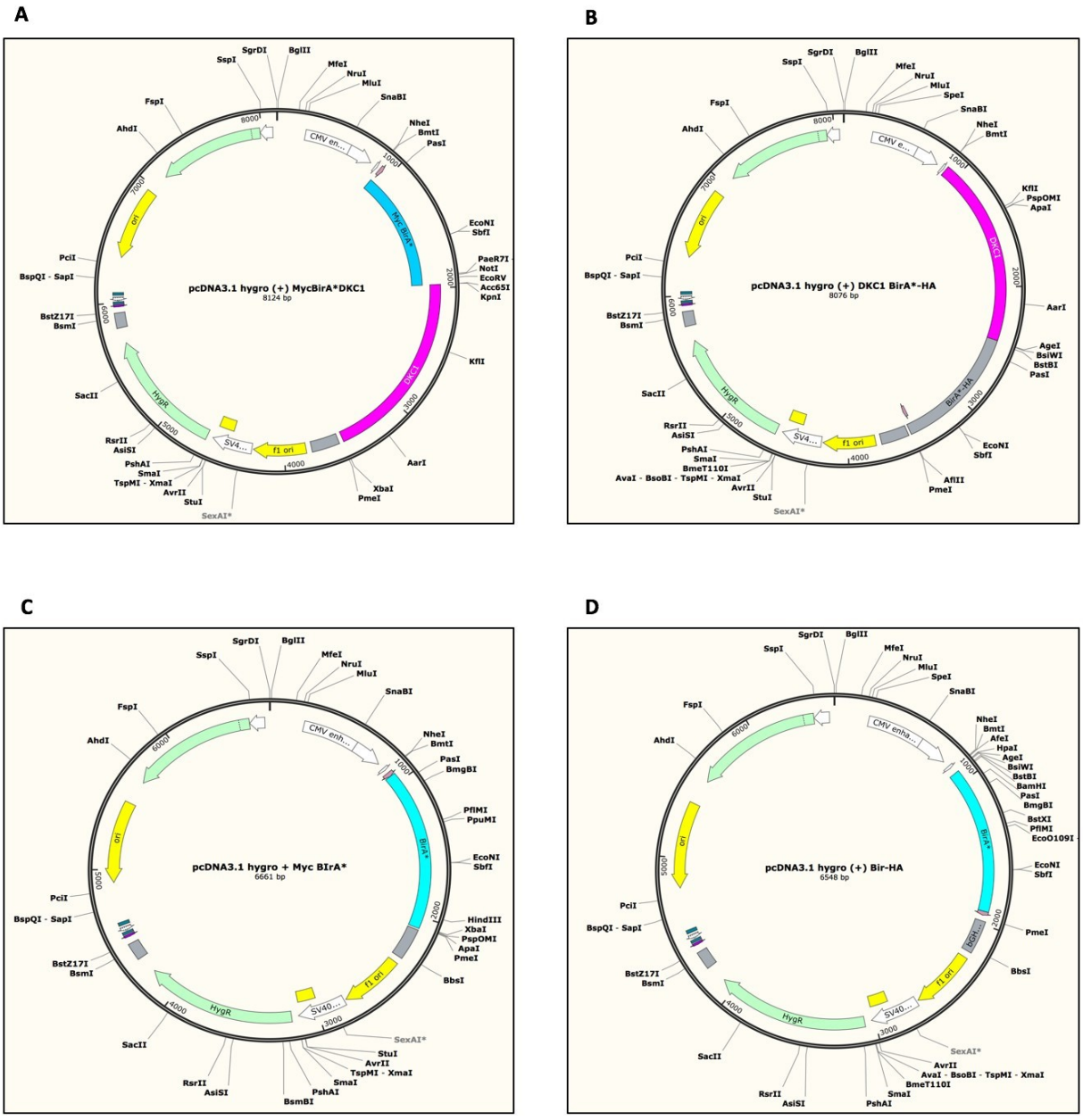

Figure 17. BioID constructs designed using dyskerin as a bait. A) MycBirA* was fused to dyskerin at the N-terminus. B) HA-BirA* was fused to dyskerin at the C-terminus. A control construct for each fusion protein was used: Myc-BirA* alone for Myc-BirA*-dyskerin (C) and HA-BirA* alone for dyskerin-BirA*HA (D).

necessary to verify fusion protein expression, localization of the fusion protein as an indication of its function and that BirA* is active (Figure 18). Cell extracts from each of the generated BioID cell lines were assessed for fusion protein expression by immunoblotting against dyskerin as well as either the Myc or HA epitope tags (Figure 18A). Both BirA*-dyskerin tagged proteins were observed at approximately 100 kDa as predicted (Figure 18A, lanes 3 and 4) and each control BirA* protein at about 40 kDa (Figure 18A, right panel, lanes 1 and 2). Second, we checked the localization of the fusion proteins using IF against each tag and TCAB1, a protein, which similarly to dyskerin, localizes to the CB. The localization for each fusion protein was observed to overlap with TCAB1 foci (Figure 18B). Additional foci in the nucleus to which the fusion proteins localized displayed a nucleolar pattern although colocalization with a nucleolar marker such as fibrillarin would be necessary to confirm that these foci are nucleolar. Finally, we performed a streptavidin purification with cell extracts prepared from each BioID cell line and used Strepatividin HRP to detect biotinylated proteins by immunoblot analysis. We observed a larger number of biotinylated proteins in the samples from cells expressing BirA* fused to dyskerin compared to the samples from cells expressing BirA* only (Figure 18C, compare lanes 1 and 2, 5 and 6), which is expected as BirA*-dyskerin should interact with more proteins than BirA* alone. The number of biotinylated proteins is further increased in samples from both HA-BirA*dyskerin and Myc-BirA*dyskerin expressing cells after the streptavidin purification confirming BirA* activity of the fusion proteins (Figure 18C, compare lanes 2 and 4, 6 and 8). Preliminary data following a first run of the mass spectrometry analysis from the streptavidin pulldown of these cell lines gave promising information. We used the integrated software ProHits developed form Anne Claude Gingras's lab, a program that allows an easy and efficient analysis of mass spectrometry based interaction proteomics[298]. The data is sorted through multiple RefSeq protein databases. Comet and Mascot were chosen for this analysis. It then lets you observe all the peptides obtained

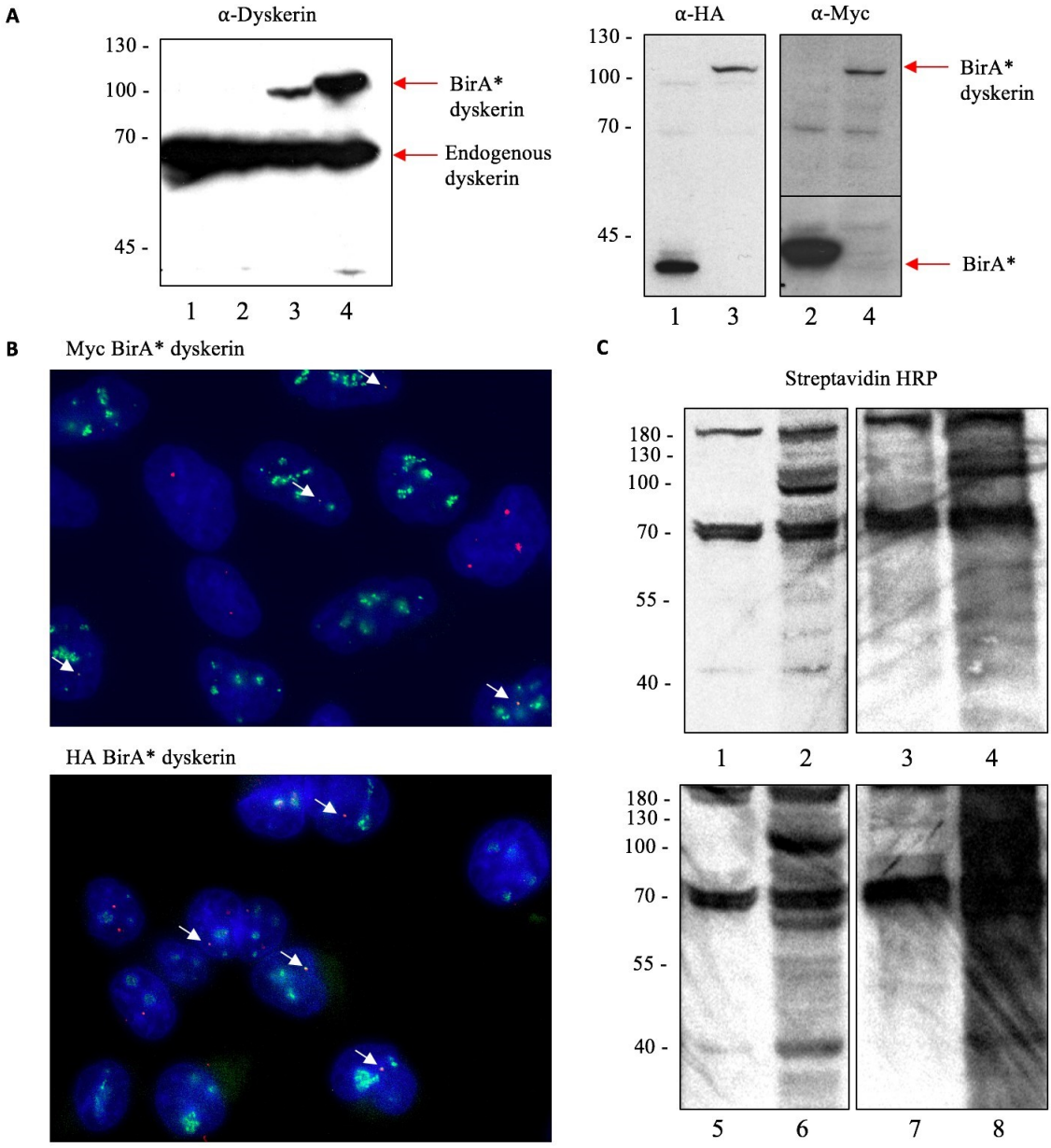

Figure 18. BirA* dyskerin fusion proteins are expressed properly, localize properly and contain an active BirA*. HEK293 cells stably expressing His-SUMO3 were stably transfected with either Myc-BirA* alone, Myc-BirA*-dyskerin, HA-BirA* alone or HA-BirA*dyskerin. A) Input samples of lysates from cells expressing HA-BirA* alone (lane 1, 39 kDa), Myc-BirA* alone (lane 2, 41 kDa), dyskerin-BirA*HA (lane 3, 109 kDa) and Myc-BirA*-dyskerin (lane 4, 111 kDa) were blotted against dyskerin, HA or Myc. B) Immunofluorescence against TCAB1 (red foci) and Myc (top picture) or HA (bottom picture) (green foci). C) Streptavidin HRP blot of input (lanes 1, 2, 5 and 6) and streptavidin pulldown (lanes 3, 4, 7 and 8) samples revealing biotinylated proteins in each cell line expressing HA-BirA* alone (lanes 1 and 3), HA-BirA* dyskerin (lanes 2 and 4), Myc-BirA* alone (lanes 5 and 7), Myc-BirA*-dyskerin (lanes 6 and 8) after 18 h incubation in 50 µM biotin. Molecular Weight markers were used for each gel and are indicated on left of the gels in kDa.

with each fusion protein, sorting them by the number of peptides for one specific protein as well as the number of unique peptides in this pool. The additional function of this tool is the significance analysis of intercactome (SAINT) algorithm which will compare the spectral count of unique peptides in our bait fusion proteins compared to our negative controls. For this experiment, we set out our Saint Score at 95 % of confidence and our False Discovery Rate at 0.02. The proteins identified as significant are then termed "hits". Interestingly, the HA tagged samples gave more reliable hits compared to the Myc samples displaying higher spectral peptide counts for the expected proteins known to interact with dyskerin. While both the HA-BirA* dyskerin and Myc-BirA* dyskerin led to the identification of H/ACA RNP subunits such as NHP2, NAF1, GAR1, NOP10 and SHQ1, the Myc-BirA*dyskerin did not identify reptin and pontin which were present for the HA-BirA* dyskerin. Also, while both showed to have significant biotinylation of telomerase specific proteins including TCAB1, only the HA-BirA* dyskerin sample pulled down SUMO specific proteins such as Ubc9, SUMO3 and SUMO1. Further analysis of the hits from the HA- BirA* dyskerin revealed clusters specific to the nucleolus (nucelolin, fibrillarin), ribosome biogenesis, translation, mitosis and some additional telomerase specific component. Therefore, this construct including its HA-BirA* control seem promising for future analysis of proteins having weak interactions with dyskerin. Specific proteins to be validated will be chosen once the experiment has been repeated two more times.

DISCUSSION

SUMOylation allows the tight regulation of multiple cellular processes via the alteration of protein localization, protein activation, or protein-protein interactions. Moreover, many studies have already linked this PTM to cell cycle progression. Both in budding yeast and mouse embryos, a Ubc9 knockdown leads to cell cycle arrest and multiple mitotic abnormalities[272]. Dyskerin has been associated to multiple functions among which we distinguish two that are cell cycle dependent: first, dyskerin is a key element of the telomerase complex as it is necessary for hTR stabilization and telomerase assembly which has an optimal activity in S phase and second, this nucleolar protein has been shown to have a role at the mitotic apparatus during mitosis with increased protein levels in G2/M. Among its multiple SUMOylation sites, maybe some conserved sites are involved in regulating the protein activity or localization at specific time points of the cell cycle. Our results reveal that dyskerin SUMOylation peaks in S phase and G2/M (Figure 8B-D) which correspond exactly to its cell cycle dependent functions described previously. Whether dyskerin SUMOylation is specific to and essential for each of these functions remains to be determined. If it is, further experiments will also be required to understand if SUMOylation regulates these dyskerin functions by regulating the localization or function of dyskerin or by recruiting other proteins. Unfortunately, it is difficult to identify SUMOylated forms of dyskerin with immunofluorescence so the tracking of the modified protein across the cell cycle would require a more advanced technique. Many experiments have used the fluorescent resonance energy transfer (FRET)[299] and bioluminescence resonance energy transfer (BRET)[300] to be able to follow quantitatively and in a time course the SUMOylation of their proteins of interest. The SUMO protein is fused to a fluorescent or bioluminescent protein termed as donor which will emit a certain wavelength when activated. The bait, for example dyskerin, is fused to an acceptor protein capable of absorbing the wavelength emitted by the donor protein and emit a different one. This way, when

SUMO interacts with the bait, the wavelength/color caught in the microscope will change. These methods have been helpful as they are highly sensitive and allow the tracking of the interaction spatiotemporally. Another alternative might be to synchronize His-SUMO3 Flag-dyskerin expressing HEK293 in G1, S phase and G2/M followed by a cell fractionation of each sample to identify the subcellular localization that is enriched in SUMOylated dyskerin at each cell cycle phase. Finally, a BioID experiment could be performed to identify enriched protein interactors in cells that are in different phases of the cell cycle after arresting them at different stages of the cell cycle using treatments such as thymidine for G1, hydroxyurea for S phase and nocodazole for G2/M. This experiment could also provide more information about dyskerin's role in the mitotic apparatus, whether it is directly interacting with mitotic elements or if it is indirectly involved due to its role in ribosomal biogenesis and translation of mitotic proteins.

As previously described, SUMOylation is highly implicated in the regulation of multiple proteins involved in the DDR such as RPA[167,234], BLM[235] or even BRCA1[232]. Multiple studies characterizing SUMOylation induce genotoxic stress using cellular models to observe if SUMOylation of proteins of interest can be induced[147]. In this part of my project, we wanted to find DNA damaging agents that could increase dyskerin SUMOylation. The first treatment that we tested was doxorubicin. We observed that dyskerin protein levels slightly increased with low amount of doxorubicin for 24 h but that, as concentrations were increased, dyskerin protein levels decreased (Figure 9A & B). Moreover, global SUMOylation levels did not seem to be impacted by the treatment (Figure 9C). Dyskerin depleted cells have been shown to be less sensitive to the damage induced by doxorubicin treatments in human breast cancers and osteosarcomas[137,278]. This decreased sensitivity seems to be due to a reduction in downstream factors involved in the cell cycle checkpoints such as p53 and p21 rather than a direct effect of dyskerin on the cell response to doxorubicin. This is further supported by research showing that

reduction of dyskerin levels leads to reduced p53 levels and that p53 deficiency also leads to reduced doxorubicin-induced cell death[137,278,301]. Studies have shown doxorubicin can downregulate the SUMOylation of KRAB domain-associated protein 1 (KAP1) relieving its repression on p21 transcription[302,303]. However, these studies mainly show that doxorubicin leads to the activation of a DDR and activates phosphorylation of key DNA repair factors such as ATM and ATR which will lead to reduced KAP1 SUMOylation due to competition by phosphorylation. Therefore, doxorubicin seems to act indirectly on protein SUMOylation states which corresponds to the observed stable levels of global SUMOylated proteins following the treatment. Moreover, doxorubicin has been shown to decrease dyskerin protein levels[135]. However, in the latter study, only one concentration of doxorubicin was tested (0.5 μg/ml) which corresponds to the highest concentration (1 μM) we used in our experiments. Doxorubicin is a DNA intercalating agent and induces a cell cycle arrest in the G1/S phase. We can hypothesize that at very low dosage, doxorubicin creates DNA damage but not sufficiently to induce cell cycle arrest. Dyskerin levels might be increased reflecting one of dyskerin's functions in DNA damage repair. As the concentration of doxorubicin keeps increasing, the cells are blocked in G1, which as observed in our cell cycle experiment, leads to decreased dyskerin protein levels (Figure 8B and 9A & B). Conducting a time-dependent treatment of doxorubicin at these different concentrations could give some insights on whether dyskerin protein levels are downregulated right after treatment administration or if it happens gradually over time. It will also show if the increase at low dosage of doxorubicin is constant or only peaks for a few hours. Finally, further experiments, such as repeating the NiNTA purification, need to be conducted to confirm that doxorubicin treatment is not impacting, directly or indirectly SUMOylated dyskerin levels. The NiNTA purification may be done with an increased number of cells to account for the fact that high dosage of doxorubicin reduced dyskerin protein levels.

SUMOylation of PML was found to be inducible with arsenic. Other studies in human cell lines have used arsenic as a mean to induces global cellular SUMOylation[146,304]. The interest in understanding the function of SUMOylation in PML bodies grew when further studies proved that their assembly leads to the SUMOylation of PML-interacting proteins such as the death domain-associated protein 6 (DAXX), X-box protein 1 and SP100 *in vivo* in human cells[305-308]. More detailed studies identified two processes allowing PML bodies to regulate cellular death through SUMOylation. First, it was shown that some PML partners contain a SIM motif allowing their recruitment to the SUMO chains on PML body proteins such as DAXX, a transcription factor inhibitor. In this case, DAXX binds to transcription factors and targets them to the PML bodies where they are degraded[308-310]. DAXX also uses its SIM to bind SUMOylated transcription factors specifically such as the androgen receptor and the CREB-binding protein[308,310,311]. The second mechanism is the SUMO-dependent recruitment of ubiquitin E3 ligases which also contain SIMs. These E3 ligases are known as STUbLs. RNF4 has been extensively studied as a PML-related STUbL that is recruited to PML bodies upon AsO_3 treatment and dependent on PML SUMOylation. It is thought that through this mechanism, PML can direct the degradation of transcription factors and other proliferation associated proteins to trigger apoptosis and senescence followed by its own degradation[226]. Here we report that SUMOylated dyskerin levels are increased upon AsO_3 treatment between 1h to 3h which corresponds to the transient SUMOylation of PML and then these higher molecular weight species are lost after 4h, a decrease which is also observed for PML (Figure 10C, bottom panel). Although PML has 3 sites of SUMOylation, the SUMOylation of only one residue (K160) is necessary for its degradation[146,226]. It is possible that different dyskerin SUMOylation sites may regulate different dyskerin functions by different pathways. SUMO-dependent degradation of dyskerin may occur as the formation of SUMO2/3 branches on proteins is the main target for this type of proteasomal-mediated degradation and

previous experiments from our lab showed that dyskerin can be poly-SUMOylated with SUMO2 *in vitro*[130]. To test if the reduction in SUMOylated dyskerin levels we observe at 4 h is due to SUMO-dependent proteasomal degradation we could perform a similar experiment in the presence of MG132 to inhibit protein degradation. MG132 is a proteasome inhibitor, therefore the treatment would prevent proteasomal degradation. If the decrease in dyskerin SUMOylation is in fact due to SUMO-dependent proteasomal degradation, the decrease at 4 h of treatment should no longer be observed.

Furthermore, arsenic has been shown to increase ubiquitination through the activation of the E3 ligase c-Cbl in human airway epithelial cells[312]. If dyskerin is in fact degraded in a SUMO-dependent manner, additional experiments will be required to be able to differentiate whether dyskerin degradation is mediated by the PML bodies specifically or whether it is an indirect effect of the arsenic treatment upregulating other factors such as the ubiquitination machinery. The High mobility group protein HMGI-C (HMGA2) transcription factor was shown to selectively decrease levels of PML bodies in a rat parotid cell line activated by AsO_3. This effect is dependent on a transient SUMOylation of HMGA2 leading PML proteins to a ubiquitin-dependent proteasomal degradation[313]. If the inhibition of HMGA2 SUMOylation also inhibits arsenic-dependent dyskerin degradation, then we will be able to conclude that it is PML-specific. On the other hand, Lin *et al.* mention a motif known as Synergy Control motif which is often found in the consensus motif of the SUMOylation site regulating degradation of proteins which contain this motif[308]. The sequence of this motif resembles P-X(0,3)- I/V-K-X-D/E-X(0,3)-P, where K is the modified lysine residue, X(0,3) is any amino acid from 0 to 3, D/E is an acidic residue and I/V is a hydrophobic residue. Interestingly, the disease associated K43 of dyskerin is located in a similar motif with the amino acid sequence **P**ESK**V**A**K**L**D**TSQW**P**. It would be interesting to see if this lysine SUMOylation specifically is enough to target dyskerin for degradation similarly

to PML[146,226]. K43 mutated dyskerin could be expressed in the His-SUMO3 expressing HEK293 and treated with the same AsO_3 treatments to assess if the degradation at 4h is still observed. If the SUMOylated levels of dyskerin remain stable then we could conclude that this SUMO site is necessary and sufficient in dyskerin for its SUMO- dependent degradation.

The extremities of telomeres can be recognized as DSBs and activate the DDR. Telomere-associated proteins and structures prevent this activation through the formation of higher tertiary structures such as T-loops and G-quadruplexes[19,23]. However, they will be detected as DNA damage and activate the damage response pathway when telomeres become critically short and can no longer be bound by the shelterin complex and form these complexes. SUMOylation has previously been implicated in the recruitment of telomerase at the sites of telomere specific damage in budding yeast where the SUMO E3 ligase Siz1 promotes the nucleoplasmic accumulation of telomerase RNA[293,314]. In this model, SUMOylation is necessary for the *de novo* addition of telomeric repeats at these DNA damage sites. Knowing the role of dyskerin in the telomerase complex and in stabilizing the telomerase RNA, we wanted to determine if inducing telomere-specific damage could be sufficient in our cell model to induce a change in dyskerin SUMOylation. We first observed that dyskerin protein levels are decreased by the induction of ROS at telomeres and this decrease becomes larger as the cells are exposed for longer times to telomere specific ROS (Figure 13A & B). It was also interesting to observe that the levels of other H/ACA proteins such as NOP10 and NHP2 did not follow the same pattern as dyskerin. While NOP10 protein levels were unaffected by the genotoxic treatment NHP2 protein levels decreased with increased exposure to light. A previous study had shown that various DNA damage treatments can lead to different effects on various H/ACA proteins[135]. Among the treatments used in the studies conducted by Lin *et al.*, chloroquine, which also induces ROS[135,315], induced changes in NOP10 and NHP2 levels similar to what we observed upon ROS generation induced by KR-TRF1.

However, no effect on dyskerin levels was observed upon chloroquine treatment. Therefore, the effect the KR-TRF1 fusion protein has on dyskerin in the His-SUMO3 Flag-dyskerin expressing HEK293 may be specifically due to the induced telomere damage. Our results could also indicate that dyskerin regulation is linked to a role dyskerin plays independently of the H/ACA RNP complexes and telomerase[129,131]. On the other hand, it may be that dyskerin is the limiting factor for the assembly of some of these H/ACA complexes and that the downregulation of dyskerin prevents their assembly. We could hypothesize that low levels of dyskerin might repress telomerase assembly through hTR instability and degradation as previously described when dyskerin levels are low[140]. Following an immunoblotting against the Flag-tag of dyskerin, we observed the formation of higher molecular weight dyskerin proteins, and the levels of these proteins increased with longer treatment (Figure 13D). This preliminary data indicates that the creation of ROS species at the telomeres may induce dyskerin SUMOylation while decreasing non-SUMOylated levels of the protein. It was intriguing to observe that inducing telomere-specific damage using a different approach, expression of a dominant negative TRF2 did not lead to the exact same effects on dyskerin. Upon telomere damage induced by the TRF2 variant we observed SUMOylated forms of dyskerin (Figure 15C) but non-SUMOylated dyskerin protein levels also increased (Figure 15A & B). Although we expected to observe similar results using two different ways to induce telomere-specific damage, the KR-TRF1 releases ROS which will also cause non-telomere specific damage [267]. Moreover, the paper characterizing this protein describes the formation of DSBs but also 8-oxo-G which is an oxidative stress specific lesion probably not induced by the expression of the TRF2 dominant negative variant. On the other hand, while KR-TRF1 does not generate unprotected telomeres, the TRF2 dominant negative does and leads to an important shortening of the G-rich strand overhang and telomere shortening[268]. Finally, Sun *et al.* suggest from their data that telomerase might contribute to cell

survival upon oxidative stress by comparing its effect on both telomerase positive and telomerase negative cells[267]. On the other hand, the TRF2 dominant negative expression does not affect telomerase activity[268] but it would be interesting to determine if telomerase negative cells would be more sensitive to the TRF2 dominant negative variant as well. In conclusion, while both these approaches create DSBs at telomeres, their additional side effects might be influencing the effect they have on dyskerin protein levels and SUMOylation.

We previously showed that overexpression of SUMO1 or SUMO3 results in increased dyskerin protein levels upon treatment with the protein synthesis inhibitor cycloheximide compared to the control where no SUMO was expressed[130]. Therefore, it may be that the increased protein levels and molecular weight shift observed after silencing SENP3 in His-SUMO3 Flag-dyskerin expressing HEK293 cells (Figure 16A) is due to an increase in the stability of dyskerin due to its post-translational modification and reveals a role for the specific protease in regulating dyskerin SUMOylation. Furthermore, the specificity of SENPs in their localization and for specific SUMO isoforms allows to further interpret that SUMOylated dyskerin is mainly localized in the nucleolus and that SENP3 is involved in removing SUMO2 or 3 from the protein as they are the isoforms it favors[193,198,269]. However, SENP3 has also been shown to deconjugate SUMO1 in rare cases[193]. Observing a role for SENP3 in dyskerin SUMOylation is further interesting as SENP3 has been shown to regulate ribosomal biogenesis through the processing of other SUMOylated proteins. One research by Haindl *et al.* shows in HEK293 cells that the nucleophosmin protein, involved in the maturation of the 28S ribosomal RNA, interacts with SENP3 and that SENP3 silencing inhibits ribosomal RNA processing[194]. Another study by Finkbeiner *et al.* further identifies a whole nucleolar complex which, after silencing each of these complex subunits in HeLa cells, they conclude this complex to be involved in the processing of the large ribosomal subunit. They further show that two of these subunits are SUMOylated and

processed by SENP3 *in vivo*[195]. SENP3 was also linked to the regulation of the G2/M transition and spindle assembly in mouse oocytes where Huang *et al.* proved that it localizes at microtubules during mitosis while its silencing leads to the spindle assembly checkpoint activation and to abnormal spindle morphogenesis[198]. The cellular processes in which SENP3 has been shown to play a role highly suggests it might also regulate dyskerin SUMOylation since dyskerin is a key regulator of ribosomal RNA maturation through pseudouridylation while playing a major function in orchestrating the G2/M progress and spindle assembly as demonstrated by Alawi *et al.*[110,131]. Further experiments would be required to confirm this hypothesis such as a cellular fractionation experiment to help confirm a dominant nucleolar localization and an *in vitro* experiment analyzing dyskerin SUMOylation with both SUMO1 or SUMO2/3 in the presence of SENP3. The characterization of the SENPs involved in dyskerin SUMOylation is important as it will allow to identify a factor that can be silenced to stabilize SUMOylated dyskerin levels. As mentioned, SUMOylation is a very transient and dynamic modification making it challenging to study in endogenous conditions. If silencing SENP3 can increase the total amount of SUMOylated dyskerin, it will have a significant impact on our ability to perform future experiments.

One important step of the characterization of dyskerin SUMOylation includes the identification of the key factors involved in this cycle. Previous experiments described the identification of SENPs involved in dyskerin SUMOylation and this experiment was meant to identify the E3 ligase involved in dyskerin SUMOylation. Here, we report the functional unbiased approach known as BioID using dyskerin as a bait where dyskerin was fused to the mutated biotin ligase BirA*. This technique allows to identify all proteins that interact with this protein, even weak interactions, or coming in close-proximity to dyskerin. The fusion was made on both the N-terminus and C-terminus of dyskerin. My experiments confirm that these fusion proteins are

properly expressed in stable HEK293 cell lines also expressing His-SUMO3, that they localize properly and that the fused BirA* is capable of biotinylation (Figure 18). Moreover, the proper growth and survival of these cell lines suggests the proper functioning of these dyskerin fusion proteins. Fusing dyskerin to BirA* on the N-terminus or the C-terminus led to the identification of different interactors and affected the efficiency of the BioID approach as the Myc-BirA* control. While the N-terminally tagged dyskerin did not lead to the identification of any SUMO-related proteins after the SAINT analysis, the C-terminally tagged dyskerin identified Ubc9, SUMO1 and SUMO3. As SUMO2 and 3 share 97 % homology, we predict that the system is not sensitive enough to detect differences in peptides for the two different SUMO isoforms. Moreover, we observed that the spectral count for the C-terminal BirA* control was lower than for the Ha-BirA* dyskerin. However, this observation is not so surprising as the HA tag is very little and does not contain any lysine residues, therefore the chances of it being biotinylated are reduced. Although these data are preliminary, the hits obtained present clustering related to the nucleolus, H/ACA proteins, RNA binding, ribosome biogenesis, telomerase and mitosis, which were anticipated from what is known of the functions of dyskerin. After repeating this MS analysis three times, it will be a useful tool to identify a SUMO E3 ligase. Some key signatures of these enzymes include a SIM motif as well as RING domains[316]. From the list obtained after the SAINT analysis, all the hits can be searched for these specific motifs. If promising enzymes are found in this search, we will then silence them or knock them down in our His-SUMO3 Flag-dyskerin expressing HEK293 cell line and observe if it can abolish SUMOylation of dyskerin. Moreover, this approach will be useful for the identification of additional proteins that will help to gain a better understanding of dyskerin functions and the mechanisms regulating these functions. First, the SIM motif can be found in many other proteins that just E3 ligases. This motif allows the recruitment of proteins to SUMOylation branches[316,317]. Any protein identified to have a SIM in our hits will

therefore give also more insights on the role of dyskerin SUMOylation. It would be interesting later to repeat this experiment using a Ubc9 dominant negative protein to abolish SUMOylation and observe the interactions that are being lost. Furthermore, some roles of dyskerin have been less characterized such as its role during mitosis. The pool of proteins identified linked to the mitotic apparatus can be more thoroughly sorted and, using immunoprecipitation against dyskerin, real interactions between dyskerin and mitotic factors can be determined. Therefore, the BioID assay with dyskerin as a bait has an important potential to uncover multiple aspects of SUMOylation-dependent dyskerin interactions and its downstream roles.

CONCLUSION

The data obtained from this research act as a stepping stone to further characterize the mechanisms regulating dyskerin SUMOylation starting with the factors involved in its SUMOylation cycle, the cellular processes it responds to but essentially the proteins recruited or interacting with the SUMO proteins bound to SUMOylated dyskerin and their function. This knowledge is important to have a better understanding of the roles of dyskerin activated or repressed by this modification and possibly its role in telomerase assembly as well as activity.

Additionally, it allows the identification of experimental conditions enhancing and stabilizing dyskerin SUMOylation that will possibly allow the detection of single SUMOylated lysine residue in dyskerin in normal biological conditions without having to overexpress dyskerin or SUMO through large scale proteomics analysis.

REFERENCE LIST

1 MacNeil, D. E., Bensoussan, H. J. & Autexier, C. Telomerase Regulation from Beginning to the End. *Genes (Basel)* **7**, doi:10.3390/genes7090064 (2016).

2 Greider, C. W. & Blackburn, E. H. The telomere terminal transferase of Tetrahymena is a ribonucleoprotein enzyme with two kinds of primer specificity. *Cell* **51**, 887-898 (1987).

3 Greider, C. W. & Blackburn, E. H. Identification of a specific telomere terminal transferase activity in Tetrahymena extracts. *Cell* **43**, 405-413 (1985).

4 Johansson, E. & Dixon, N. Replicative DNA polymerases. *Cold Spring Harb Perspect Biol* **5**, doi:10.1101/cshperspect.a012799 (2013).

5 Kornbeg, A. B., T. *DNA replication*. 2nd edn, (W.H. Freeman and Company, New York, 1991).

6 Shore, D. & Bianchi, A. Telomere length regulation: coupling DNA end processing to feedback regulation of telomerase. *EMBO J* **28**, 2309-2322, doi:10.1038/emboj.2009.195 (2009).

7 Levin, D. S., Bai, W., Yao, N., O'Donnell, M. & Tomkinson, A. E. An interaction between DNA ligase I and proliferating cell nuclear antigen: implications for Okazaki fragment synthesis and joining. *Proc Natl Acad Sci U S A* **94**, 12863-12868 (1997).

8 Maloy, S. R. & Hughes, K. T. *Brenner's encyclopedia of genetics*. Second edition. edn, (Elsevier/Academic Press, 2013).

9 Watson, J. D. Origin of concatemeric T7 DNA. *Nat New Biol* **239**, 197-201 (1972).

10 Olovnikov, A. M. A theory of marginotomy. The incomplete copying of template margin in enzymic synthesis of polynucleotides and biological significance of the phenomenon. *J Theor Biol* **41**, 181-190 (1973).

11 Harley, C. B., Futcher, A. B. & Greider, C. W. Telomeres shorten during ageing of human fibroblasts. *Nature* **345**, 458-460, doi:10.1038/345458a0 (1990).

12 Shay, J. W. & Wright, W. E. Hayflick, his limit, and cellular ageing. *Nat Rev Mol Cell Biol* **1**, 72-76, doi:10.1038/35036093 (2000).

13 McEachern, M. J. & Blackburn, E. H. A conserved sequence motif within the exceptionally diverse telomeric sequences of budding yeasts. *Proc Natl Acad Sci U S A* **91**, 3453-3457 (1994).

14 Moyzis, R. K. *et al.* A highly conserved repetitive DNA sequence, (TTAGGG)n, present at the telomeres of human chromosomes. *Proc Natl Acad Sci U S A* **85**, 6622-6626 (1988).

15 Calado, R. T. & Dumitriu, B. Telomere dynamics in mice and humans. *Semin Hematol* **50**, 165-174, doi:10.1053/j.seminhematol.2013.03.030 (2013).

16 Houghtaling, B. R., Cuttonaro, L., Chang, W. & Smith, S. A dynamic molecular link between the telomere length regulator TRF1 and the chromosome end protector TRF2. *Curr Biol* **14**, 1621-1631, doi:10.1016/j.cub.2004.08.052 (2004).

17 Liu, D. *et al.* PTOP interacts with POT1 and regulates its localization to telomeres. *Nat Cell Biol* **6**, 673-680, doi:10.1038/ncb1142 (2004).

18 Ye, J. Z. *et al.* POT1-interacting protein PIP1: a telomere length regulator that recruits POT1 to the TIN2/TRF1 complex. *Genes Dev* **18**, 1649-1654, doi:10.1101/gad.1215404 (2004).

19 de Lange, T. Protection of mammalian telomeres. *Oncogene* **21**, 532-540, doi:10.1038/sj.onc.1205080 (2002).

20 Liu, D., O'Connor, M. S., Qin, J. & Songyang, Z. Telosome, a mammalian telomere-associated complex formed by multiple telomeric proteins. *J Biol Chem* **279**, 51338-51342, doi:10.1074/jbc.M409293200 (2004).
21 Janouskova, E. *et al.* Human Rap1 modulates TRF2 attraction to telomeric DNA. *Nucleic Acids Res* **43**, 2691-2700, doi:10.1093/nar/gkv097 (2015).
22 Giardini, M. A., Segatto, M., da Silva, M. S., Nunes, V. S. & Cano, M. I. Telomere and telomerase biology. *Prog Mol Biol Transl Sci* **125**, 1-40, doi:10.1016/B978-0-12-397898-1.00001-3 (2014).
23 Neidle, S. & Parkinson, G. N. The structure of telomeric DNA. *Curr Opin Struct Biol* **13**, 275-283 (2003).
24 Bai, Y. & Murnane, J. P. Telomere instability in a human tumor cell line expressing a dominant-negative WRN protein. *Hum Genet* **113**, 337-347, doi:10.1007/s00439-003-0972-y (2003).
25 Weinrich, S. L. *et al.* Reconstitution of human telomerase with the template RNA component hTR and the catalytic protein subunit hTRT. *Nat Genet* **17**, 498-502, doi:10.1038/ng1297-498 (1997).
26 Khanna, A. & Stamm, S. Regulation of alternative splicing by short non-coding nuclear RNAs. *RNA Biol* **7**, 480-485 (2010).
27 Wang, P., Yang, L., Gao, Y. Q. & Zhao, X. S. Accurate placement of substrate RNA by Gar1 in H/ACA RNA-guided pseudouridylation. *Nucleic Acids Res* **43**, 7207-7216, doi:10.1093/nar/gkv757 (2015).
28 Ge, J. & Yu, Y. T. RNA pseudouridylation: new insights into an old modification. *Trends Biochem Sci* **38**, 210-218, doi:10.1016/j.tibs.2013.01.002 (2013).
29 McMahon, M., Contreras, A. & Ruggero, D. Small RNAs with big implications: new insights into H/ACA snoRNA function and their role in human disease. *Wiley Interdiscip Rev RNA* **6**, 173-189, doi:10.1002/wrna.1266 (2015).
30 Pederson, T. The nucleolus. *Cold Spring Harb Perspect Biol* **3**, doi:10.1101/cshperspect.a000638 (2011).
31 Kiss, T., Fayet-Lebaron, E. & Jady, B. E. Box H/ACA small ribonucleoproteins. *Mol Cell* **37**, 597-606, doi:10.1016/j.molcel.2010.01.032 (2010).
32 Venteicher, A. S. & Artandi, S. E. TCAB1: driving telomerase to Cajal bodies. *Cell Cycle* **8**, 1329-1331, doi:10.4161/cc.8.9.8288 (2009).
33 Fu, D. & Collins, K. Distinct biogenesis pathways for human telomerase RNA and H/ACA small nucleolar RNAs. *Mol Cell* **11**, 1361-1372 (2003).
34 Theimer, C. A. *et al.* Structural and functional characterization of human telomerase RNA processing and cajal body localization signals. *Mol Cell* **27**, 869-881, doi:10.1016/j.molcel.2007.07.017 (2007).
35 Marrone, A. *et al.* Functional characterization of novel telomerase RNA (TERC) mutations in patients with diverse clinical and pathological presentations. *Haematologica* **92**, 1013-1020 (2007).
36 Bachand, F. & Autexier, C. Functional regions of human telomerase reverse transcriptase and human telomerase RNA required for telomerase activity and RNA-protein interactions. *Mol Cell Biol* **21**, 1888-1897, doi:10.1128/MCB.21.5.1888-1897.2001 (2001).

37 Autexier, C., Pruzan, R., Funk, W. D. & Greider, C. W. Reconstitution of human telomerase activity and identification of a minimal functional region of the human telomerase RNA. *EMBO J* **15**, 5928-5935 (1996).
38 Chen, J. L., Blasco, M. A. & Greider, C. W. Secondary structure of vertebrate telomerase RNA. *Cell* **100**, 503-514 (2000).
39 Martin-Rivera, L. & Blasco, M. A. Identification of functional domains and dominant negative mutations in vertebrate telomerase RNA using an in vivo reconstitution system. *J Biol Chem* **276**, 5856-5865, doi:10.1074/jbc.M008419200 (2001).
40 Kim, N. K., Zhang, Q. & Feigon, J. Structure and sequence elements of the CR4/5 domain of medaka telomerase RNA important for telomerase function. *Nucleic Acids Res* **42**, 3395-3408, doi:10.1093/nar/gkt1276 (2014).
41 Mitchell, J. R. & Collins, K. Human telomerase activation requires two independent interactions between telomerase RNA and telomerase reverse transcriptase. *Mol Cell* **6**, 361-371 (2000).
42 Jady, B. E., Bertrand, E. & Kiss, T. Human telomerase RNA and box H/ACA scaRNAs share a common Cajal body-specific localization signal. *J Cell Biol* **164**, 647-652, doi:10.1083/jcb.200310138 (2004).
43 Venteicher, A. S. *et al.* A human telomerase holoenzyme protein required for Cajal body localization and telomere synthesis. *Science* **323**, 644-648, doi:10.1126/science.1165357 (2009).
44 Vogan, J. M. *et al.* Minimized human telomerase maintains telomeres and resolves endogenous roles of H/ACA proteins, TCAB1, and Cajal bodies. *Elife* **5**, doi:10.7554/eLife.18221 (2016).
45 Egan, E. D. & Collins, K. Specificity and stoichiometry of subunit interactions in the human telomerase holoenzyme assembled in vivo. *Mol Cell Biol* **30**, 2775-2786, doi:10.1128/MCB.00151-10 (2010).
46 Wang, C. & Meier, U. T. Architecture and assembly of mammalian H/ACA small nucleolar and telomerase ribonucleoproteins. *EMBO J* **23**, 1857-1867, doi:10.1038/sj.emboj.7600181 (2004).
47 Egan, E. D. & Collins, K. Biogenesis of telomerase ribonucleoproteins. *RNA* **18**, 1747-1759, doi:10.1261/rna.034629.112 (2012).
48 Huang, C., Karijolich, J. & Yu, Y. T. Post-transcriptional modification of RNAs by artificial Box H/ACA and Box C/D RNPs. *Methods Mol Biol* **718**, 227-244, doi:10.1007/978-1-61779-018-8_14 (2011).
49 Fu, D. & Collins, K. Purification of human telomerase complexes identifies factors involved in telomerase biogenesis and telomere length regulation. *Mol Cell* **28**, 773-785, doi:10.1016/j.molcel.2007.09.023 (2007).
50 Darzacq, X. *et al.* Stepwise RNP assembly at the site of H/ACA RNA transcription in human cells. *J Cell Biol* **173**, 207-218, doi:10.1083/jcb.200601105 (2006).
51 Trahan, C., Martel, C. & Dragon, F. Effects of dyskeratosis congenita mutations in dyskerin, NHP2 and NOP10 on assembly of H/ACA pre-RNPs. *Hum Mol Genet* **19**, 825-836, doi:10.1093/hmg/ddp551 (2010).
52 Ballarino, M., Morlando, M., Pagano, F., Fatica, A. & Bozzoni, I. The cotranscriptional assembly of snoRNPs controls the biosynthesis of H/ACA snoRNAs in Saccharomyces cerevisiae. *Mol Cell Biol* **25**, 5396-5403, doi:10.1128/MCB.25.13.5396-5403.2005 (2005).

53 Hoareau-Aveilla, C., Bonoli, M., Caizergues-Ferrer, M. & Henry, Y. hNaf1 is required for accumulation of human box H/ACA snoRNPs, scaRNPs, and telomerase. *RNA* **12**, 832-840, doi:10.1261/rna.2344106 (2006).
54 Stanley, S. E. *et al.* Loss-of-function mutations in the RNA biogenesis factor NAF1 predispose to pulmonary fibrosis-emphysema. *Sci Transl Med* **8**, 351ra107, doi:10.1126/scitranslmed.aaf7837 (2016).
55 Walbott, H. *et al.* The H/ACA RNP assembly factor SHQ1 functions as an RNA mimic. *Genes Dev* **25**, 2398-2408, doi:10.1101/gad.176834.111 (2011).
56 Grozdanov, P. N., Roy, S., Kittur, N. & Meier, U. T. SHQ1 is required prior to NAF1 for assembly of H/ACA small nucleolar and telomerase RNPs. *RNA* **15**, 1188-1197, doi:10.1261/rna.1532109 (2009).
57 Grozdanov, P. N., Fernandez-Fuentes, N., Fiser, A. & Meier, U. T. Pathogenic NAP57 mutations decrease ribonucleoprotein assembly in dyskeratosis congenita. *Hum Mol Genet* **18**, 4546-4551, doi:10.1093/hmg/ddp416 (2009).
58 Li, S., Duan, J., Li, D., Ma, S. & Ye, K. Structure of the Shq1-Cbf5-Nop10-Gar1 complex and implications for H/ACA RNP biogenesis and dyskeratosis congenita. *EMBO J* **30**, 5010-5020, doi:10.1038/emboj.2011.427 (2011).
59 Singh, M., Wang, Z., Cascio, D. & Feigon, J. Structure and interactions of the CS domain of human H/ACA RNP assembly protein Shq1. *J Mol Biol* **427**, 807-823, doi:10.1016/j.jmb.2014.12.012 (2015).
60 Machado-Pinilla, R., Liger, D., Leulliot, N. & Meier, U. T. Mechanism of the AAA+ ATPases pontin and reptin in the biogenesis of H/ACA RNPs. *RNA* **18**, 1833-1845, doi:10.1261/rna.034942.112 (2012).
61 Venteicher, A. S., Meng, Z., Mason, P. J., Veenstra, T. D. & Artandi, S. E. Identification of ATPases pontin and reptin as telomerase components essential for holoenzyme assembly. *Cell* **132**, 945-957, doi:10.1016/j.cell.2008.01.019 (2008).
62 Autexier, C. & Lue, N. F. The structure and function of telomerase reverse transcriptase. *Annu Rev Biochem* **75**, 493-517, doi:10.1146/annurev.biochem.75.103004.142412 (2006).
63 Wyatt, H. D., West, S. C. & Beattie, T. L. InTERTpreting telomerase structure and function. *Nucleic Acids Res* **38**, 5609-5622, doi:10.1093/nar/gkq370 (2010).
64 Lingner, J. *et al.* Reverse transcriptase motifs in the catalytic subunit of telomerase. *Science* **276**, 561-567 (1997).
65 Nakamura, T. M. *et al.* Telomerase catalytic subunit homologs from fission yeast and human. *Science* **277**, 955-959 (1997).
66 Chu, T. W., D'Souza, Y. & Autexier, C. The Insertion in Fingers Domain in Human Telomerase Can Mediate Enzyme Processivity and Telomerase Recruitment to Telomeres in a TPP1-Dependent Manner. *Mol Cell Biol* **36**, 210-222, doi:10.1128/MCB.00746-15 (2016).
67 Chu, T. W., MacNeil, D. E. & Autexier, C. Multiple Mechanisms Contribute to the Cell Growth Defects Imparted by Human Telomerase Insertion in Fingers Domain Mutations Associated with Premature Aging Diseases. *J Biol Chem* **291**, 8374-8386, doi:10.1074/jbc.M116.714782 (2016).
68 Lue, N. F., Lin, Y. C. & Mian, I. S. A conserved telomerase motif within the catalytic domain of telomerase reverse transcriptase is specifically required for repeat addition processivity. *Mol Cell Biol* **23**, 8440-8449 (2003).

69 O'Connor, C. M., Lai, C. K. & Collins, K. Two purified domains of telomerase reverse transcriptase reconstitute sequence-specific interactions with RNA. *J Biol Chem* **280**, 17533-17539, doi:10.1074/jbc.M501211200 (2005).
70 Jacobs, S. A., Podell, E. R. & Cech, T. R. Crystal structure of the essential N-terminal domain of telomerase reverse transcriptase. *Nat Struct Mol Biol* **13**, 218-225, doi:10.1038/nsmb1054 (2006).
71 Sealey, D. C. *et al.* The N-terminus of hTERT contains a DNA-binding domain and is required for telomerase activity and cellular immortalization. *Nucleic Acids Res* **38**, 2019-2035, doi:10.1093/nar/gkp1160 (2010).
72 Zhu, Y., Tomlinson, R. L., Lukowiak, A. A., Terns, R. M. & Terns, M. P. Telomerase RNA accumulates in Cajal bodies in human cancer cells. *Mol Biol Cell* **15**, 81-90, doi:10.1091/mbc.E03-07-0525 (2004).
73 Heiss, N. S. *et al.* Dyskerin localizes to the nucleolus and its mislocalization is unlikely to play a role in the pathogenesis of dyskeratosis congenita. *Hum Mol Genet* **8**, 2515-2524 (1999).
74 Richard, P. *et al.* A common sequence motif determines the Cajal body-specific localization of box H/ACA scaRNAs. *EMBO J* **22**, 4283-4293, doi:10.1093/emboj/cdg394 (2003).
75 Tycowski, K. T., Shu, M. D., Kukoyi, A. & Steitz, J. A. A conserved WD40 protein binds the Cajal body localization signal of scaRNP particles. *Mol Cell* **34**, 47-57, doi:10.1016/j.molcel.2009.02.020 (2009).
76 Cristofari, G. *et al.* Human telomerase RNA accumulation in Cajal bodies facilitates telomerase recruitment to telomeres and telomere elongation. *Mol Cell* **27**, 882-889, doi:10.1016/j.molcel.2007.07.020 (2007).
77 Yuan, P. *et al.* Telomerase Cajal body protein 1 depletion inhibits telomerase trafficking to telomeres and induces G1 cell cycle arrest in A549 cells. *Oncol Lett* **8**, 1009-1016, doi:10.3892/ol.2014.2306 (2014).
78 Chen, Y. *et al.* Human cells lacking coilin and Cajal bodies are proficient in telomerase assembly, trafficking and telomere maintenance. *Nucleic Acids Res* **43**, 385-395, doi:10.1093/nar/gku1277 (2015).
79 Tomlinson, R. L., Li, J., Culp, B. R., Terns, R. M. & Terns, M. P. A Cajal body-independent pathway for telomerase trafficking in mice. *Exp Cell Res* **316**, 2797-2809, doi:10.1016/j.yexcr.2010.07.001 (2010).
80 Poole, A. R. & Hebert, M. D. SMN and coilin negatively regulate dyskerin association with telomerase RNA. *Biol Open* **5**, 726-735, doi:10.1242/bio.018804 (2016).
81 Stern, J. L., Zyner, K. G., Pickett, H. A., Cohen, S. B. & Bryan, T. M. Telomerase recruitment requires both TCAB1 and Cajal bodies independently. *Mol Cell Biol* **32**, 2384-2395, doi:10.1128/MCB.00379-12 (2012).
82 Platani, M., Goldberg, I., Swedlow, J. R. & Lamond, A. I. In vivo analysis of Cajal body movement, separation, and joining in live human cells. *J Cell Biol* **151**, 1561-1574 (2000).
83 Jady, B. E., Richard, P., Bertrand, E. & Kiss, T. Cell cycle-dependent recruitment of telomerase RNA and Cajal bodies to human telomeres. *Mol Biol Cell* **17**, 944-954, doi:10.1091/mbc.E05-09-0904 (2006).
84 Tomlinson, R. L., Ziegler, T. D., Supakorndej, T., Terns, R. M. & Terns, M. P. Cell cycle-regulated trafficking of human telomerase to telomeres. *Mol Biol Cell* **17**, 955-965, doi:10.1091/mbc.E05-09-0903 (2006).

85 Vogan, J. M. & Collins, K. Dynamics of Human Telomerase Holoenzyme Assembly and Subunit Exchange across the Cell Cycle. *J Biol Chem* **290**, 21320-21335, doi:10.1074/jbc.M115.659359 (2015).
86 Tajrishi, M. M., Tuteja, R. & Tuteja, N. Nucleolin: The most abundant multifunctional phosphoprotein of nucleolus. *Commun Integr Biol* **4**, 267-275, doi:10.4161/cib.4.3.14884 (2011).
87 Lee, J. H. *et al.* Catalytically active telomerase holoenzyme is assembled in the dense fibrillar component of the nucleolus during S phase. *Histochem Cell Biol* **141**, 137-152, doi:10.1007/s00418-013-1166-x (2014).
88 Dalby, A. B., Hofr, C. & Cech, T. R. Contributions of the TEL-patch amino acid cluster on TPP1 to telomeric DNA synthesis by human telomerase. *J Mol Biol* **427**, 1291-1303, doi:10.1016/j.jmb.2015.01.008 (2015).
89 Nandakumar, J. *et al.* The TEL patch of telomere protein TPP1 mediates telomerase recruitment and processivity. *Nature* **492**, 285-289, doi:10.1038/nature11648 (2012).
90 D'Souza, Y., Chu, T. W. & Autexier, C. A translocation-defective telomerase with low levels of activity and processivity stabilizes short telomeres and confers immortalization. *Mol Biol Cell* **24**, 1469-1479, doi:10.1091/mbc.E12-12-0889 (2013).
91 Jiang, J. *et al.* Structure of Tetrahymena telomerase reveals previously unknown subunits, functions, and interactions. *Science* **350**, aab4070, doi:10.1126/science.aab4070 (2015).
92 Cheung, D. H., Kung, H. F., Huang, J. J. & Shaw, P. C. PinX1 is involved in telomerase recruitment and regulates telomerase function by mediating its localization. *FEBS Lett* **586**, 3166-3171, doi:10.1016/j.febslet.2012.06.028 (2012).
93 Tong, A. S. *et al.* ATM and ATR Signaling Regulate the Recruitment of Human Telomerase to Telomeres. *Cell Rep* **13**, 1633-1646, doi:10.1016/j.celrep.2015.10.041 (2015).
94 McKerlie, M., Lin, S. & Zhu, X. D. ATM regulates proteasome-dependent subnuclear localization of TRF1, which is important for telomere maintenance. *Nucleic Acids Res* **40**, 3975-3989, doi:10.1093/nar/gks035 (2012).
95 Lee, S. S., Bohrson, C., Pike, A. M., Wheelan, S. J. & Greider, C. W. ATM Kinase Is Required for Telomere Elongation in Mouse and Human Cells. *Cell Rep* **13**, 1623-1632, doi:10.1016/j.celrep.2015.10.035 (2015).
96 Chandra, A., Hughes, T. R., Nugent, C. I. & Lundblad, V. Cdc13 both positively and negatively regulates telomere replication. *Genes Dev* **15**, 404-414, doi:10.1101/gad.861001 (2001).
97 Takai, H. *et al.* A POT1 mutation implicates defective telomere end fill-in and telomere truncations in Coats plus. *Genes Dev* **30**, 812-826, doi:10.1101/gad.276873.115 (2016).
98 Cong, Y. S., Wen, J. & Bacchetti, S. The human telomerase catalytic subunit hTERT: organization of the gene and characterization of the promoter. *Hum Mol Genet* **8**, 137-142 (1999).
99 Vinagre, J. *et al.* Frequency of TERT promoter mutations in human cancers. *Nat Commun* **4**, 2185, doi:10.1038/ncomms3185 (2013).
100 Horn, S. *et al.* TERT promoter mutations in familial and sporadic melanoma. *Science* **339**, 959-961, doi:10.1126/science.1230062 (2013).
101 Heidenreich, B. & Kumar, R. TERT promoter mutations in telomere biology. *Mutat Res* **771**, 15-31, doi:10.1016/j.mrrev.2016.11.002 (2017).

102 Avigad, S. *et al.* Short telomeres: a novel potential predictor of relapse in Ewing sarcoma. *Clin Cancer Res* **13**, 5777-5783, doi:10.1158/1078-0432.CCR-07-0308 (2007).
103 Gramatges, M. M. *et al.* Telomere content and risk of second malignant neoplasm in survivors of childhood cancer: a report from the Childhood Cancer Survivor Study. *Clin Cancer Res* **20**, 904-911, doi:10.1158/1078-0432.CCR-13-2076 (2014).
104 Shay, J. W. & Wright, W. E. Role of telomeres and telomerase in cancer. *Semin Cancer Biol* **21**, 349-353, doi:10.1016/j.semcancer.2011.10.001 (2011).
105 Shay, J. W., Pereira-Smith, O. M. & Wright, W. E. A role for both RB and p53 in the regulation of human cellular senescence. *Exp Cell Res* **196**, 33-39 (1991).
106 Muller, P. A. & Vousden, K. H. p53 mutations in cancer. *Nat Cell Biol* **15**, 2-8, doi:10.1038/ncb2641 (2013).
107 Marrone, A., Walne, A. & Dokal, I. Dyskeratosis congenita: telomerase, telomeres and anticipation. *Curr Opin Genet Dev* **15**, 249-257, doi:10.1016/j.gde.2005.04.004 (2005).
108 Heiss, N. S. *et al.* X-linked dyskeratosis congenita is caused by mutations in a highly conserved gene with putative nucleolar functions. *Nat Genet* **19**, 32-38, doi:10.1038/ng0598-32 (1998).
109 Mitchell, J. R., Wood, E. & Collins, K. A telomerase component is defective in the human disease dyskeratosis congenita. *Nature* **402**, 551-555, doi:10.1038/990141 (1999).
110 Angrisani, A., Vicidomini, R., Turano, M. & Furia, M. Human dyskerin: beyond telomeres. *Biol Chem* **395**, 593-610, doi:10.1515/hsz-2013-0287 (2014).
111 Carrillo, J. *et al.* High resolution melting analysis for the identification of novel mutations in DKC1 and TERT genes in patients with dyskeratosis congenita. *Blood Cells Mol Dis* **49**, 140-146, doi:10.1016/j.bcmd.2012.05.008 (2012).
112 Vulliamy, T. *et al.* The RNA component of telomerase is mutated in autosomal dominant dyskeratosis congenita. *Nature* **413**, 432-435, doi:10.1038/35096585 (2001).
113 Trahan, C. & Dragon, F. Dyskeratosis congenita mutations in the H/ACA domain of human telomerase RNA affect its assembly into a pre-RNP. *RNA* **15**, 235-243, doi:10.1261/rna.1354009 (2009).
114 Ueda, Y. *et al.* A mutation in the H/ACA box of telomerase RNA component gene (TERC) in a young patient with myelodysplastic syndrome. *BMC Med Genet* **15**, 68, doi:10.1186/1471-2350-15-68 (2014).
115 Blasco, M. A. *et al.* Telomere shortening and tumor formation by mouse cells lacking telomerase RNA. *Cell* **91**, 25-34 (1997).
116 Bakar, O., Isik, U., Canpolat, C. & Alanay, Y. Hoyeraal-Hreidarsson Syndrome: An Extremely Rare Dyskeratosis Congenita Phenotype. *Pediatr Dermatol* **32**, e263-266, doi:10.1111/pde.12693 (2015).
117 Alter, B. P., Giri, N., Savage, S. A. & Rosenberg, P. S. Cancer in dyskeratosis congenita. *Blood* **113**, 6549-6557, doi:10.1182/blood-2008-12-192880 (2009).
118 Montanaro, L. Dyskerin and cancer: more than telomerase. The defect in mRNA translation helps in explaining how a proliferative defect leads to cancer. *J Pathol* **222**, 345-349, doi:10.1002/path.2777 (2010).
119 Jiang, W., Middleton, K., Yoon, H. J., Fouquet, C. & Carbon, J. An essential yeast protein, CBF5p, binds in vitro to centromeres and microtubules. *Mol Cell Biol* **13**, 4884-4893 (1993).
120 Meier, U. T. & Blobel, G. NAP57, a mammalian nucleolar protein with a putative homolog in yeast and bacteria. *J Cell Biol* **127**, 1505-1514 (1994).

121 Phillips, B. *et al.* The Nop60B gene of Drosophila encodes an essential nucleolar protein that functions in yeast. *Mol Gen Genet* **260**, 20-29 (1998).
122 Lermontova, I., Schubert, V., Bornke, F., Macas, J. & Schubert, I. Arabidopsis CBF5 interacts with the H/ACA snoRNP assembly factor NAF1. *Plant Mol Biol* **65**, 615-626, doi:10.1007/s11103-007-9226-z (2007).
123 Kannan, K., Nelson, A. D. & Shippen, D. E. Dyskerin is a component of the Arabidopsis telomerase RNP required for telomere maintenance. *Mol Cell Biol* **28**, 2332-2341, doi:10.1128/MCB.01490-07 (2008).
124 Kauffman, T., Tran, J. & DiNardo, S. Mutations in Nop60B, the Drosophila homolog of human dyskeratosis congenita 1, affect the maintenance of the germ-line stem cell lineage during spermatogenesis. *Dev Biol* **253**, 189-199 (2003).
125 Cerrudo, C. S., Ghiringhelli, P. D. & Gomez, D. E. Protein universe containing a PUA RNA-binding domain. *FEBS J* **281**, 74-87, doi:10.1111/febs.12602 (2014).
126 Li, L. & Ye, K. Crystal structure of an H/ACA box ribonucleoprotein particle. *Nature* **443**, 302-307, doi:10.1038/nature05151 (2006).
127 Li, S. *et al.* Reconstitution and structural analysis of the yeast box H/ACA RNA-guided pseudouridine synthase. *Genes Dev* **25**, 2409-2421, doi:10.1101/gad.175299.111 (2011).
128 Rashid, R. *et al.* Crystal structure of a Cbf5-Nop10-Gar1 complex and implications in RNA-guided pseudouridylation and dyskeratosis congenita. *Mol Cell* **21**, 249-260, doi:10.1016/j.molcel.2005.11.017 (2006).
129 Alawi, F. & Lin, P. Dyskerin is required for tumor cell growth through mechanisms that are independent of its role in telomerase and only partially related to its function in precursor rRNA processing. *Mol Carcinog* **50**, 334-345, doi:10.1002/mc.20715 (2011).
130 Brault, M. E., Lauzon, C. & Autexier, C. Dyskeratosis congenita mutations in dyskerin SUMOylation consensus sites lead to impaired telomerase RNA accumulation and telomere defects. *Hum Mol Genet* **22**, 3498-3507, doi:10.1093/hmg/ddt204 (2013).
131 Alawi, F. & Lin, P. Dyskerin localizes to the mitotic apparatus and is required for orderly mitosis in human cells. *PLoS One* **8**, e80805, doi:10.1371/journal.pone.0080805 (2013).
132 Gu, B. W., Bessler, M. & Mason, P. J. A pathogenic dyskerin mutation impairs proliferation and activates a DNA damage response independent of telomere length in mice. *Proc Natl Acad Sci U S A* **105**, 10173-10178, doi:10.1073/pnas.0803559105 (2008).
133 Pereboeva, L., Hubbard, M., Goldman, F. D. & Westin, E. R. Robust DNA Damage Response and Elevated Reactive Oxygen Species in TINF2-Mutated Dyskeratosis Congenita Cells. *PLoS One* **11**, e0148793, doi:10.1371/journal.pone.0148793 (2016).
134 Liu, H. *et al.* hTERT promotes cell adhesion and migration independent of telomerase activity. *Sci Rep* **6**, 22886, doi:10.1038/srep22886 (2016).
135 Lin, P. *et al.* Differential requirements for H/ACA ribonucleoprotein components in cell proliferation and response to DNA damage. *Histochem Cell Biol* **144**, 543-558, doi:10.1007/s00418-015-1359-6 (2015).
136 Jobert, L. *et al.* The human base excision repair enzyme SMUG1 directly interacts with DKC1 and contributes to RNA quality control. *Mol Cell* **49**, 339-345, doi:10.1016/j.molcel.2012.11.010 (2013).
137 Montanaro, L. *et al.* Novel dyskerin-mediated mechanism of p53 inactivation through defective mRNA translation. *Cancer Res* **70**, 4767-4777, doi:10.1158/0008-5472.CAN-09-4024 (2010).

138 Bellodi, C. *et al.* H/ACA small RNA dysfunctions in disease reveal key roles for noncoding RNA modifications in hematopoietic stem cell differentiation. *Cell Rep* **3**, 1493-1502, doi:10.1016/j.celrep.2013.04.030 (2013).
139 Bellodi, C. *et al.* Loss of function of the tumor suppressor DKC1 perturbs p27 translation control and contributes to pituitary tumorigenesis. *Cancer Res* **70**, 6026-6035, doi:10.1158/0008-5472.CAN-09-4730 (2010).
140 Montanaro, L. *et al.* Dyskerin expression influences the level of ribosomal RNA pseudo-uridylation and telomerase RNA component in human breast cancer. *J Pathol* **210**, 10-18, doi:10.1002/path.2023 (2006).
141 Sieron, P. *et al.* DKC1 overexpression associated with prostate cancer progression. *Br J Cancer* **101**, 1410-1416, doi:10.1038/sj.bjc.6605299 (2009).
142 von Stedingk, K. *et al.* snoRNPs Regulate Telomerase Activity in Neuroblastoma and Are Associated with Poor Prognosis. *Transl Oncol* **6**, 447-457 (2013).
143 Angrisani, A., Turano, M., Paparo, L., Di Mauro, C. & Furia, M. A new human dyskerin isoform with cytoplasmic localization. *Biochim Biophys Acta* **1810**, 1361-1368, doi:10.1016/j.bbagen.2011.07.012 (2011).
144 Kim, W. *et al.* Systematic and quantitative assessment of the ubiquitin-modified proteome. *Mol Cell* **44**, 325-340, doi:10.1016/j.molcel.2011.08.025 (2011).
145 Manza, L. L. *et al.* Global shifts in protein sumoylation in response to electrophile and oxidative stress. *Chem Res Toxicol* **17**, 1706-1715, doi:10.1021/tx049767l (2004).
146 Galisson, F. *et al.* A novel proteomics approach to identify SUMOylated proteins and their modification sites in human cells. *Mol Cell Proteomics* **10**, M110 004796, doi:10.1074/mcp.M110.004796 (2011).
147 Westman, B. J. *et al.* A proteomic screen for nucleolar SUMO targets shows SUMOylation modulates the function of Nop5/Nop58. *Mol Cell* **39**, 618-631, doi:10.1016/j.molcel.2010.07.025 (2010).
148 Lamoliatte, F., McManus, F. P., Maarifi, G., Chelbi-Alix, M. K. & Thibault, P. Uncovering the SUMOylation and ubiquitylation crosstalk in human cells using sequential peptide immunopurification. *Nat Commun* **8**, 14109, doi:10.1038/ncomms14109 (2017).
149 Meluh, P. B. & Koshland, D. Evidence that the MIF2 gene of Saccharomyces cerevisiae encodes a centromere protein with homology to the mammalian centromere protein CENP-C. *Mol Biol Cell* **6**, 793-807 (1995).
150 Okura, T. *et al.* Protection against Fas/APO-1- and tumor necrosis factor-mediated cell death by a novel protein, sentrin. *J Immunol* **157**, 4277-4281 (1996).
151 Beauclair, G., Bridier-Nahmias, A., Zagury, J. F., Saib, A. & Zamborlini, A. JASSA: a comprehensive tool for prediction of SUMOylation sites and SIMs. *Bioinformatics* **31**, 3483-3491, doi:10.1093/bioinformatics/btv403 (2015).
152 Yang, S. H., Galanis, A., Witty, J. & Sharrocks, A. D. An extended consensus motif enhances the specificity of substrate modification by SUMO. *EMBO J* **25**, 5083-5093, doi:10.1038/sj.emboj.7601383 (2006).
153 Ivanov, A. V. *et al.* PHD domain-mediated E3 ligase activity directs intramolecular sumoylation of an adjacent bromodomain required for gene silencing. *Mol Cell* **28**, 823-837, doi:10.1016/j.molcel.2007.11.012 (2007).
154 Yavuz, A. S. & Sezerman, O. U. Predicting sumoylation sites using support vector machines based on various sequence features, conformational flexibility and disorder. *BMC Genomics* **15 Suppl 9**, S18, doi:10.1186/1471-2164-15-S9-S18 (2014).

155 Matic, I. *et al.* Site-specific identification of SUMO-2 targets in cells reveals an inverted SUMOylation motif and a hydrophobic cluster SUMOylation motif. *Mol Cell* **39**, 641-652, doi:10.1016/j.molcel.2010.07.026 (2010).
156 Tatham, M. H. *et al.* Polymeric chains of SUMO-2 and SUMO-3 are conjugated to protein substrates by SAE1/SAE2 and Ubc9. *J Biol Chem* **276**, 35368-35374, doi:10.1074/jbc.M104214200 (2001).
157 Kamitani, T., Kito, K., Nguyen, H. P., Fukuda-Kamitani, T. & Yeh, E. T. Characterization of a second member of the sentrin family of ubiquitin-like proteins. *J Biol Chem* **273**, 11349-11353 (1998).
158 Saitoh, H. & Hinchey, J. Functional heterogeneity of small ubiquitin-related protein modifiers SUMO-1 versus SUMO-2/3. *J Biol Chem* **275**, 6252-6258 (2000).
159 Wilkinson, K. A. & Henley, J. M. Mechanisms, regulation and consequences of protein SUMOylation. *Biochem J* **428**, 133-145, doi:10.1042/BJ20100158 (2010).
160 Guo, D. *et al.* A functional variant of SUMO4, a new I kappa B alpha modifier, is associated with type 1 diabetes. *Nat Genet* **36**, 837-841, doi:10.1038/ng1391 (2004).
161 Wang, C. Y., Yang, P., Li, M. & Gong, F. Characterization of a negative feedback network between SUMO4 expression and NFkappaB transcriptional activity. *Biochem Biophys Res Commun* **381**, 477-481, doi:10.1016/j.bbrc.2009.02.060 (2009).
162 Lin, H. Y. *et al.* Small ubiquitin-like modifier-4 Met55Val polymorphism is associated with glycemic control of Type 2 diabetes mellitus in Taiwan. *J Endocrinol Invest* **33**, 401-405, doi:10.3275/6624
10.1007/BF03346611 (2010).
163 Owerbach, D., McKay, E. M., Yeh, E. T., Gabbay, K. H. & Bohren, K. M. A proline-90 residue unique to SUMO-4 prevents maturation and sumoylation. *Biochem Biophys Res Commun* **337**, 517-520, doi:10.1016/j.bbrc.2005.09.090 (2005).
164 Liang, Y. C. *et al.* SUMO5, a Novel Poly-SUMO Isoform, Regulates PML Nuclear Bodies. *Sci Rep* **6**, 26509, doi:10.1038/srep26509 (2016).
165 Bernardi, R. & Pandolfi, P. P. Structure, dynamics and functions of promyelocytic leukaemia nuclear bodies. *Nat Rev Mol Cell Biol* **8**, 1006-1016, doi:10.1038/nrm2277 (2007).
166 Geiss-Friedlander, R. & Melchior, F. Concepts in sumoylation: a decade on. *Nat Rev Mol Cell Biol* **8**, 947-956, doi:10.1038/nrm2293 (2007).
167 Dou, H., Huang, C., Van Nguyen, T., Lu, L. S. & Yeh, E. T. SUMOylation and de-SUMOylation in response to DNA damage. *FEBS Lett* **585**, 2891-2896, doi:10.1016/j.febslet.2011.04.002 (2011).
168 Desterro, J. M., Rodriguez, M. S., Kemp, G. D. & Hay, R. T. Identification of the enzyme required for activation of the small ubiquitin-like protein SUMO-1. *J Biol Chem* **274**, 10618-10624 (1999).
169 Johnson, E. S., Schwienhorst, I., Dohmen, R. J. & Blobel, G. The ubiquitin-like protein Smt3p is activated for conjugation to other proteins by an Aos1p/Uba2p heterodimer. *EMBO J* **16**, 5509-5519, doi:10.1093/emboj/16.18.5509 (1997).
170 Giraud, M. F., Desterro, J. M. & Naismith, J. H. Structure of ubiquitin-conjugating enzyme 9 displays significant differences with other ubiquitin-conjugating enzymes which may reflect its specificity for sumo rather than ubiquitin. *Acta Crystallogr D Biol Crystallogr* **54**, 891-898 (1998).

171 Tatham, M. H., Chen, Y. & Hay, R. T. Role of two residues proximal to the active site of Ubc9 in substrate recognition by the Ubc9.SUMO-1 thiolester complex. *Biochemistry* **42**, 3168-3179, doi:10.1021/bi026861x (2003).
172 Hayashi, T. *et al.* Ubc9 is essential for viability of higher eukaryotic cells. *Exp Cell Res* **280**, 212-221 (2002).
173 Nacerddine, K. *et al.* The SUMO pathway is essential for nuclear integrity and chromosome segregation in mice. *Dev Cell* **9**, 769-779, doi:10.1016/j.devcel.2005.10.007 (2005).
174 Demarque, M. D. *et al.* Sumoylation by Ubc9 regulates the stem cell compartment and structure and function of the intestinal epithelium in mice. *Gastroenterology* **140**, 286-296, doi:10.1053/j.gastro.2010.10.002 (2011).
175 Flotho, A. & Melchior, F. Sumoylation: a regulatory protein modification in health and disease. *Annu Rev Biochem* **82**, 357-385, doi:10.1146/annurev-biochem-061909-093311 (2013).
176 Schmidt, D. & Muller, S. Members of the PIAS family act as SUMO ligases for c-Jun and p53 and repress p53 activity. *Proc Natl Acad Sci U S A* **99**, 2872-2877, doi:10.1073/pnas.052559499 (2002).
177 Weger, S., Hammer, E. & Heilbronn, R. Topors acts as a SUMO-1 E3 ligase for p53 in vitro and in vivo. *FEBS Lett* **579**, 5007-5012, doi:10.1016/j.febslet.2005.07.088 (2005).
178 Sakin, V., Richter, S. M., Hsiao, H. H., Urlaub, H. & Melchior, F. Sumoylation of the GTPase Ran by the RanBP2 SUMO E3 Ligase Complex. *J Biol Chem* **290**, 23589-23602, doi:10.1074/jbc.M115.660118 (2015).
179 Werner, A., Flotho, A. & Melchior, F. The RanBP2/RanGAP1*SUMO1/Ubc9 complex is a multisubunit SUMO E3 ligase. *Mol Cell* **46**, 287-298, doi:10.1016/j.molcel.2012.02.017 (2012).
180 Minty, A., Dumont, X., Kaghad, M. & Caput, D. Covalent modification of p73alpha by SUMO-1. Two-hybrid screening with p73 identifies novel SUMO-1-interacting proteins and a SUMO-1 interaction motif. *J Biol Chem* **275**, 36316-36323, doi:10.1074/jbc.M004293200 (2000).
181 Song, J., Durrin, L. K., Wilkinson, T. A., Krontiris, T. G. & Chen, Y. Identification of a SUMO-binding motif that recognizes SUMO-modified proteins. *Proc Natl Acad Sci U S A* **101**, 14373-14378, doi:10.1073/pnas.0403498101 (2004).
182 Song, J., Zhang, Z., Hu, W. & Chen, Y. Small ubiquitin-like modifier (SUMO) recognition of a SUMO binding motif: a reversal of the bound orientation. *J Biol Chem* **280**, 40122-40129, doi:10.1074/jbc.M507059200 (2005).
183 Baba, D. *et al.* Crystal structure of SUMO-3-modified thymine-DNA glycosylase. *J Mol Biol* **359**, 137-147, doi:10.1016/j.jmb.2006.03.036 (2006).
184 Chupreta, S., Holmstrom, S., Subramanian, L. & Iniguez-Lluhi, J. A. A small conserved surface in SUMO is the critical structural determinant of its transcriptional inhibitory properties. *Mol Cell Biol* **25**, 4272-4282, doi:10.1128/MCB.25.10.4272-4282.2005 (2005).
185 Metzger, M. B., Pruneda, J. N., Klevit, R. E. & Weissman, A. M. RING-type E3 ligases: master manipulators of E2 ubiquitin-conjugating enzymes and ubiquitination. *Biochim Biophys Acta* **1843**, 47-60, doi:10.1016/j.bbamcr.2013.05.026 (2014).
186 Xu, Z. & Au, S. W. Mapping residues of SUMO precursors essential in differential maturation by SUMO-specific protease, SENP1. *Biochem J* **386**, 325-330, doi:10.1042/BJ20041210 (2005).

187 Shen, L. N., Dong, C., Liu, H., Naismith, J. H. & Hay, R. T. The structure of SENP1-SUMO-2 complex suggests a structural basis for discrimination between SUMO paralogues during processing. *Biochem J* **397**, 279-288, doi:10.1042/BJ20052030 (2006).
188 Xu, Z. *et al.* Crystal structure of the SENP1 mutant C603S-SUMO complex reveals the hydrolytic mechanism of SUMO-specific protease. *Biochem J* **398**, 345-352, doi:10.1042/BJ20060526 (2006).
189 Kolli, N. *et al.* Distribution and paralogue specificity of mammalian deSUMOylating enzymes. *Biochem J* **430**, 335-344, doi:10.1042/BJ20100504 (2010).
190 Shen, L. *et al.* SUMO protease SENP1 induces isomerization of the scissile peptide bond. *Nat Struct Mol Biol* **13**, 1069-1077, doi:10.1038/nsmb1172 (2006).
191 Sharma, P., Yamada, S., Lualdi, M., Dasso, M. & Kuehn, M. R. Senp1 is essential for desumoylating Sumo1-modified proteins but dispensable for Sumo2 and Sumo3 deconjugation in the mouse embryo. *Cell Rep* **3**, 1640-1650, doi:10.1016/j.celrep.2013.04.016 (2013).
192 Nayak, A. & Muller, S. SUMO-specific proteases/isopeptidases: SENPs and beyond. *Genome Biol* **15**, 422, doi:10.1186/s13059-014-0422-2 (2014).
193 Gong, L. & Yeh, E. T. Characterization of a family of nucleolar SUMO-specific proteases with preference for SUMO-2 or SUMO-3. *J Biol Chem* **281**, 15869-15877, doi:10.1074/jbc.M511658200 (2006).
194 Haindl, M., Harasim, T., Eick, D. & Muller, S. The nucleolar SUMO-specific protease SENP3 reverses SUMO modification of nucleophosmin and is required for rRNA processing. *EMBO Rep* **9**, 273-279, doi:10.1038/embor.2008.3 (2008).
195 Finkbeiner, E., Haindl, M. & Muller, S. The SUMO system controls nucleolar partitioning of a novel mammalian ribosome biogenesis complex. *EMBO J* **30**, 1067-1078, doi:10.1038/emboj.2011.33 (2011).
196 Klein, U. R., Haindl, M., Nigg, E. A. & Muller, S. RanBP2 and SENP3 function in a mitotic SUMO2/3 conjugation-deconjugation cycle on Borealin. *Mol Biol Cell* **20**, 410-418, doi:10.1091/mbc.E08-05-0511 (2009).
197 Gillies, J. *et al.* SUMO Pathway Modulation of Regulatory Protein Binding at the Ribosomal DNA Locus in Saccharomyces cerevisiae. *Genetics* **202**, 1377-1394, doi:10.1534/genetics.116.187252 (2016).
198 Huang, C. J., Wu, D., Khan, F. A. & Huo, L. J. The SUMO Protease SENP3 Orchestrates G2-M Transition and Spindle Assembly in Mouse Oocytes. *Sci Rep* **5**, 15600, doi:10.1038/srep15600 (2015).
199 Lima, C. D. & Reverter, D. Structure of the human SENP7 catalytic domain and poly-SUMO deconjugation activities for SENP6 and SENP7. *J Biol Chem* **283**, 32045-32055, doi:10.1074/jbc.M805655200 (2008).
200 Alegre, K. O. & Reverter, D. Swapping small ubiquitin-like modifier (SUMO) isoform specificity of SUMO proteases SENP6 and SENP7. *J Biol Chem* **286**, 36142-36151, doi:10.1074/jbc.M111.268847 (2011).
201 Shen, L. N., Geoffroy, M. C., Jaffray, E. G. & Hay, R. T. Characterization of SENP7, a SUMO-2/3-specific isopeptidase. *Biochem J* **421**, 223-230, doi:10.1042/BJ20090246 (2009).
202 Melchior, F. SUMO--nonclassical ubiquitin. *Annu Rev Cell Dev Biol* **16**, 591-626, doi:10.1146/annurev.cellbio.16.1.591 (2000).

203 Muller, S., Hoege, C., Pyrowolakis, G. & Jentsch, S. SUMO, ubiquitin's mysterious cousin. *Nat Rev Mol Cell Biol* **2**, 202-210, doi:10.1038/35056591 (2001).
204 Dohmen, R. J. SUMO protein modification. *Biochim Biophys Acta* **1695**, 113-131, doi:10.1016/j.bbamcr.2004.09.021 (2004).
205 Bies, J., Markus, J. & Wolff, L. Covalent attachment of the SUMO-1 protein to the negative regulatory domain of the c-Myb transcription factor modifies its stability and transactivation capacity. *J Biol Chem* **277**, 8999-9009, doi:10.1074/jbc.M110453200 (2002).
206 Dahle, O. *et al.* Transactivation properties of c-Myb are critically dependent on two SUMO-1 acceptor sites that are conjugated in a PIASy enhanced manner. *Eur J Biochem* **270**, 1338-1348 (2003).
207 Desterro, J. M., Rodriguez, M. S. & Hay, R. T. SUMO-1 modification of IkappaBalpha inhibits NF-kappaB activation. *Mol Cell* **2**, 233-239 (1998).
208 Gostissa, M. *et al.* Activation of p53 by conjugation to the ubiquitin-like protein SUMO-1. *EMBO J* **18**, 6462-6471, doi:10.1093/emboj/18.22.6462 (1999).
209 Rodriguez, M. S. *et al.* SUMO-1 modification activates the transcriptional response of p53. *EMBO J* **18**, 6455-6461, doi:10.1093/emboj/18.22.6455 (1999).
210 Chen, L. & Chen, J. MDM2-ARF complex regulates p53 sumoylation. *Oncogene* **22**, 5348-5357, doi:10.1038/sj.onc.1206851 (2003).
211 Santiago, A., Li, D., Zhao, L. Y., Godsey, A. & Liao, D. p53 SUMOylation promotes its nuclear export by facilitating its release from the nuclear export receptor CRM1. *Mol Biol Cell* **24**, 2739-2752, doi:10.1091/mbc.E12-10-0771 (2013).
212 Stindt, M. H., Carter, S., Vigneron, A. M., Ryan, K. M. & Vousden, K. H. MDM2 promotes SUMO-2/3 modification of p53 to modulate transcriptional activity. *Cell Cycle* **10**, 3176-3188, doi:10.4161/cc.10.18.17436 (2011).
213 Honda, R. & Yasuda, H. Association of p19(ARF) with Mdm2 inhibits ubiquitin ligase activity of Mdm2 for tumor suppressor p53. *EMBO J* **18**, 22-27, doi:10.1093/emboj/18.1.22 (1999).
214 Buschmann, T., Fuchs, S. Y., Lee, C. G., Pan, Z. Q. & Ronai, Z. SUMO-1 modification of Mdm2 prevents its self-ubiquitination and increases Mdm2 ability to ubiquitinate p53. *Cell* **101**, 753-762 (2000).
215 Lohrum, M. A., Woods, D. B., Ludwig, R. L., Balint, E. & Vousden, K. H. C-terminal ubiquitination of p53 contributes to nuclear export. *Mol Cell Biol* **21**, 8521-8532, doi:10.1128/MCB.21.24.8521-8532.2001 (2001).
216 Klenk, C., Humrich, J., Quitterer, U. & Lohse, M. J. SUMO-1 controls the protein stability and the biological function of phosducin. *J Biol Chem* **281**, 8357-8364, doi:10.1074/jbc.M513703200 (2006).
217 Schimmel, J. *et al.* The ubiquitin-proteasome system is a key component of the SUMO-2/3 cycle. *Mol Cell Proteomics* **7**, 2107-2122, doi:10.1074/mcp.M800025-MCP200 (2008).
218 Sriramachandran, A. M. & Dohmen, R. J. SUMO-targeted ubiquitin ligases. *Biochim Biophys Acta* **1843**, 75-85, doi:10.1016/j.bbamcr.2013.08.022 (2014).
219 Kerscher, O. SUMO junction-what's your function? New insights through SUMO-interacting motifs. *EMBO Rep* **8**, 550-555, doi:10.1038/sj.embor.7400980 (2007).
220 Mullen, J. R. & Brill, S. J. Activation of the Slx5-Slx8 ubiquitin ligase by poly-small ubiquitin-like modifier conjugates. *J Biol Chem* **283**, 19912-19921, doi:10.1074/jbc.M802690200 (2008).

221 Uzunova, K. *et al.* Ubiquitin-dependent proteolytic control of SUMO conjugates. *J Biol Chem* **282**, 34167-34175, doi:10.1074/jbc.M706505200 (2007).
222 Chen, R. H., Lee, Y. R. & Yuan, W. C. The role of PML ubiquitination in human malignancies. *J Biomed Sci* **19**, 81, doi:10.1186/1423-0127-19-81 (2012).
223 Salomoni, P. & Pandolfi, P. P. The role of PML in tumor suppression. *Cell* **108**, 165-170 (2002).
224 Muller, S., Matunis, M. J. & Dejean, A. Conjugation with the ubiquitin-related modifier SUMO-1 regulates the partitioning of PML within the nucleus. *EMBO J* **17**, 61-70, doi:10.1093/emboj/17.1.61 (1998).
225 Tatham, M. H. *et al.* RNF4 is a poly-SUMO-specific E3 ubiquitin ligase required for arsenic-induced PML degradation. *Nat Cell Biol* **10**, 538-546, doi:10.1038/ncb1716 (2008).
226 Lallemand-Breitenbach, V. *et al.* Role of promyelocytic leukemia (PML) sumolation in nuclear body formation, 11S proteasome recruitment, and As2O3-induced PML or PML/retinoic acid receptor alpha degradation. *J Exp Med* **193**, 1361-1371 (2001).
227 Geoffroy, M. C., Jaffray, E. G., Walker, K. J. & Hay, R. T. Arsenic-induced SUMO-dependent recruitment of RNF4 into PML nuclear bodies. *Mol Biol Cell* **21**, 4227-4239, doi:10.1091/mbc.E10-05-0449 (2010).
228 van Hagen, M., Overmeer, R. M., Abolvardi, S. S. & Vertegaal, A. C. RNF4 and VHL regulate the proteasomal degradation of SUMO-conjugated Hypoxia-Inducible Factor-2alpha. *Nucleic Acids Res* **38**, 1922-1931, doi:10.1093/nar/gkp1157 (2010).
229 Yang, Y. C., Yoshikai, Y., Hsu, S. W., Saitoh, H. & Chang, L. K. Role of RNF4 in the ubiquitination of Rta of Epstein-Barr virus. *J Biol Chem* **288**, 12866-12879, doi:10.1074/jbc.M112.413393 (2013).
230 Guzzo, C. M. & Matunis, M. J. Expanding SUMO and ubiquitin-mediated signaling through hybrid SUMO-ubiquitin chains and their receptors. *Cell Cycle* **12**, 1015-1017, doi:10.4161/cc.24332 (2013).
231 Hofmann, K. & Falquet, L. A ubiquitin-interacting motif conserved in components of the proteasomal and lysosomal protein degradation systems. *Trends Biochem Sci* **26**, 347-350 (2001).
232 Guzzo, C. M. *et al.* RNF4-dependent hybrid SUMO-ubiquitin chains are signals for RAP80 and thereby mediate the recruitment of BRCA1 to sites of DNA damage. *Sci Signal* **5**, ra88, doi:10.1126/scisignal.2003485 (2012).
233 Ciccia, A. & Elledge, S. J. The DNA damage response: making it safe to play with knives. *Mol Cell* **40**, 179-204, doi:10.1016/j.molcel.2010.09.019 (2010).
234 Dou, H., Huang, C., Singh, M., Carpenter, P. B. & Yeh, E. T. Regulation of DNA repair through deSUMOylation and SUMOylation of replication protein A complex. *Mol Cell* **39**, 333-345, doi:10.1016/j.molcel.2010.07.021 (2010).
235 Ouyang, K. J. *et al.* SUMO modification regulates BLM and RAD51 interaction at damaged replication forks. *PLoS Biol* **7**, e1000252, doi:10.1371/journal.pbio.1000252 (2009).
236 Halas, A., Krawczyk, M. & Sledziewska-Gojska, E. PCNA SUMOylation protects against PCNA polyubiquitination-mediated, Rad59-dependent, spontaneous, intrachromosomal gene conversion. *Mutat Res* **791-792**, 10-18, doi:10.1016/j.mrfmmm.2016.08.001 (2016).
237 Strauss, C. & Goldberg, M. Recruitment of proteins to DNA double-strand breaks: MDC1 directly recruits RAP80. *Cell Cycle* **10**, 2850-2857, doi:10.4161/cc.10.17.17341 (2011).

238 Hu, Y. & Parvin, J. D. Small ubiquitin-like modifier (SUMO) isoforms and conjugation-independent function in DNA double-strand break repair pathways. *J Biol Chem* **289**, 21289-21295, doi:10.1074/jbc.C114.582122 (2014).
239 Galanty, Y., Belotserkovskaya, R., Coates, J. & Jackson, S. P. RNF4, a SUMO-targeted ubiquitin E3 ligase, promotes DNA double-strand break repair. *Genes Dev* **26**, 1179-1195, doi:10.1101/gad.188284.112 (2012).
240 Vyas, R. *et al.* RNF4 is required for DNA double-strand break repair in vivo. *Cell Death Differ* **20**, 490-502, doi:10.1038/cdd.2012.145 (2013).
241 Nie, M., Moser, B. A., Nakamura, T. M. & Boddy, M. N. SUMO-targeted ubiquitin ligase activity can either suppress or promote genome instability, depending on the nature of the DNA lesion. *PLoS Genet* **13**, e1006776, doi:10.1371/journal.pgen.1006776 (2017).
242 Chung, I. & Zhao, X. A STUbL wards off telomere fusions. *EMBO J* **32**, 775-777, doi:10.1038/emboj.2013.39 (2013).
243 Tanaka, K. *et al.* Characterization of a fission yeast SUMO-1 homologue, pmt3p, required for multiple nuclear events, including the control of telomere length and chromosome segregation. *Mol Cell Biol* **19**, 8660-8672 (1999).
244 Hang, L. E., Liu, X., Cheung, I., Yang, Y. & Zhao, X. SUMOylation regulates telomere length homeostasis by targeting Cdc13. *Nat Struct Mol Biol* **18**, 920-926, doi:10.1038/nsmb.2100 (2011).
245 O'Connor, M. S., Safari, A., Liu, D., Qin, J. & Songyang, Z. The human Rap1 protein complex and modulation of telomere length. *J Biol Chem* **279**, 28585-28591, doi:10.1074/jbc.M312913200 (2004).
246 Lescasse, R., Pobiega, S., Callebaut, I. & Marcand, S. End-joining inhibition at telomeres requires the translocase and polySUMO-dependent ubiquitin ligase Uls1. *EMBO J* **32**, 805-815, doi:10.1038/emboj.2013.24 (2013).
247 Garg, M. *et al.* Tpz1TPP1 SUMOylation reveals evolutionary conservation of SUMO-dependent Stn1 telomere association. *EMBO Rep* **15**, 871-877, doi:10.15252/embr.201438919 (2014).
248 Miyagawa, K. *et al.* SUMOylation regulates telomere length by targeting the shelterin subunit Tpz1(Tpp1) to modulate shelterin-Stn1 interaction in fission yeast. *Proc Natl Acad Sci U S A* **111**, 5950-5955, doi:10.1073/pnas.1401359111 (2014).
249 Rogan, E. M. *et al.* Alterations in p53 and p16INK4 expression and telomere length during spontaneous immortalization of Li-Fraumeni syndrome fibroblasts. *Mol Cell Biol* **15**, 4745-4753 (1995).
250 Yeager, T. R. *et al.* Telomerase-negative immortalized human cells contain a novel type of promyelocytic leukemia (PML) body. *Cancer Res* **59**, 4175-4179 (1999).
251 Potts, P. R. & Yu, H. The SMC5/6 complex maintains telomere length in ALT cancer cells through SUMOylation of telomere-binding proteins. *Nat Struct Mol Biol* **14**, 581-590, doi:10.1038/nsmb1259 (2007).
252 Churikov, D. *et al.* SUMO-Dependent Relocalization of Eroded Telomeres to Nuclear Pore Complexes Controls Telomere Recombination. *Cell Rep* **15**, 1242-1253, doi:10.1016/j.celrep.2016.04.008 (2016).
253 Sarge, K. D. & Park-Sarge, O. K. Sumoylation and human disease pathogenesis. *Trends Biochem Sci* **34**, 200-205, doi:10.1016/j.tibs.2009.01.004 (2009).
254 Dorval, V. & Fraser, P. E. SUMO on the road to neurodegeneration. *Biochim Biophys Acta* **1773**, 694-706, doi:10.1016/j.bbamcr.2007.03.017 (2007).

255 Steffan, J. S. *et al.* SUMO modification of Huntingtin and Huntington's disease pathology. *Science* **304**, 100-104, doi:10.1126/science.1092194 (2004).
256 Zhang, Y. Q. & Sarge, K. D. Sumoylation regulates lamin A function and is lost in lamin A mutants associated with familial cardiomyopathies. *J Cell Biol* **182**, 35-39, doi:10.1083/jcb.200712124 (2008).
257 Villalva, C. *et al.* Isolation of differentially expressed genes in NPM-ALK-positive anaplastic large cell lymphoma. *Br J Haematol* **118**, 791-798 (2002).
258 Wang, L. & Banerjee, S. Differential PIAS3 expression in human malignancy. *Oncol Rep* **11**, 1319-1324 (2004).
259 Mo, Y. Y., Yu, Y., Theodosiou, E., Ee, P. L. & Beck, W. T. A role for Ubc9 in tumorigenesis. *Oncogene* **24**, 2677-2683, doi:10.1038/sj.onc.1208210 (2005).
260 McDoniels-Silvers, A. L., Nimri, C. F., Stoner, G. D., Lubet, R. A. & You, M. Differential gene expression in human lung adenocarcinomas and squamous cell carcinomas. *Clin Cancer Res* **8**, 1127-1138 (2002).
261 Kim, J. H. *et al.* Roles of sumoylation of a reptin chromatin-remodelling complex in cancer metastasis. *Nat Cell Biol* **8**, 631-639, doi:10.1038/ncb1415 (2006).
262 Cheng, J., Bawa, T., Lee, P., Gong, L. & Yeh, E. T. Role of desumoylation in the development of prostate cancer. *Neoplasia* **8**, 667-676, doi:10.1593/neo.06445 (2006).
263 Karin, M. Nuclear factor-kappaB in cancer development and progression. *Nature* **441**, 431-436, doi:10.1038/nature04870 (2006).
264 Karin, M. & Greten, F. R. NF-kappaB: linking inflammation and immunity to cancer development and progression. *Nat Rev Immunol* **5**, 749-759, doi:10.1038/nri1703 (2005).
265 Reddel, R. R. A SUMO ligase for ALT. *Nat Struct Mol Biol* **14**, 570-571, doi:10.1038/nsmb0707-570 (2007).
266 Lamoliatte, F. *et al.* Large-scale analysis of lysine SUMOylation by SUMO remnant immunoaffinity profiling. *Nat Commun* **5**, 5409, doi:10.1038/ncomms6409 (2014).
267 Sun, L. *et al.* Targeted DNA damage at individual telomeres disrupts their integrity and triggers cell death. *Nucleic Acids Res* **43**, 6334-6347, doi:10.1093/nar/gkv598 (2015).
268 van Steensel, B., Smogorzewska, A. & de Lange, T. TRF2 protects human telomeres from end-to-end fusions. *Cell* **92**, 401-413 (1998).
269 Huang, C. *et al.* SENP3 is responsible for HIF-1 transactivation under mild oxidative stress via p300 de-SUMOylation. *EMBO J* **28**, 2748-2762, doi:10.1038/emboj.2009.210 (2009).
270 Li, X. *et al.* SENP1 mediates TNF-induced desumoylation and cytoplasmic translocation of HIPK1 to enhance ASK1-dependent apoptosis. *Cell Death Differ* **15**, 739-750, doi:10.1038/sj.cdd.4402303 (2008).
271 Mallette, F. A. & Richard, S. JMJD2A promotes cellular transformation by blocking cellular senescence through transcriptional repression of the tumor suppressor CHD5. *Cell Rep* **2**, 1233-1243, doi:10.1016/j.celrep.2012.09.033 (2012).
272 Eifler, K. & Vertegaal, A. C. SUMOylation-Mediated Regulation of Cell Cycle Progression and Cancer. *Trends Biochem Sci* **40**, 779-793, doi:10.1016/j.tibs.2015.09.006 (2015).
273 Masutomi, K. *et al.* Telomerase maintains telomere structure in normal human cells. *Cell* **114**, 241-253 (2003).
274 Cohen, S. B. *et al.* Protein composition of catalytically active human telomerase from immortal cells. *Science* **315**, 1850-1853, doi:10.1126/science.1138596 (2007).

275 Galanty, Y. *et al.* Mammalian SUMO E3-ligases PIAS1 and PIAS4 promote responses to DNA double-strand breaks. *Nature* **462**, 935-939, doi:10.1038/nature08657 (2009).
276 Morris, J. R. *et al.* The SUMO modification pathway is involved in the BRCA1 response to genotoxic stress. *Nature* **462**, 886-890, doi:10.1038/nature08593 (2009).
277 Hendriks, I. A. *et al.* Uncovering global SUMOylation signaling networks in a site-specific manner. *Nat Struct Mol Biol* **21**, 927-936, doi:10.1038/nsmb.2890 (2014).
278 Lin, P., Mobasher, M. E. & Alawi, F. Acute dyskerin depletion triggers cellular senescence and renders osteosarcoma cells resistant to genotoxic stress-induced apoptosis. *Biochem Biophys Res Commun* **446**, 1268-1275, doi:10.1016/j.bbrc.2014.03.114 (2014).
279 Li, D., Morimoto, K., Takeshita, T. & Lu, Y. Arsenic induces DNA damage via reactive oxygen species in human cells. *Environ Health Prev Med* **6**, 27-32, doi:10.1007/BF02897306 (2001).
280 Sahin, U., Lallemand-Breitenbach, V. & de The, H. PML nuclear bodies: regulation, function and therapeutic perspectives. *J Pathol* **234**, 289-291, doi:10.1002/path.4426 (2014).
281 Kamitani, T. *et al.* Identification of three major sentrinization sites in PML. *J Biol Chem* **273**, 26675-26682 (1998).
282 Arnoult, N. & Karlseder, J. Complex interactions between the DNA-damage response and mammalian telomeres. *Nat Struct Mol Biol* **22**, 859-866, doi:10.1038/nsmb.3092 (2015).
283 Maser, R. S. & DePinho, R. A. Telomeres and the DNA damage response: why the fox is guarding the henhouse. *DNA Repair (Amst)* **3**, 979-988, doi:10.1016/j.dnarep.2004.05.009 (2004).
284 Fu, X. H. *et al.* Telomere recombination preferentially occurs at short telomeres in telomerase-null type II survivors. *PLoS One* **9**, e90644, doi:10.1371/journal.pone.0090644 (2014).
285 Cusanelli, E., Romero, C. A. & Chartrand, P. Telomeric noncoding RNA TERRA is induced by telomere shortening to nucleate telomerase molecules at short telomeres. *Mol Cell* **51**, 780-791, doi:10.1016/j.molcel.2013.08.029 (2013).
286 Schmidt, J. C., Zaug, A. J. & Cech, T. R. Live Cell Imaging Reveals the Dynamics of Telomerase Recruitment to Telomeres. *Cell* **166**, 1188-1197 e1189, doi:10.1016/j.cell.2016.07.033 (2016).
287 Bianchi, A. & Shore, D. Increased association of telomerase with short telomeres in yeast. *Genes Dev* **21**, 1726-1730, doi:10.1101/gad.438907 (2007).
288 Britt-Compton, B., Capper, R., Rowson, J. & Baird, D. M. Short telomeres are preferentially elongated by telomerase in human cells. *FEBS Lett* **583**, 3076-3080, doi:10.1016/j.febslet.2009.08.029 (2009).
289 Ge, Y. *et al.* Preferential extension of short telomeres induced by low extracellular pH. *Nucleic Acids Res* **44**, 8086-8096, doi:10.1093/nar/gkw464 (2016).
290 Cristofari, G. & Lingner, J. Telomere length homeostasis requires that telomerase levels are limiting. *EMBO J* **25**, 565-574, doi:10.1038/sj.emboj.7600952 (2006).
291 Wong, J. M., Kusdra, L. & Collins, K. Subnuclear shuttling of human telomerase induced by transformation and DNA damage. *Nat Cell Biol* **4**, 731-736, doi:10.1038/ncb846 (2002).
292 Masutomi, K. *et al.* The telomerase reverse transcriptase regulates chromatin state and DNA damage responses. *Proc Natl Acad Sci U S A* **102**, 8222-8227, doi:10.1073/pnas.0503095102 (2005).

293 Ouenzar, F. *et al.* Cell cycle-dependent spatial segregation of telomerase from sites of DNA damage. *J Cell Biol*, doi:10.1083/jcb.201610071 (2017).
294 Bulina, M. E. *et al.* A genetically encoded photosensitizer. *Nat Biotechnol* **24**, 95-99, doi:10.1038/nbt1175 (2006).
295 Vegh, R. B. *et al.* Reactive oxygen species in photochemistry of the red fluorescent protein "Killer Red". *Chem Commun (Camb)* **47**, 4887-4889, doi:10.1039/c0cc05713d (2011).
296 Zhang, P. *et al.* TRF2 dysfunction elicits DNA damage responses associated with senescence in proliferating neural cells and differentiation of neurons. *J Neurochem* **97**, 567-581, doi:10.1111/j.1471-4159.2006.03779.x (2006).
297 Murtif, V. L. & Samols, D. Mutagenesis affecting the carboxyl terminus of the biotinyl subunit of transcarboxylase. Effects on biotination. *J Biol Chem* **262**, 11813-11816 (1987).
298 Knight, J. D. *et al.* A web-tool for visualizing quantitative protein-protein interaction data. *Proteomics* **15**, 1432-1436, doi:10.1002/pmic.201400429 (2015).
299 Song, Y., Madahar, V. & Liao, J. Development of FRET assay into quantitative and high-throughput screening technology platforms for protein-protein interactions. *Ann Biomed Eng* **39**, 1224-1234, doi:10.1007/s10439-010-0225-x (2011).
300 Kim, Y. P. *et al.* Analysis of in vitro SUMOylation using bioluminescence resonance energy transfer (BRET). *Biochem Biophys Res Commun* **382**, 530-534, doi:10.1016/j.bbrc.2009.03.055 (2009).
301 Jiang, M., Chiu, S. Y. & Hsu, W. SUMO-specific protease 2 in Mdm2-mediated regulation of p53. *Cell Death Differ* **18**, 1005-1015, doi:10.1038/cdd.2010.168 (2011).
302 Lee, Y. K., Thomas, S. N., Yang, A. J. & Ann, D. K. Doxorubicin down-regulates Kruppel-associated box domain-associated protein 1 sumoylation that relieves its transcription repression on p21WAF1/CIP1 in breast cancer MCF-7 cells. *J Biol Chem* **282**, 1595-1606, doi:10.1074/jbc.M606306200 (2007).
303 Li, X. *et al.* Role for KAP1 serine 824 phosphorylation and sumoylation/desumoylation switch in regulating KAP1-mediated transcriptional repression. *J Biol Chem* **282**, 36177-36189, doi:10.1074/jbc.M706912200 (2007).
304 Weisshaar, S. R. *et al.* Arsenic trioxide stimulates SUMO-2/3 modification leading to RNF4-dependent proteolytic targeting of PML. *FEBS Lett* **582**, 3174-3178, doi:10.1016/j.febslet.2008.08.008 (2008).
305 Sahin, U. *et al.* Oxidative stress-induced assembly of PML nuclear bodies controls sumoylation of partner proteins. *J Cell Biol* **204**, 931-945, doi:10.1083/jcb.201305148 (2014).
306 Wang, F. F. *et al.* Deficiency of SUMO-specific protease 1 induces arsenic trioxide-mediated apoptosis by regulating XBP1 activity in human acute promyelocytic leukemia. *Oncol Lett* **12**, 3755-3762, doi:10.3892/ol.2016.5162 (2016).
307 Mann, K. K. & Miller, W. H., Jr. Death by arsenic: implications of PML sumoylation. *Cancer Cell* **5**, 307-309 (2004).
308 Lin, D. Y. *et al.* Negative modulation of androgen receptor transcriptional activity by Daxx. *Mol Cell Biol* **24**, 10529-10541, doi:10.1128/MCB.24.24.10529-10541.2004 (2004).
309 Lin, D. Y. *et al.* Role of SUMO-interacting motif in Daxx SUMO modification, subnuclear localization, and repression of sumoylated transcription factors. *Mol Cell* **24**, 341-354, doi:10.1016/j.molcel.2006.10.019 (2006).

310 Shih, H. M., Chang, C. C., Kuo, H. Y. & Lin, D. Y. Daxx mediates SUMO-dependent transcriptional control and subnuclear compartmentalization. *Biochem Soc Trans* **35**, 1397-1400, doi:10.1042/BST0351397 (2007).
311 Kuo, H. Y. *et al.* SUMO modification negatively modulates the transcriptional activity of CREB-binding protein via the recruitment of Daxx. *Proc Natl Acad Sci U S A* **102**, 16973-16978, doi:10.1073/pnas.0504460102 (2005).
312 Bomberger, J. M., Coutermarsh, B. A., Barnaby, R. L. & Stanton, B. A. Arsenic promotes ubiquitinylation and lysosomal degradation of cystic fibrosis transmembrane conductance regulator (CFTR) chloride channels in human airway epithelial cells. *J Biol Chem* **287**, 17130-17139, doi:10.1074/jbc.M111.338855 (2012).
313 Cao, X. *et al.* SUMOylation of HMGA2: selective destabilization of promyelocytic leukemia protein via proteasome. *Mol Cancer Ther* **7**, 923-934, doi:10.1158/1535-7163.MCT-07-0540 (2008).
314 Verdun, R. E. & Karlseder, J. Replication and protection of telomeres. *Nature* **447**, 924-931, doi:10.1038/nature05976 (2007).
315 Toler, S. M., Noe, D. & Sharma, A. Selective enhancement of cellular oxidative stress by chloroquine: implications for the treatment of glioblastoma multiforme. *Neurosurg Focus* **21**, E10 (2006).
316 Gareau, J. R. & Lima, C. D. The SUMO pathway: emerging mechanisms that shape specificity, conjugation and recognition. *Nat Rev Mol Cell Biol* **11**, 861-871, doi:10.1038/nrm3011 (2010).
317 Hecker, C. M., Rabiller, M., Haglund, K., Bayer, P. & Dikic, I. Specification of SUMO1- and SUMO2-interacting motifs. *J Biol Chem* **281**, 16117-16127, doi:10.1074/jbc.M512757200 (2006).